Electronic Supplementary Material (ESI) for Organic & Biomolecular Chemistry.

Index

Gene cloning, recombination and transformation

Primers used for amplification of lyase genes

Overhangs for cloning are highlighted in bold.

Designation	Sequence
IB001f_AAV94883	ATGACCCAGACCGACCCCGC
IB001r_AAV94883	TCATATCTCTCCCTCCGGAT
IB002f_AAV94883	**GGCAGCCATATGGCTAGCATGACTGGTGGA**ATGACCCAGACCGACCCCGC
IB002r_AAV94883	**TCTCAGTGGTGGTGGTGGTGGTGCTCGAGT**TCATATCTCTCCCTCCGGAT
IB005f_YP165716	ATGACCGCCATGCTCGACAG
IB005r_YP165716	TCAGGCGCTGGCGGTGAACC
IB006f_YP165716	**GGCAGCCATATGGCTAGCATGACTGGTGGA**ATGACCGCCATGCTCGACAG
IB006r_YP165716	**TCTCAGTGGTGGTGGTGGTGGTGCTCGAGT**TCAGGCGCTGGCGGTGAACC
IB017f_AAV95561.	ATGCGCGAACATCGCTGG
IB017r_AAV95561.1	CTAGGCCTGTCCCATCAACG
IB018f_AAV95561.1	**GGCAGCCATATGGCTAGCATGACTGGTGGA**ATGCGCGAACATCGCTGG
IB018r_AAV95561.1	**TCTCAGTGGTGGTGGTGGTGGTGCTCGAGT**CTAGGCCTGTCCCATCAACG
NB003f_DddP_NcoI	**GGACAGCCATGG**CCAGCGATACCTTCG
NB003r_DddP_XhoI	**ACCTCACTCGAG**ACGGGTGGTGCCCATC

The genes for DddQ, DddW and DddP were amplified from genomic DNA of *Ruegeria pomeroyi* DSS-3 using the primer pairs IB001f_AAV94883 / IB001r_AAV94883, IB005f_YP165716 / IB005r_YP165716 and IB017f_AAV95561.1 / IB018r_AAV95561.1. The obtained DNA encoding for DddQ, DddW and DddP was elongated and amplified with 30 bp homology arms fitting to the pYE-Express vector[1] using the primer pairs IB002f_AAV94883 / IB002r_AAV94883, IB006f_YP165716 / IB006r_YP165716, IB018f_AAV95561.1 / IB018r_AAV95561.1. Homologous recombination was carried out by transforming *S. cerevisae* FY834 with digested pYE-Express vector (HindIII and EcoRI) and the respective PCR product following the LiOAc/ salmon sperm carrier DNA protocol.[2] The transformed yeast was grown on freshly prepared SM-URA agar plates (0.17 g yeast nitrogen base, 0.50 g ammonium sulfate, 2.00 g glucose, 0.077 g nutritional supplement minus uracil, 20.0 g agar, 1L water) for 3 d at 28 °C. Plasmid DNA was extracted from the yeast colonies using the Zymoprep yeast plasmid miniprep II kit (Zymo Research, Irvine, USA), following the instructions of the manufacturer.

As DddP could not be obtained in soluble, active form after transformation and expression (see next chapter), the gene for DddP from *Phaeobacter inhibens* DSM 17395 was amplified from the genomic DNA of *P. inhibens* using the primer pair NB003f_DddP_NcoI/ NB 003r_DddP_XhoI. The primers and the pET28c vector plasmid (Novagen) were digested using restriction enzymes NcoI and XhoI, mixed and heterologously recombined using T4 DNA ligase.

All recombinant plasmid constructs were transformed into *E. coli* BL21 by electroporation. Transformed bacteria were plated on 2YT agar (16 g tryptone, 10 g yeast extract, 5 g NaCl, 15 g agar, pH 7.2, 1 L water) containing kanamycin (50 mg/L) at 37 °C overnight. Single colonies were picked and cultured in 2YT containing kanamycin (50 mg/L). Recombinant plasmids were extracted from these cultures using the pure yield plasmid miniprep kit (Promega), following the instructions of the manufacturer, and checked by sequencing.

Expression and purification of recombinant enzymes

E. coli BL21 cells carrying the expression plasmid for expression of a respective lyase gene were precultured in 35 mL LB medium (10 g tryptone, 5 g yeast extract, 5 g NaCl, pH 7.2, 1 L water) containing kanamycin (50 mg/L) at 37 °C and 160 rpm overnight. An aliquot from these cultures was used to inoculate LB medium containing kanamycin (50 mg/L). The expression cultures were grown to OD_{600} = 0.5 (37 °C, 160 rpm) and cooled for 45 min (18 °C, 160 rpm) before expression was induced by addition of IPTG (400 µM) and continued for 18 h (18 °C, 160 rpm). Cell harvesting by centrifugation (5100 g, 1 h) yielded a bacterial cell pellet that was taken up in washing/ lysis buffer (For DddW and DddQ: 10 mM Tris, 200 mM NaCl, 20 mM imidazole, pH 8; for DddP: 20 mM MES, 50 mM NaCl, 20 mM imidazole, pH 6; 15 mL for 1 L of cell culture) and ultra sonicated (7x 1 min intervals). Cell debris was separated from the soluble components by centrifugation (12900 g, 2x 10 min) and the soluble fraction was passed through a 20 µm cellulose filter. Purification of the desired enzyme was carried out via Ni^{2+}-NTA-affinity chromatography with Ni^{2+}-NTA superflow (Qiagen, 30 mL) using lysis / binding buffer for washing (2x 20 mL) and elution buffer for elution of DddW (10 mM Tris, 200 mM NaCl, 500 mM imidazole, pH 8, 3x 10 mL) and DddQ (10 mM Tris, 200 mM NaCl, 100 mM imidazole, pH 8, 3x 10 mL). DddP was eluted using elution buffer (20 mM MES, 50 mM NaCl, pH 6) with an imidazole gradient (subsequently 50 mM imidazole 2x 7 mL and 100 mM imidazole 3x 7 mL). All fractions were checked by SDS-PAGE. Enzyme purity in the elution fractions was determined via gel densometry using ImageJ for DddW > 95 %, for DddQ > 95 % and for DddP > 85 %. The purified enzyme containing fractions of the respective lyases were dialysed (3x 1000 fold volume dialysis buffer (DddQ and DddW: 10 mM Tris, 200 mM NaCl, pH 8; DddP: 20 mM MES, 200 mM NaCl, pH 6) gentle agitation, 6-8 h, 4 °C) to eliminate imidazole. Glycerin (10% v/v) was added and the enzyme solutions were aliquotted in 1 mL portions, shock frosted in liquid nitrogen and stored at –80 °C until use. The enzyme concentration was estimated via calculation of their extinction coefficient and measuring the UV absorption at 280 nm[3] and Bradford assays.

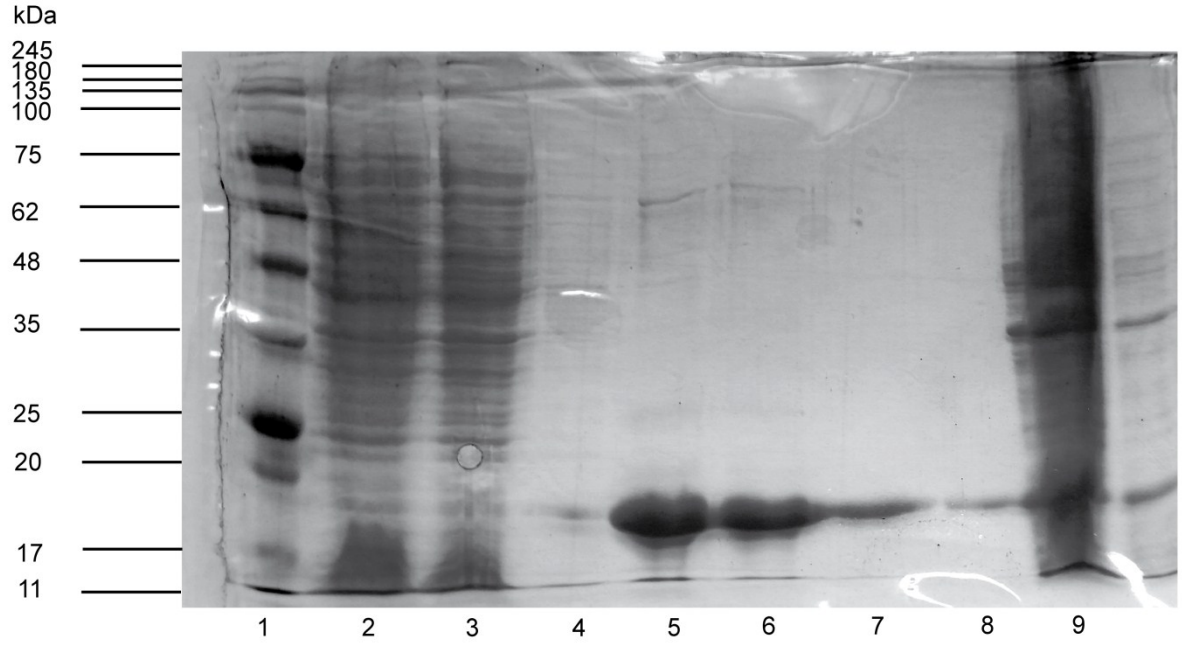

Figure S1 SDS-PAGE analysis of recombinant DddW. Lanes: 1: Marker, 2: flow-through, 3: first wash fraction, 4: second wash fraction, 5: first elution fraction, 6: second elution fraction, 7 third elution fraction, 8: fourth elution fraction, 9: insoluble fraction.

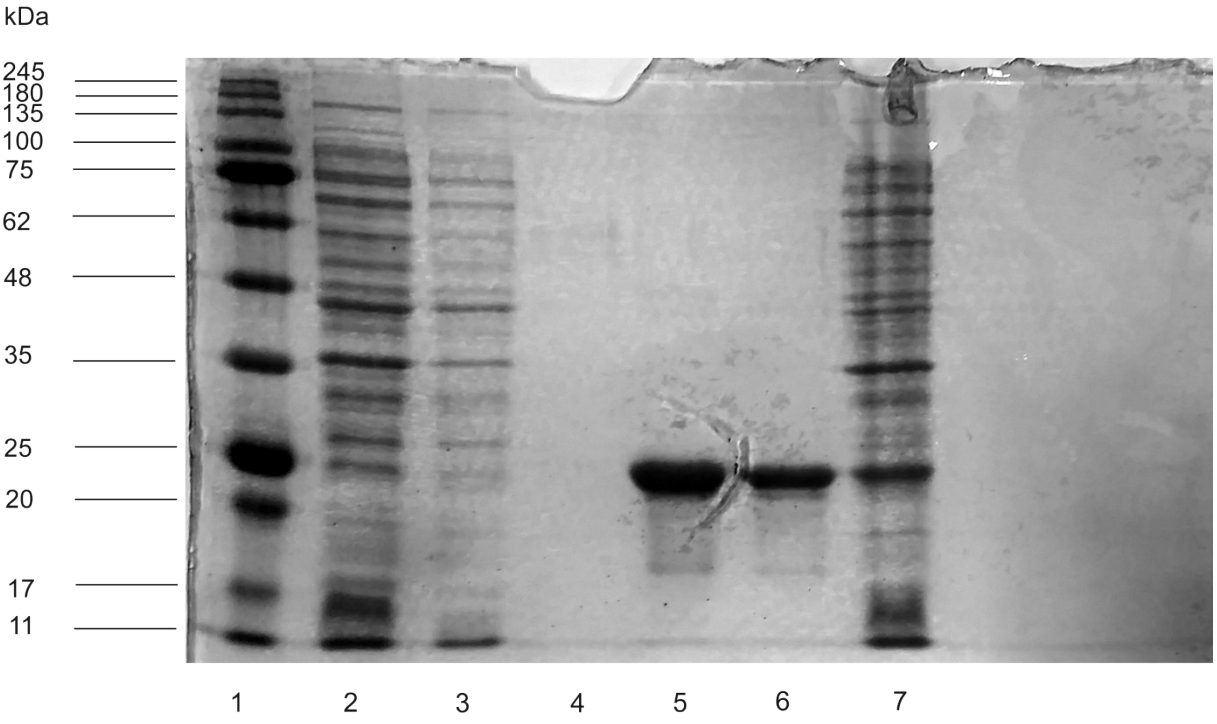

Figure S2 SDS-PAGE analysis of recombinant DddQ. Lanes: 1: Marker, 2: flow-through, 3: first wash fraction, 4: second wash fraction, 5: first elution fraction, 6: second elution fraction, 7 insoluble fraction.

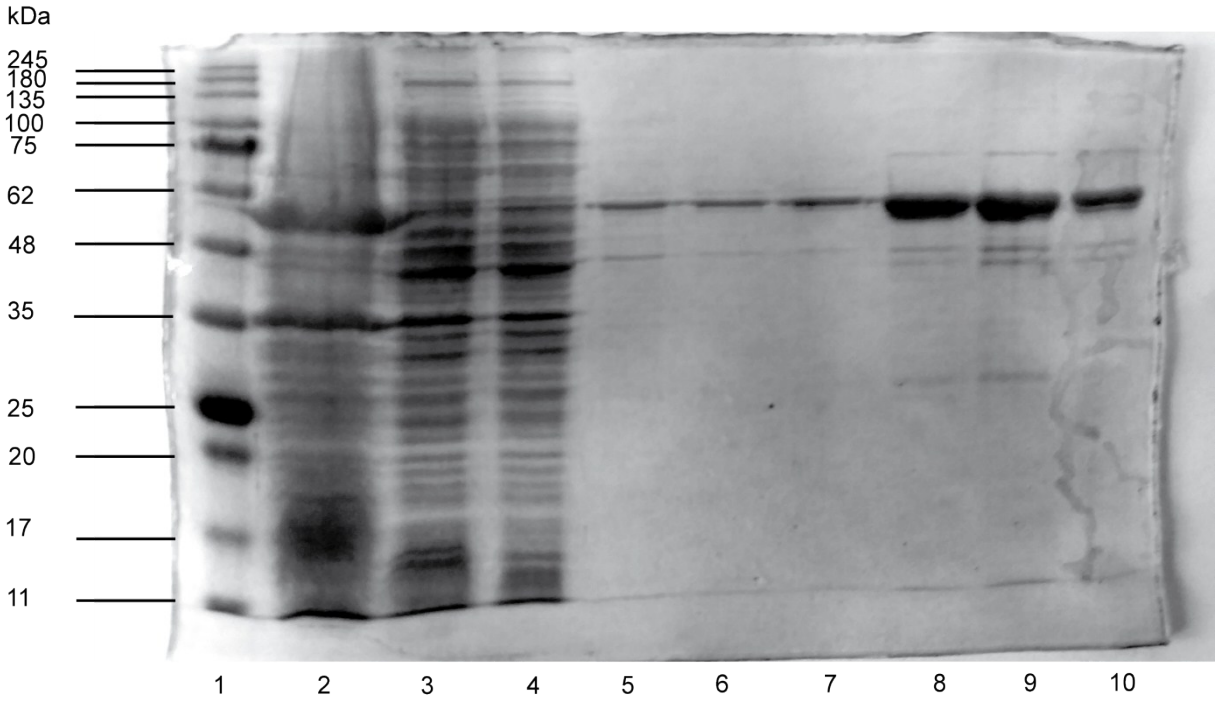

Figure S3 SDS-PAGE analysis of recombinant DddP. Lanes: 1: Marker, 2: flow-through (20 mM imidazole) , 3: first wash fraction (20 mM imidazole), 4: second wash fraction (20 mM imidazole), 5: third wash fraction (50 mM imidazole), 6: fourth wash fraction (50 mM imidazole), 7: fifth wash fraction (50 mM imidazole), 8: first elution fraction (100 mM imidazole), 9: second elution fraction (100 mM imidazole), 10: third elution fraction (100 mM imidazole).

General synthetic and analytical methods

Chemicals were purchased from Acros Organics (Geel, Belgium) or Sigma Aldrich Chemie GmbH (Steinheim, Germany) and used without purification. Thin-layer chromatography was performed with 0.2 mm precoated plastic sheets Polygram® Sil G/UV254 (Machery-Nagel). Column chromatography was carried out using Merck silica gel 60 (70-200 mesh). ^{1}H NMR and ^{13}C NMR spectra were recorded on Bruker AV I (400 MHz), AV III HD Prodigy (500 MHz) and AV III HD Cryo (700 MHz) spectrometers, and were referenced against $CDCl_3$ (δ = 7.26 ppm) and C_6D_6 (δ = 7.16 ppm) for ^{1}H-NMR and $CDCl_3$ (δ = 77.01 ppm) and C_6D_6 (δ = 128.06 ppm) for ^{13}C-NMR. GC-MS analyses were carried out with a HP 7890B gas chromatograph connected to a HP 5977A inert mass detector fitted with a HP5-MS silica capillary column (30m, 0.25mm i. d., 0.50 μm film). Used parameters were (1) inlet pressure, 77.1 kPa, He 23.3 mL min^{-1}, (2) injection volume, 1 μL, (3) transfer line, 250 °C, and (4) electron energy 70 eV. The GC was programmed as follows: 5 min at 50 °C increasing at 10 °C min^{-1} to 320 °C, and operated in split mode (50:1, 60 s valve time). The carrier gas was He at 1 mL min^{-1}. For determination of the enantiomeric excess of **20**, different samples (Fig. S4) were subjected to GC/MS analysis on the same gas chromatograph using a Cyclosil-B column (Agilent, 30 m length, 0.25 mm diameter, 0.25 μm film) with the program: start at 50 °C, increasing at 2.5 °C min^{-1} to 170 °C, then increasing at 20 °C min^{-1} to 245 °C. Retention indices (*I*) were determined from a homologous series of *n*-alkanes (C_8-C_{40}). Optical rotary powers were recorded on a P8000 Polarimeter (Krüss). UV/Vis spectra and single wavelength measurements were recorded on a Cary 100 UV/Vis spectrometer (Agilent).

Procedure for anion exchange of ionic compounds

Before use the OH^- form of the anion exchange resin (Amberlite® IRA-96) was flushed with two column volumes HCl (1 M) and afterwards washed with distilled water until pH 6 was reached. The aqueous solution containing the salt for exchange was carefully laid on the resin and slowly eluted with two column volumes of distilled water. Lyophilisation of the elution fractions yielded the product. After use, the resin was washed with three column volumes NaOH solution (3% w/v) and stored in water at room temperature.

Synthetic procedures for DMSP analogues

(*R*)-4-Isopropyl-5,5-dimethyl-3-propionyloxazolidin-2-one (**22**)

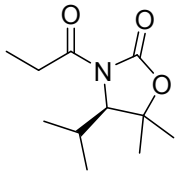

n-BuLi (1.6 mM in hexanes, 13.6 mL, 21.7 mmol, 1.20 eq) was added dropwise to a solution of (*R*)-4-isopropyl-5,5-dimethyloxazolidin-2-one ((*R*)-**21**, 2.84 g, 18.1 mmol, 1.00 eq) in anhydrous THF (75 mL) under argon atmosphere at –78 °C. The resulting mixture was stirred for 30 min before propionyl chloride (2.01 g, 21.7 mmol, 1.20 eq) was added dropwise at the same temperature. After additional stirring for 3 h at –78 °C the mixture was allowed to warm to room temperature overnight and subsequently quenched by the addition of 0.5 M HCl. The mixture was diluted with water (70 mL), the phases were separated and the aqueous phase was extracted with EtOAc (2x 40 mL). The combined organic layers were washed with $NaHCO_3$ (sat. solution, 3x 70 mL), dried over $MgSO_4$ and filtrated before the solvent was removed in vacuo, leaving a colourless oil. Column chromatography (silica gel, EtOAc/cyclohexane 1:7 changing to 1:2) yielded **22** (3.32 g, 15.6 mmol, 86 %) as a colourless solid.

Optical rotary power: $[\alpha]_D^{21.5}$ = –34.2 (*c* 1, EtOH). **TLC** (cyclohexane/EtOAc 5:1): R_f = 0.43. **GC** (HP-5): *I* = 1425. **^{1}H-NMR** (500 MHz, $CDCl_3$): δ = 4.16 (d, $^3J_{H,H}$ = 3.6 Hz, 1H, CH), 3.02 (dq, $^2J_{H,H}$ = 17.4 Hz, $^3J_{H,H}$ = 7.4 Hz, 1H, CH_2), 2.92 (dq, $^3J_{H,H}$ = 7.4 Hz, $^2J_{H,H}$ = 17.4 Hz, 1H, CH_2), 2.15 (m, 1H, CH), 1.52 (s, 3H, CH_3), 1.39 (s, 3H, CH_3), 1.19 (dd, $^3J_{H,H}$ = 7.3 Hz, $^3J_{H,H}$ = 7.3 Hz, 3H, CH_3), 1.04 (d, $^3J_{H,H}$ = 7.1 Hz, 3H, CH_3), 0.95 (d, $^3J_{H,H}$ = 6.9 Hz, 3H, CH_3) ppm. **^{13}C-NMR** (125 MHz, $CDCl_3$): δ = 174.8 (C_q), 153.7 (C_q), 82.9 (C_q), 66.4 (CH), 29.6 (CH_3), 29.2 (CH_2), 28.9 (CH_3), 21.6 (CH), 21.5 (CH_3), 17.2 (CH_3), 8.9 (CH_3) ppm. **IR** (ATR): $\tilde{\nu}$ = 2981 (m), 2957 (w), 2940 (w), 2880 (w), 1756 (s), 1701 (s), 1457 (w), 1338 (s), 1359 (s), 1309 (s), 1279 (m), 1238 (s), 1216 (m), 1171 (s), 1119 (s), 1093 (m), 1063 (s), 1019 (m), 1012 (m), 964 (m), 945 (m), 936 (m), 804 (m), 791 (m), 759 (m), 708 (m), 634 (w), 610 (w), 594 (w), 575 (w) cm^{-1}. **UV/Vis** (EtOH): λ_{max} (lg ε): 212 (4.271) nm. **EI-MS** (70 eV): *m*/*z* (%) = 213 (4), 170 (51), 114 (81), 98 (4), 97 (3), 96 (3), 83 (3), 71 (5), 70 (21), 57 (100), 43 (13). **HRESIMS** calcd. for $C_{11}H_{20}NO_3^+$: 214.1438, found: 214.1438.

(*S*)-4-Isopropyl-5,5-dimethyl-3-propionyloxazolidin-2-one ((*ent*)-**22**)

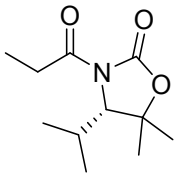

Starting material ((*S*)-**21**, 3.00 g, 19.1 mmol, 1.00 eq) yielded (*ent*)-**22** (3.36 g, 15.8 mmol, 83 %) by following the same procedure as for **22**. All recorded spectral data with exception of the rotary power were the same as for **22**.

Optical rotary power: $[\alpha]_D^{21.5}$ = +35.5 (*c* 1, EtOH).

(*R*)-3-((*S*)-3-Hydroxy-2-methylpropanoyl)-4-isopropyl-5,5-dimethyloxazolidin-2-one (**23**)

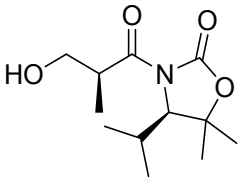

To a solution of **22** (3.00 g, 14.1 mmol, 1.0 eq) in dry DCM (80 mL) freshly distilled $TiCl_4$ (2.67 g, 14.1 mmol, 1.0 eq) was added dropwise over 5 min at 0 °C under argon atmosphere. The resulting clear orange solution was treated dropwise with DIPEA (2.00 g, 15.5 mmol, 1.1 eq) over 10 min at the same temperature whereupon its colour changed to deep blackberry. The mixture was stirred at 0 °C for 50 min before 1,3,5-trioxane (1.52 g, 16.9 mmol, 1.2 eq, in 10 mL dry DCM) and $TiCl_4$ (2.67 g, 14.1 mmol, 1.0 eq) were added dropwise and simultaneously over 30 min at the same temperature. After stirring for 3.5 h at 0 °C additional $TiCl_4$ (400 mg, 2.1 mmol, 0.15 eq) was added and stirring was continued for 40 min. The reaction was quenched with NH_4Cl (sat. solution, 80 mL) and diluted with water (80 mL). The layers were separated and the aqueous layer was extracted with DCM (2x 40 mL). The combined organic layers were washed subsequently with $NaHCO_3$ (half concentrated solution, 100 mL) and NH_4Cl (half concentrated solution, 100 mL), dried over $MgSO_4$ and filtrated. After removal of

the solvent in vacuo and column chromatography (silica gel, cyclohexane/EtOAc 2:1) **23** (2.89 g, 11.9 mmol, 85 %) was obtained as a colourless solid. NMR analysis showed exclusively one diastereoisomer.

Optical rotary power: $[\alpha]_D^{21.5}$ = –11.8 (*c* 1, EtOH) **TLC** (cyclohexane/EtOAc 2:1): R_f = 0.33. **GC** (HP-5): *I* = 1634. **^{1}H-NMR** (500 MHz, $CDCl_3$): δ = 4.16 (d, $^3J_{H,H}$ = 3.3 Hz, 1H, CH), 4.02-3.96 (m, 1H, CH), 3.82 (dd, $^3J_{H,H}$ = 10.9 Hz, $^3J_{H,H}$ = 4.6 Hz, 1H, CH_2), 3.76 (dd, $^3J_{H,H}$ = 11.0 Hz, $^3J_{H,H}$ = 7.6 Hz, 1H, CH_2), 2.28 (s, 1H, OH), 2.16-2.12 (m, 1H, CH), 1.51 (s, 3H, CH_3), 1.37 (s, 3H, CH_3), 1.15 (d, $^3J_{H,H}$ = 6.9 Hz, 3H, CH_3), 1.02 (d, $^3J_{H,H}$ = 7.0 Hz, 3H, CH_3), 0.95 (d, $^3J_{H,H}$ = 6.8 Hz, 3H, CH_3) ppm. **^{13}C-NMR** (125 MHz, $CDCl_3$): δ = 176.6 (C_q), 153.9 (C_q), 83.2 (C_q), 66.7 (CH), 65.7 (CH_2), 40.3 (CH), 29.7 (CH_3), 28.9 (CH_3), 21.6 (CH_3), 21.4 (CH), 17.1 (CH_3), 13.4 (CH_3) ppm. **IR** (ATR): $\tilde{\nu}$ = 3520 (m), 2967 (w), 2937 (w), 2882 (w), 2838 (w), 1762 (s), 1687 (s), 1465 (w), 1388 (m), 1359 (m), 1310 (s), 1281 (s), 1258 (m), 1217 (s), 1173 (s), 1116 (s), 1067 (s), 1032 (s), 972 (m), 954 (m), 912 (w), 857 (w), 813 (m), 791 (w), 758 (w), 733 (m), 624 (w), 609 (w), 471 (w), 425 (w).cm^{-1}. **UV/Vis** (EtOH): λ_{max} (lg ε): 208 (3.632) nm. **EI-MS** (70 eV): *m*/*z* (%) = 243 (1), 226 (4), 213 (6), 200 (5), 184 (2), 170 (2), 139 (5), 114 (100), 99 (6), 98 (7), 97 (6), 87 (12), 70 (57), 69 (18), 59 (30), 57 (11), 56 (10), 55 (12), 43 (19), 41 (17). **HRESIMS** calcd. for $C_{12}H_{22}NO_4^+$: 244.1543, found: 244.1544.

(*S*)-3-((*R*)-3-Hydroxy-2-methylpropanoyl)-4-isopropyl-5,5-dimethyloxazolidin-2-one ((*ent*)-**23**)

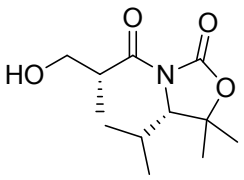

The starting material ((*ent*) **22**, 1.50 g, 7.1 mmol, 1.0 eq) yielded (*ent*)-**23** (1.47 g, 15.8 mmol, 86 %) by following the same procedure as for **23**. All recorded physical data with exception of the rotary power were the same as for **23**.

Optical rotary power: $[\alpha]_D^{21.5}$ = +11.3 (*c* 1, EtOH).

S-((*R*)-3-((*R*)-4-Isopropyl-5,5-dimethyl-2-oxooxazolidin-3-yl)-2-methyl-3-oxopropyl) ethanethioate (**24**)

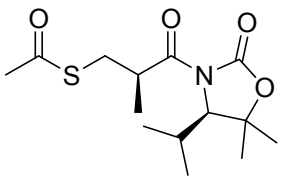

DIAD (3.11 g in 7 mL dry THF, 14.4 mmol, 1.3 eq) was added dropwise to a solution of triphenylphosphine (3.79 g, 14.4 mmol, 1.3 eq) in dry THF (100 mL) under argon atmosphere at 0 °C. The mixture was stirred for 10 min at the same temperature before **23** (2.70 g in 7 mL dry THF, 11.1 mmol, 1.0 eq) was added dropwise at 0 °C. The resulting colourless emulsion was stirred for 30 min maintaining the same temperature and thioacetic acid (1.02 g, 13.3 mmol, 1.3 eq) was added dropwise. The resulting green emulsion was allowed to come to room temperature overnight, changing its colour to yellow. The solvent was removed in vacuo and the obtained crude oil was subjected to column chromatography (silica gel, cyclohexane/EtOAc 6:1) yielding **24** (3.05 g, 10.1 mmol, 91 %) as a colourless oil.

Optical rotary power: $[\alpha]_D^{21.5}$ = +34.1 (*c* 1, $CHCl_3$). **TLC** (cyclohexane/EtOAc 2:1): R_f = 0.59. **GC** (HP-5): *I* = 1957. **^{1}H-NMR** (500 MHz, C_6D_6): δ = 4.31 (ddq, $^3J_{H,H}$ = 7.7 Hz, $^3J_{H,H}$ = 6.8 Hz, $^3J_{H,H}$ = 5.9 Hz, 1H, CH), 3.92 (d, $^3J_{H,H}$ = 3.0 Hz, 1H, CH), 3.31 (dd, $^2J_{H,H}$ = 13.1 Hz, $^3J_{H,H}$ = 7.8 Hz, 1H, CH_2), 3.28 (dd, $^2J_{H,H}$ = 13.3 Hz, $^3J_{H,H}$ = 5.8 Hz, 1H, CH_2), 1.83 (s, 3H, CH_3), 1.73-1.66 (m, 1H, CH), 1.14 (d, $^3J_{H,H}$ = 6.9 Hz, 3H, CH_3), 0.95 (d, $^3J_{H,H}$ = 7.0 Hz, 3H, CH_3), 0.93 (s, 3H, CH_3), 0.85 (s, 3H, CH_3), 0.81 (d, $^3J_{H,H}$ = 6.8 Hz, 3H, CH_3) ppm. **^{13}C-NMR** (125 MHz, C_6D_6): δ = 193.7 (C_q), 176.7 (C_q), 153.1 (C_q), 82.1 (C_q), 66.3 (CH), 39.0 (CH), 32.3 (CH_2), 30.1 (CH_3), 29.8 (CH_3), 28.3 (CH_3), 21.9 (CH), 20.9 (CH_3), 17.2 (CH_3), 17.0 (CH_3) ppm. **IR** (ATR): $\tilde{\nu}$ = 2973 (w), 2934 (w), 2879 (w), 1770 (s), 1692 (s), 1456 (w), 1392 (s), 1311 (m), 1277 (s), 1252 (m), 1239 (m), 1219 (s), 1169 (s), 1117 (s), 1069 (s), 973 (m), 953 (s), 913 (w), 857 (w), 786 (m), 745 (w), 729 (w), 684 (w), 623 (s) cm^{-1}. **UV/Vis** (EtOH): λ_{max} (lg ε): 209 (3.236) nm. **EI-MS** (70 eV): *m*/*z* (%) = 301 (1), 258 (4), 226 (33), 200 (3), 182 (5), 158 (29), 145 (13), 139 (7), 130 (4), 114 (30), 97 (26), 88 (24), 83 (5), 71 (13), 70 (25), 69 (23), 55 (20), 43 (100), 42 (16), 41 (31). **HRESIMS** calcd. for $C_{14}H_{24}NO_4S^+$: 302.1421, found: 302.1421.

S-((*S*)-3-((*S*)-4-Isopropyl-5,5-dimethyl-2-oxooxazolidin-3-yl)-2-methyl-3-oxopropyl) ethanethioate ((*ent*)-**24**)

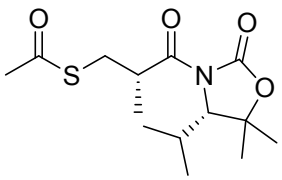

Starting material ((*ent*)-**23**, 1.20 g, 4.94 mmol, 1.0 eq) yielded (*ent*)-**24** (1.39 g, 4.61 mmol, 94 %) by following the same procedure as for **24**. All recorded physical data with exception of the rotary power were the same as for **24**.

Optical rotary power: $[\alpha]_D^{21.5}$ = –34.0 (*c* 1, $CHCl_3$).

(*R*)-4-Isopropyl-5,5-dimethyl-3-((*R*)-2-methyl-3-(methylthio)propanoyl)oxazolidin-2-one (**25**)

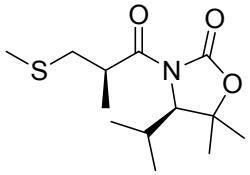

Compound **24** (2.37 g, 7.87 mmol, 1.0 eq) was solved in MeOH (60 mL) before MeI (1.34 g, 9.45 mmol, 1.2 eq) and $NaHCO_3$ (1.65 g, 19.7 mmol, 2.5 eq) were added at room temperature. The reaction suspension was stirred for 5 d at room temperature. After 2 and 3 d additional portions of MeI (134 mg, 0.94 mmol, 0.1 eq) were added. The mixture was diluted with water (200 mL), neutralised with NH_4Cl (sat. solution) and extracted with EtOAc (3x 150 mL). The combined organic layers were dried over $MgSO_4$ and filtrated and the solvent was removed in vacuo. Column chromatography (silica gel, cyclohexane/EtOAc 8:1) yielded **25** (1.03 g, 3.76 mmol, 48 %) as a colourless oil.

Optical rotary power: $[\alpha]_D^{21.5}$ = +28.4 (*c* 1.56, MeOH). **TLC** (cyclohexane/EtOAc 5:1): R_f = 0.34. **GC** (HP-5): *I* = 1828. **^{1}H-NMR** (500 MHz, $CDCl_3$): δ = 4.19 (d, $^3J_{H,H}$ = 3.0 Hz, 1H, CH), 4.19-4.15 (m, 1H, CH), 2.95 (dd, $^2J_{H,H}$ = 13.2 Hz, $^3J_{H,H}$ = 8.1 Hz, 1H, CH_2), 2.53 (dd, $^2J_{H,H}$ = 13.2 Hz, $^3J_{H,H}$ = 6.3 Hz, 1H, CH_2), 2.15 (s, 3H, CH_3), 2.17-2.11 (m,

1H, CH), 1.50 (s, 3H, CH_3), 1.36 (s, 3H, CH_3), 1.22 (d, $^3J_{H,H}$ = 6.8 Hz, 3H, CH_3), 1.04 (d, $^3J_{H,H}$ = 7.0 Hz, 3H, CH_3), 0.97 (d, $^3J_{H,H}$ = 6.8 Hz, 3H, CH_3) ppm. **^{13}C-NMR** (125 MHz, $CDCl_3$): δ = 176.4 (C_q), 153.5 (C_q), 82.8 (C_q), 66.5 (CH), 38.1 (CH_2), 37.6 (CH), 29.8 (CH_3), 29.0 (CH), 21.6 (CH_3), 21.4 (CH_3), 17.00 (CH_3), 16.98 (CH_3), 15.9 (CH_3) ppm. **IR** (ATR): $\tilde{\nu}$ = 2971 (w), 2929 (w), 2877 (w), 1768 (s), 1697 (s), 1455 (s), 1413 (s), 1385 (s), 1369 (s), 1356 (s), 1311 (s), 1277 (s), 1242 (s), 1216 (s), 1116 (s), 1093 (s), 1065 (m), 1036 (w), 1010 (w), 974 (s), 956 (s), 912 (w), 868 (w), 857 (w), 815 (w), 857 (w), 814 (s), 786 (m), 754 (m), 727 (m), 699 (m), 688 (m), 623 (m), 698 (m), 559 (w), 412 (m) cm^{-1}. **UV/Vis** (EtOH): λ_{max} (lg ε): 206 (3.922) nm. **EI-MS** (70 eV): *m*/*z* (%) = 273 (18), 226 (44), 182 (13), 158 (13), 130 (10), 117 (17), 97 (38), 89 (54), 88 (100), 69 (30), 61 (36), 55 (17), 43 (18), 41 (31). **HREIMS** calcd. for $C_{13}H_{23}NO_3S^{\bullet+}$: 273.1393, found: 273.1383.

(*S*)-4-Isopropyl-5,5-dimethyl-3-((*S*)-2-methyl-3-(methylthio)propanoyl)oxazolidin-2-one ((*ent*)-**25**)

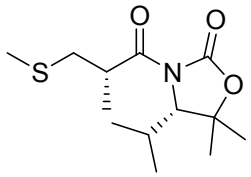

The starting material ((*ent*)-**24**, 1.16 g, 3.85 mmol, 1 eq) yielded (*ent*)-**25** (535 mg, 1.96 mmol, 51 %) by following the same procedure as for **25**. All recorded physical data with exception of the rotary power were the same as for **25**.

Optical rotary power: $[\alpha]_D^{21.5}$ = –27.4 (*c* 1, MeOH).

(*R*)-2-Methyl-3-(methylthio)propanoic acid ((*R*)-**20**)

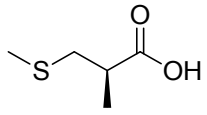

A solution of **25** (970 mg, 3.55 mmol, 1.0 eq) in THF (5 mL) was added to HCl (2 M, 71 mL) and the mixture was heated to 120 °C. After 6 d TLC analysis showed complete conversion of the starting material and the reaction was cooled to room temperature. The aqueous mixture was extracted with EtOAc (5x 30mL) and the combined organic layers were dried over $MgSO_4$, filtrated and concentrated in vacuo. Column

chromatography (silica gel, cyclohexane/EtOAc 1:1) yielded (*R*)-**20** (393 mg, 2.93 mmol, 83 %) as a colourless oil. GC-analysis on a homochiral stationary phase showed an enantiomeric excess of >98 % (Fig. S4).

Optical rotary power: $[\alpha]_D^{21.5}$ = +22.0 (*c* 1, EtOH). **TLC** (cyclohexane/EtOAc 1:1): R_f = 0.70. **GC** (HP-5): *I* = 1407. **^{1}H-NMR** (500 MHz, $CDCl_3$): δ = 2.84 (dd, $^2J_{H,H}$ = 12.8 Hz, $^3J_{H,H}$ = 7.0 Hz, 1H, CH_2), 2.73 (ddq, $^3J_{H,H}$ = 7.0 Hz, $^3J_{H,H}$ = 7.0 Hz, $^3J_{H,H}$ = 7.0 Hz, 1H, CH), 2.56 (dd, $^2J_{H,H}$ = 12.8 Hz, $^3J_{H,H}$ = 6.5 Hz, 1H, CH_2), 2.12 (s, 3H, CH_3), 1.29 (d, $^3J_{H,H}$ = 6.9 Hz, 3H, CH_3) ppm. **^{13}C-NMR** (125 MHz, $CDCl_3$): δ = 181.8 (C_q), 39.8 (CH), 37.4 (CH_2), 16.7 (CH_3), 16.2 (CH_3) ppm. **IR** (ATR): $\tilde{\nu}$ = 3000 (m, br), 2976 (m), 2917 (m), 2656 (w, br), 1700 (s), 1462 (m), 1423 (m), 1376 (w), 1294 (m), 1235 (s), 1193 (m), 1113 (w), 1067 (w), 1040 (w), 928 (m), 807 (m), 634 (w), 533 (m) cm^{-1}. **UV/Vis** (EtOH): λ_{max} (lg ε): No absorption over 200 nm. **EI-MS** (70 eV): *m*/*z* (%) = 134 (36), 101 (3), 87 (6), 73 (7), 61 (100), 45 (14), 41 (16). **HREIMS** calcd. for $C_5H_{10}O_2S^{\bullet+}$: 134.0396, found: 134.0392.

(*S*)-2-Methyl-3-(methylthio)propanoic acid ((*S*)-**20**)

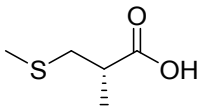

Starting material (*ent*)-**25** (470 mg, 1.72 mmol, 1.0 eq) yielded (*S*)-**20** (160 mg, 1.19 mmol, 69 %) as a colourless oil by following the same procedure as for (*R*)-**20**. All recorded physical data with exception of the rotary power were the same as for (*R*)-**20**.

Optical rotary power: $[\alpha]_D^{21.5}$ = –22.9 (*c* 1, EtOH).

(2*R*)-(2-Methyl-dimethylsulfoniopropionate hydrochloride ((*R*)-Me-DMSP, (*R*)-**17**)

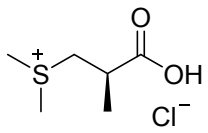

Compound (*R*)-**20** (211 mg, 1.57 mmol, 1.0 eq) was dissolved in nitromethane (317 mg, 5.18 mmol, 3.2 eq) and treated with MeI (602 mg, 4.24 mmol, 2.7 eq). The mixture was stirred for 48 h before Et_2O was added and stirring was continued for 30 min while a brown solid precipitated. The Et_2O was carefully decanted and the solid residue was dissolved in H_2O (20 mL) and washed with DCM (3x 15 mL). After residual DCM was removed in vacuo, the aqueous layer was subjected to ion exchange chromatography. The elution fractions yielded (*R*)-**17** (243 mg, 1.32 mmol, 84 %) as a colourless solid after lyophilisation. An aliquot was dissolved in water and treated with $AgNO_3$ solution. The formed precipitate completely dissolved after addition of ammonia, showing the absence of iodide anions.

Optical rotary power: $[\alpha]_D^{21.5}$ = +26.9 (*c* 1, H_2O). **^{1}H-NMR** (500 MHz, D_2O): δ = 3.63 (dd, $^2J_{H,H}$ = 13.5 Hz, $^3J_{H,H}$ = 8.7 Hz, 1H, CH_2), 3.47 (dd, $^2J_{H,H}$ = 13.3 Hz, $^3J_{H,H}$ = 5.4 Hz, 1H, CH_2), 3.15 (ddt, $^3J_{H,H}$ = 5.4 Hz, $^3J_{H,H}$ = 7.0 Hz, $^3J_{H,H}$ = 8.7 Hz, 1H, CH), 2.979 (s, 3H, CH_3), 2.976 (s, 3H, CH_3), 1.39 (d, $^3J_{H,H}$ = 7.3 Hz, 3H, CH_3) ppm. **^{13}C-NMR** (125 MHz, $CDCl_3$): δ = 176.8 (C_q), 46.3 (CH), 35.7 (CH_2), 26.1 (CH_3), 25.6 (CH_3), 16.1 (CH_3) ppm. **IR** (ATR): $\tilde{\nu}$ = 3000 (m, br), 2976 (m), 2917 (m), 2656 (w, br), 1700 (s), 1462 (m), 1423 (m), 1376 (w), 1294 (m), 1235 (s), 1193 (m), 1113 (w), 1067 (w), 1040 (w), 928 (m), 807 (m), 634 (w), 533 (m) cm^{-1}. **UV/Vis** (EtOH): λ_{max} (lg ε): No absorption over 200 nm. **HRESIMS** calcd. for $C_6H_{13}O_2S^+$: 149.0631, found: 149.0631.

(2*S*)-(2-Methyl-dimethylsulfoniopropionate hydrochloride ((*S*)-Me-DMSP, (*S*)-**17**)

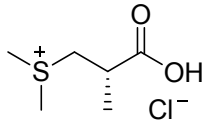

Starting material (*S*)-**20 (**215 mg, 1.60 mmol, 1.0 eq) yielded (*S*)-**17** (243 mg, 1.32 mmol, 83 %) as a colourless solid by following the same procedure as for (*R*)-**17**. All recorded physical data with exception of the rotary power were the same as for (*R*)-**17**.

Optical rotary power: $[\alpha]_D^{21.5}$ = –25.6 (*c* 1, H_2O).

3-(Methylthio)propanoic acid (**2**)

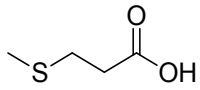

Potassium hydroxide (16.05 g, 243.17 mmol, 2.58 eq, solved in 20 mL MeOH) was added to a solution of 3-mercaptopropionic acid (10.0 g, 94.3 mmol, 1.00 eq) in MeOH (40 mL) at 0 °C before MeI (15.9 g, 112 mmol, 1.19 eq) was added dropwise over 10 min at the same temperature. The reaction mixture was stirred 1 h at 0 °C and warmed to room temperature overnight. The resulting suspension was diluted with water (70 mL), adjusted to pH = 3 using HCl (6 M) and extracted with EtOAc (3x 100 mL). The combined organic layers were dried over $MgSO_4$ and concentrated in vacuo, yielding **2** (10.7 g, 89.0 mmol, 94 %) as a yellow oil.

GC (HP-5): *I* = 1167. **^{1}H-NMR** (500 MHz, $CDCl_3$): δ = 2.78-2.75 (m, 2H, CH_2), 2.69-2.66 (m, 2H, CH_2), 2.13 (s, 3H, CH_3) ppm. **^{13}C-NMR** (125 MHz, $CDCl_3$): δ = 178.4 (C_q), 34.3 (CH_2), 28.8 (CH_2), 15.7 (CH_3) ppm. **IR** (ATR): $\tilde{\nu}$ = 2975 (w, br), 2918 (w), 2662 (w, br), 1702 (s), 1427 (m), 1412 (m), 1261 (m), 1240 (m), 1198 (m), 1144 (m), 934 (m), 810 (m), 651 (m), 631 (m), 487 (m) cm^{-1}. **UV/Vis** (EtOH): λ_{max} (lg ε): 267 (1.979). **EI-MS** (70 eV): *m*/*z* (%) = 120 (78), 105 (7), 87 (14), 74 (47), 61 (100), 55 (12), 47 (32), 45 (42), 41 (14), 35 (10). **HREIMS** calcd. for $C_4H_8O_2S^{\bullet+}$: 120.0240, found: 120.0237.

Methyl 3-(methylthio)propanoate (**28**)

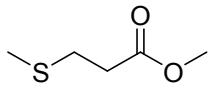

To a solution of **2** (5.00 g, 41.7 mmol, 1.00 eq) in dry MeOH (83 mL) $SOCl_2$ (5.50 g, 46.25 mmol, 1.11 eq) was added dropwise at –10 °C under argon atmosphere. The reaction mixture was stirred 10 min at –10 °C, allowed to warm to room temperature and stirred for further 10 min at room temperature before being heated to reflux for 2.5 h. The reaction was cooled to room temperature, carefully treated with $NaHCO_3$ (sat.) and stirred until no further gas evolution was observed. The mixture was diluted with

water (160 mL) and Et_2O (80 mL) and the layers were separated. The organic layer was washed with $NaHCO_3$ (sat., 3x 100 mL) dried over $MgSO_4$, filtrated and concentrated in vacuo, yielding **28** (4.30 g, 32.1 mmol, 77 %) as a colourless oil.

TLC (cyclohexane/EtOAc 20:1): R_f = 0.15. **GC** (HP-5): I = 1019. **^{1}H-NMR** (500 MHz, $CDCl_3$): δ = 3.69 (s, 3H, CH_3), 2.75 (t, $^3J_{H,H}$ = 7.5 Hz, 2H, CH_2), 2.61 (t, $^3J_{H,H}$ = 7.2 Hz, 2H, CH_2), 2.11 (s, 3H, CH_3) ppm. **^{13}C-NMR** (125 MHz, $CDCl_3$): δ = 172.5 (C_q), 51.9 (CH_3), 34.3 (CH_2), 29.2 (CH_2), 15.6 (CH_3) ppm. **IR** (ATR): $\tilde{\nu}$ = 2969 (w), 2952 (w), 2918 (w), 2842 (w), 1733 (s), 1435 (m), 1356 (m), 1244 (s), 1216 (s), 1197 (s), 1170 (s), 1144 (s), 1020 (w), 984 (w), 935 (w), 894 (w), 820 (w), 672 (w), 435 (w) cm^{-1}. **UV/Vis** (EtOH): λ_{max} (lg ε): No absorption over 200 nm. **EI-MS** (70 eV): *m*/*z* (%) = 134 (100), 119 (5), 103 (20), 87 (21), 75 (35), 74 (94), 61 (84), 59 (39), 47 (19), 45 (21). **HREIMS** calcd. for $C_5H_{10}O_2S^{\bullet+}$: 134.0402, found: 134.0404.

3-(Methylthio)propanamide (**18**)

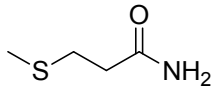

Compound **28** (2.50 g, 18.7 mmol, 1.0 eq) was added to ammonia (conc., 19 mL), forming a blurry emulsion, and stirred vigorously for 18 h at room temperature, turning into a clear solution. The mixture was diluted with water (40 mL) and washed with Et_2O (3x 20 mL). The aqueous layer was concentrated in vacuo. The pasty residue was taken up in water and lyophilised, yielding **18** (1.91 g, 16.1 mmol, 86 %) as a colourless powder.

^{1}H-NMR (500 MHz, DMSO-d_6): δ = 7.34 (s, 1H, NH_2), 6.82 (s, 1H, NH_2), 2.62 (t, $^3J_{H,H}$ = 7.2 Hz, 2H, CH_2), 2.33 (t, $^3J_{H,H}$ = 7.2 Hz, 2H, CH_2), 2.04 (s, 3H, CH_3) ppm. **^{13}C-NMR** (125 MHz, $CDCl_3$): δ = 172.8 (C_q), 35.2 (CH_2), 29.2 (CH_2), 14.7 (CH_3) ppm. **IR** (ATR): $\tilde{\nu}$ = 3351 (s, br), 3174 (s, br), 2915 (w), 1651 (s), 1628 (s), 1412 (s), 1320 (w), 1300 (m), 1214 (m), 1153 (w), 1130 (w), 1061 (w), 1015 (w), 958 (w), 933 (w), 883 (w), 806 (m), 624 (s), 616 (s), 480 (w), 462 (s) cm^{-1}. **UV/Vis** (EtOH): λ_{max} (lg ε): No absorption over 200 nm. **HRESIMS** calcd. for $C_4H_{10}NOS^+$: 120.0477, found: 120.0479.

Dimethylsulfoniopropionamide chloride (DMSPA (**16**))

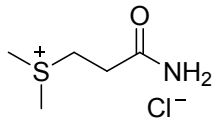

A solution of **18** (1.30 g, 10.9 mmol, 1.00 eq) in $MeNO_2$ (8.00 g, 131 mmol, 12.0 eq) was treated with MeI (1.86 g, 13.2 mmol, 1.21 eq) and stirred at room temperature for 20 hresulting in precipitation of a colourless solid. The mixture was diluted with Et_2O (20 mL), the solid material mechanically dispersed and the resulting suspension stirred vigorously for 20 min. The solvent was decanted and the procedure was repeated twice. Residual solvent was removed in vacuo, leaving a solid, which was taken up in a minimum volume of water and subjected to anion exchange chromatography. Lyophilisation of the elution fractions yielded **16** (1.64 g, 9.67 mmol, 89 %) as a colourless solid. An aliquot was dissolved in water and treated with $AgNO_3$ solution. The formed precipitate completely dissolved after addition of ammonia, showing the absence of iodide anions. **^{1}H-NMR** (500 MHz, D_2O): δ = 3.47 (t, $^3J_{H,H}$ = 6.9 Hz, 2H, CH_2), 2.88 (s, 6H, 2x CH_3), 2.86 (t, $^3J_{H,H}$ = 6.9 Hz, 2H, CH_2) ppm. **^{13}C-NMR** (125 MHz, D_2O): δ = 173.9 (C_q), 39.2 (CH_2), 29.0 (CH_2), 25.2 (2x CH_3) ppm. **IR** (ATR): $\tilde{\nu}$ = 3311 (s), 3135 (s), 3002 (s), 2983 (s), 2914 (m), 1665 (s), 1626 (s), 1407 (s), 1338 (m), 1301 (s), 1284 (s), 1220 (m), 1185 (m), 1171 (m), 1125 (m), 1056 (m), 1023 (m), 1012 (m), 983 (w), 952 (w), 926 (w), 907 (w), 793 (m), 753 (w), 702 (m), 657 (s), 630 (s), 556 (s), 546 (s), 486 (w), 460 (w) cm^{-1}. **UV/Vis** (H_2O): λ_{max} (lg ε): No absorption over 200 nm. **HRESIMS** calcd. for $C_5H_{12}NOS^+$: 134.0634, found: 134.0632.

2-Methyl-3-(methylthio)propanoic acid ((*rac*)-**20**)

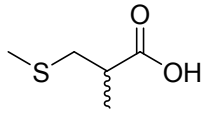

(*rac*)-2-Methyl-3-mercaptopropionic acid (**19**, 2.00 g, 16.6 mmol, 1.0 eq) was dissolved in MeOH (8 mL) and KOH (85 %, 2.75 g, 41.7 mmol, 2.5 eq, in 6 mL MeOH) was added dropwise at 0 °C. MeI (2.83 g, 20.0 mmol, 1.2 eq) was added dropwise at the same temperature. The resulting mixture was allowed to warm to room temperature and stirred for 18 h. The reaction was diluted with water (40 mL), adjusted to pH = 3 using concentrated HCl and extracted with EtOAc (3x 30 mL). The combined organic layers were dried over $MgSO_4$, filtrated and concentrated in vacuo, producing (*rac*)-**20** (2.06 g, 15.4 mmol, 92 %) as a yellow oil.

All recorded physical data were the same as for (*R*)-**20**.

(*rac*)-2-Methyl-dimethylsulfoniopionate hydrochloride ((*rac*)-Me-DMSP, (*rac*)-**17**)

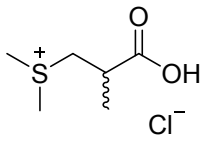

Compound (*rac*)-**20** (1.50 g, 11.2 mmol, 1.0 eq) was dissolved in $MeNO_2$ (2.19 g, 35.8 mmol, 3.2 eq) and treated with MeI (4.29 g, 30.2 mmol, 2.7 eq). The mixture was stirred at room temperature for 24 h and subsequently diluted with Et_2O (20 mL). Water (20 mL) was added, the layers were separated and the aqueous layer was extracted with Et_2O (3x 20 mL). The aqueous solution was concentrated to a volume of 10 mL and subjected to anion exchange chromatography. Lyophilisation of the elution fractions yielded (*rac*)-**17** (1.43 g, 7.76 mmol, 69 %) as a colourless solid. An aliquot was dissolved in water and treated with $AgNO_3$ solution. The formed precipitate completely dissolved after addition of ammonia (conc.), showing the absence of iodide anions.

All recorded physical data were the same as for (*R*)-**17**.

Trimethylphosphoniopropionate hydrochloride (TMPP, **15**)

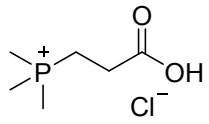

Trimethylphosphine (1 M in THF, 20 mL, 20.0 mmol, 1.0 eq) was added to a solution of 3-bromopropionic acid (3.04 g, 20.0 mmol, 1.0 eq) in dry acetonitrile under argon atmosphere at room temperature. The mixture was heated to 80 °C for 5 h. After cooling to room temperature a colourless precipitate had formed, which was separated by filtration, washed with acetonitrile and dried in vacuo. Subsequent uptake in water, anion exchange and lyophilisation yielded **15** (2.49 g, 13.6 mmol, 68 %) as a colourless solid. An aliquot was dissolved in water and treated with $AgNO_3$ solution. The formed precipitate completely dissolved after addition of ammonia, showing the absence of iodide anions.

^{1}H-NMR (500 MHz, D_2O): δ = 2.81 (ddd, $^3J_{P,H}$ = 14.0, $^3J_{H,H}$ = 8.3, $^3J_{H,H}$ = 7.0 Hz, 2H, CH_2), 2.55 (ddd, $^2J_{P,H}$ = 13.8, $^3J_{H,H}$ = 8.3, $^3J_{H,H}$ = 7.0 Hz, 2H, CH_2), 1.92 (d, $^2J_{P,H}$ = 14.4 Hz, 9H, 3x CH_3) ppm. **^{13}C-NMR** (125 MHz, D_2O): δ = 175.0 (C_q, d, $^3J_{P,C}$ = 13.5 Hz), 26.0 (CH_2, d, $^2J_{P,C}$ = 3.2 Hz), 18.6 (d, $^1J_{P,C}$ = 55.6 Hz, CH_2), 7.5 (d, $^1J_{P,C}$ = 55.4 Hz, 3x CH_3) ppm. **^{31}P-NMR** (202 MHz, D_2O): δ = 27.1 (s) ppm. **IR** (ATR): $\tilde{\nu}$ = 3368 (w), 3288 (w), 2972 (w), 2908 (w), 2763 (w, br), 2696 (w, br), 2540 (w), 2482 (w), 1731 (m), 1692 (s), 1417 (m), 1299 (m), 1261 (w), 1232 (m), 1177 (m), 987 (s), 966 (s), 912 (m), 895 (s), 780 (m), 728 (w), 645 (w), 627 (m), 491 (w), 465 (w) cm^{-1}. **UV/Vis** (H_2O): λ_{max} (lg ε): No absorption over 200 nm. **HRESIMS** calcd. for $C_6H_{14}O_2P^+$: 149.0726, found: 149.0726.

Synthesis of superquat-auxiliary

The chiral auxiliaries were synthesized from D- and L-Valin via a 4 step synthesis to obtain the corresponding enantiomers.

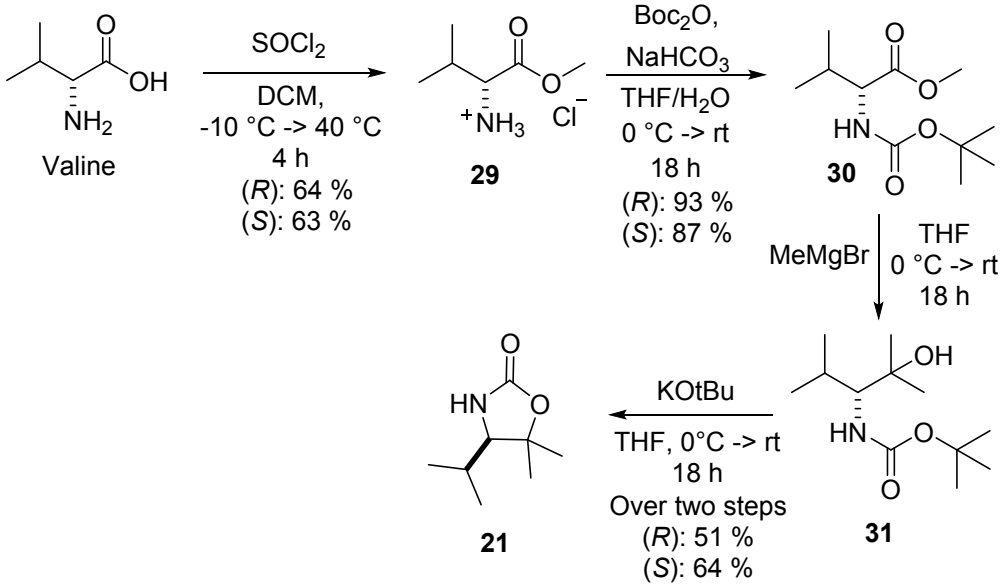

Scheme S1 Synthetic route towards superquat auxiliaries.

(*R*)-1-Methoxy-3-methyl-1-oxobutan-2-aminium chloride ((*R*)-**29**)

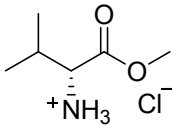

$SOCl_2$ (11.3 g, 9.48 mmol, 1.11 eq) was added dropwise over 15 min to a fine suspension of D-Valine (10.0 g, 8.54 mmol, 1.00 eq) in dry MeOH (65 mL) at –10 °C under argon atmosphere. After complete addition the reaction mixture was stirred 10 min at –10 °C, warmed to room temperature, stirred until the solution became clear and pale yellow, and finally heated to reflux for 3 h. The reaction was cooled to room temperature and the solvent was removed in vacuo. Recrystallisation of the residue from Et_2O/MeOH produced (*R*)-**29** (9.16 g, 54.7 mmol, 64 %) as a colourless solid.

Optical rotary power: $[\alpha]_D^{21.5}$ = –27.8 (*c* 0.55, MeOH).**^{1}H-NMR** (400 MHz, DMSO-d_6): δ = 8.69 (s, 3H, NH_3^+), 3.82 (d, $^3J_{H,H}$ = 4.8 Hz, 1H, CH), 3.73 (s, 3H, CH_3), 2.20 (m, 1H, CH), 0.98 (d, $^3J_{H,H}$ = 7.0 Hz, 3H, CH_3), 0.93 (d, $^3J_{H,H}$ = 7.0 Hz, 3H, CH_3). **^{13}C-NMR** (100 MHz, DMSO-d_6): δ =169.1 (C_q), 57.2 (CH_3), 52.4 (CH), 29.2 (CH), 18.4 (CH_3),

17.5 (CH_3). **IR** (ATR): $\tilde{\nu}$ = 2997 (m, br), 2966 (m), 2827 (m, br), 2669 (w), 2605 (w), 1736 (s), 1593 (w), 1569 (w), 1505 (s), 1434 (m), 1378 (w), 1286 (m), 1237 (s), 1174 (w), 1157 (w), 1107 (w), 1071 (w), 1038 (m), 1020 (w), 972 (m), 927 (w), 879 (w), 813 (w), 771 (w), 752 (w), 651 (w), 580 (w), 521 (w), 424 (w) cm^{-1}.

(*S*)-1-Methoxy-3-methyl-1-oxobutan-2-aminium chloride ((*S*)-**29**)

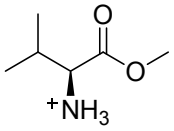

L-Valine (20.0 g, 171 mmol, 1.00 eq) yielded (*S*)-**29** (18.1 g, 108 mmol, 63 %) as a colourless solid by following the same procedure as for (*R*)-**29**. All recorded physical data with exception of the rotary power were the same as for (*R*)-**29**.

Optical rotary power: $[\alpha]_D^{21.5}$ = +26.9 (*c* 1, MeOH).

(*R*)-Methyl 2-((*tert*-butoxycarbonyl)amino)-3-methylbutanoate ((*R*)-**30**)

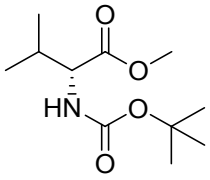

$NaHCO_3$ (11.3 g, 134 mmol, 3.0 eq) and Boc_2O (14.6 g, 67.0 mmol, 1.5 eq) were added subsequently in one portion to a solution of (*R*)-**29** (7.50 g, 44.6 mmol, 1.0 eq) in dry THF/MeOH (108 mL - 12 mL) at 0 °C under argon atmosphere. After complete addition the mixture was stirred for 5 min at 0 °C and allowed to warm to room temperature. Stirring was continued for 20 h, before the reaction was diluted with water (100 mL) and extracted with EtOAc (3x 80 mL). The combined organic layers were washed with $NaHCO_3$ solution (sat., 2x 100 mL) and NaCl solution (sat., 2x 100 mL), dried over $MgSO_4$, filtrated and concentrated in vacuo. Column chromatography (silica gel, cyclohexane/EtOAc 10:1) of the oily residue yielded (*R*)-**30** (8.96 g, 38.7 mmol, 87 %) as a colourless oil.

Optical rotary power: $[\alpha]_D^{21.5}$ = –11.5 (*c* 0.42, $CHCl_3$). **^{1}H-NMR** (500 MHz, $CDCl_3$): δ = 5.01 (d, $^3J_{H,H}$ = 7.8 Hz, 1H, NH), 4.21 (dd, $^3J_{H,H}$ = 8.9 Hz, $^3J_{H,H}$ = 4.8 Hz, 1H, CH),

3.73 (s, 3H, CH_3), 2.11 (m, 1H, CH), 1.44 (s, 9H, 3x CH_3) 0.95 (d, $^3J_{H,H}$ = 6.7 Hz, 3H, CH_3), 0.88 (d, $^3J_{H,H}$ = 6.9 Hz, 3H, CH_3). **^{13}C-NMR** (125 MHz, $CDCl_3$): δ = 172.9 (C_q), 155.6 (C_q), 79.7 (C_q), 58.5 (CH), 52.0 (CH_3), 31.3 (CH), 28.3 (3x CH_3), 18.9 (CH_3), 17.6 (CH_3). **IR** (ATR): $\tilde{\nu}$ = 3446 (w, br), 3369 (w, br), 2969 (m), 2935 (w), 2877 (w), 1741 (s), 1712 (s), 1500 (m), 1456 (m), 1437 (m), 1391 (m), 1366 (s), 1311 (m), 1239 (m), 1206 (m), 1155 (s), 1090 (m), 1042 (m), 1014 (m), 1001 (m), 907 (w), 867 (w), 779 (w), 665 (w), 527 (w), 462 (w) cm^{-1}.

(*S*)-Methyl 2-((*tert*-butoxycarbonyl)amino)-3-methylbutanoate ((*S*)-**30**)

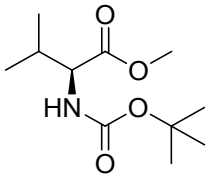

Starting material ((*S*)-**29**, 7.50 g, 44.60 mmol, 1.0 eq) yielded (*S*)-**30** (8.96 g, 42.0 mmol, 94 %) as a colourless oil by following the same procedure as for (*R*)-**30**. All recorded physical data with exception of the rotary power were the same as for (*R*)-**30**.

Optical rotary power: $[\alpha]_D^{21.5}$ = +11.9 (*c* 1, $CHCl_3$).

(*R*)-4-Isopropyl-5,5-dimethyloxazolidin-2-one ((*R*)-**21**)

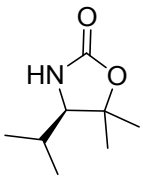

MeMgBr (3 M in Et_2O, 54 mL, 162 mmol, 4.0 eq) was added dropwise over 45 min to a solution of (*R*)-**30** (9.40 g, 40.4 mmol, 1.0 eq) in THF (195 mL) at 0 °C under argon atmosphere. After initial gas evolution a colourless precipitate formed and the reaction was stirred at room temperature overnight, forming a clear yellow solution. The mixture was cooled to 0 °C and quenched dropwise with NH_4Cl solution (sat.) until no more gas evolution was observed, diluted with water (400 mL) and extracted with EtOAc (3x 150 mL). The combined organic layers were dried over $MgSO_4$, filtrated and concentrated in vacuo. Column chromatography (silica gel, cyclohexane/EtOAc 3:1) yielded the tertiary alcohol (*R*)-**31** as a colourless oil (8.33 g).

The tertiary alcohol (*R*)-**31** (7.26 g, 31.4 mmol, 1.0 eq) was dissolved in THF (140 mL) at 0 °C under argon atmosphere, treated with KOtBu (3.91 g, 34.9 mmol, 1.1 eq) and stirred overnight, warming to room temperature. The reaction was quenched by addition of NH_4Cl solution (sat., 50 mL) and diluted with water (300 mL) and EtOAc (100 mL). The layers were separated and the aqueous layer was extracted with EtOAc (2x 100 mL). The combined organic layers were washed with NaCl solution (sat., 200 mL), dried over $MgSO_4$, filtrated and concentrated in vacuo, leaving a yellow solid. The crude product was suspended in a cyclohexane/EtOAc mixture (2:1, 2 mL) and diluted with pentane (7 °C), leaving a colourless solid, which was, after decanting the solvent, washed with pentane (3x 15 mL). Evaporation of residual solvent yielded analytically pure (*R*)-**21** (2.99 g, 19.0 mmol, 54 % over two steps) as a colourless solid.

Optical rotary power: $[\alpha]_D^{21.5}$ = –22.6 (*c* 0.55, $CHCl_3$). **TLC** (cyclohexane/EtOAc 5:1): R_f = 0.34. **^{1}H-NMR** (500 MHz, $CDCl_3$): δ = 6.63 (br s, 1H, NH), 3.18 (d, $^3J_{H,H}$ = 8.6 Hz, 1H, CH), 1.82 (m, 1H, CH), 1.47 (s, 3H, CH_3), 1.37 (s, 3H, CH_3), 0.99 (d, $^3J_{H,H}$ = 6.6 Hz, 3H, CH_3), 0.91 (d, $^3J_{H,H}$ = 6.6 Hz, 3H, CH_3). **^{13}C-NMR** (125 MHz, $CDCl_3$): δ = 159.3 (C_q), 83.9 (C_q), 68.4 (CH), 28.7 (CH_3), 28.6 (CH_3), 21.3 (CH), 20.1 (CH_3), 20.0 (CH_3). **IR** (ATR): $\tilde{\nu}$ = 3229 (m), 3131 (w), 2977 (w), 2963 (w), 2938 (w), 2915 (w), 2874 (w), 2844 (w), 1729 (s), 1554 (w), 1471 (m), 1429 (m), 1389 (m), 1375 (m), 1357 (m), 1305 (m), 1282 (w), 1245 (w), 1202 (w), 1177 (w), 1151 (w), 1132 (w), 1085 (m), 1002 (s), 946 (w), 894 (m), 859 (m), 776 (m), 719 (m), 612 (m), 591 (w), 489 (w), 469 (w), 421 (w) cm^{-1}. **UV/Vis** (EtOH): λ_{max} (lg ε): No absorption over 200 nm.

(*S*)-4-Isopropyl-5,5-dimethyloxazolidin-2-one ((*S*)-**21**)

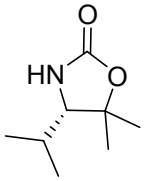

Starting material (*S*)-**30** (8.90 g, 38.5 mmol, 1.0 eq) yielded 8.73 g of crude tertiary alcohol (*S*)-**31**, which was directly subjected to the followup reaction yielding (*S*)-**21** (3.86 g, 24.5 mmol, 64 % over two steps) by following the same procedure as for (*R*)-**21**. All recorded physical data with exception of the rotary power were the same as for (*R*)-**21**.

Optical rotary power: $[\alpha]_D^{21.5}$ = +22.5 (*c* 1, $CHCl_3$).

GC analysis of 20 on a homochiral stationary phase

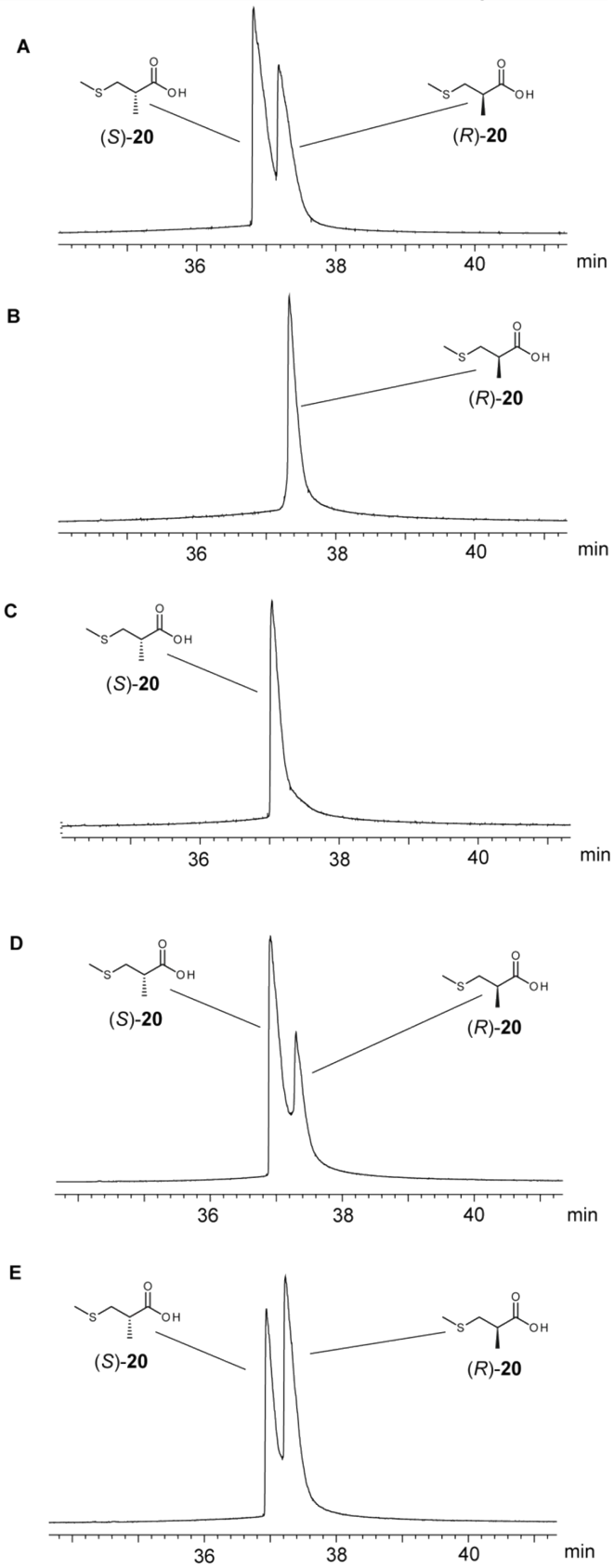

Figure S4 GC analysis of (*R*)-**20** and (*S*)-**20** on a homochiral stationary phase. (A) Pseudoracemic mixture of both enantiomers. (B) Pure (*R*)-**20**. (C) Pure (*S*)-**20**. (D) Coinjection of (*S*)-**20** and pseudoracemic mixture. (E) Coinjection of (*R*)-**20** and pseudoracemic mixture. Both enantiomers were pure to the detection limit.

Activity assay via detection of volatile products

In a 20 mL test tube containing a volume of 8 mL of enzyme specific SPME buffer (For DddW and DddQ: 10 mM Tris, 200 mM NaCl, pH 8; for DddP: 20 mM MES, 50 mM NaCl, pH 6), the respective substrate (2 mM final concentration) and enzyme (3 µM final concentration) were mixed and agitated gently for 30 min at 30 °C. The rection vessel was closed with an aluminium foil cap and a SPME fiber was put through the cap inside the gas volume above the reaction throughout the whole reaction time to adsorb evolving volatile products (Figs. S5 – S13). Subsequently the SPME fiber was subjected directly to GC/MS analysis. A negative control was carried out for each substrate, employing the same experimental setup without adding enzyme to the mixture.

The results are shown whether as total ion chromatograms (TIC) or extracted ion chromatograms (EIC). In case of EIC the detected mass is given. Chromatogram 1 always shows the result of the enzymatic reaction, chromatogram 2 shows the result of the corresponding negative control. Chromatogram pairs are always displayed with the same scaling.

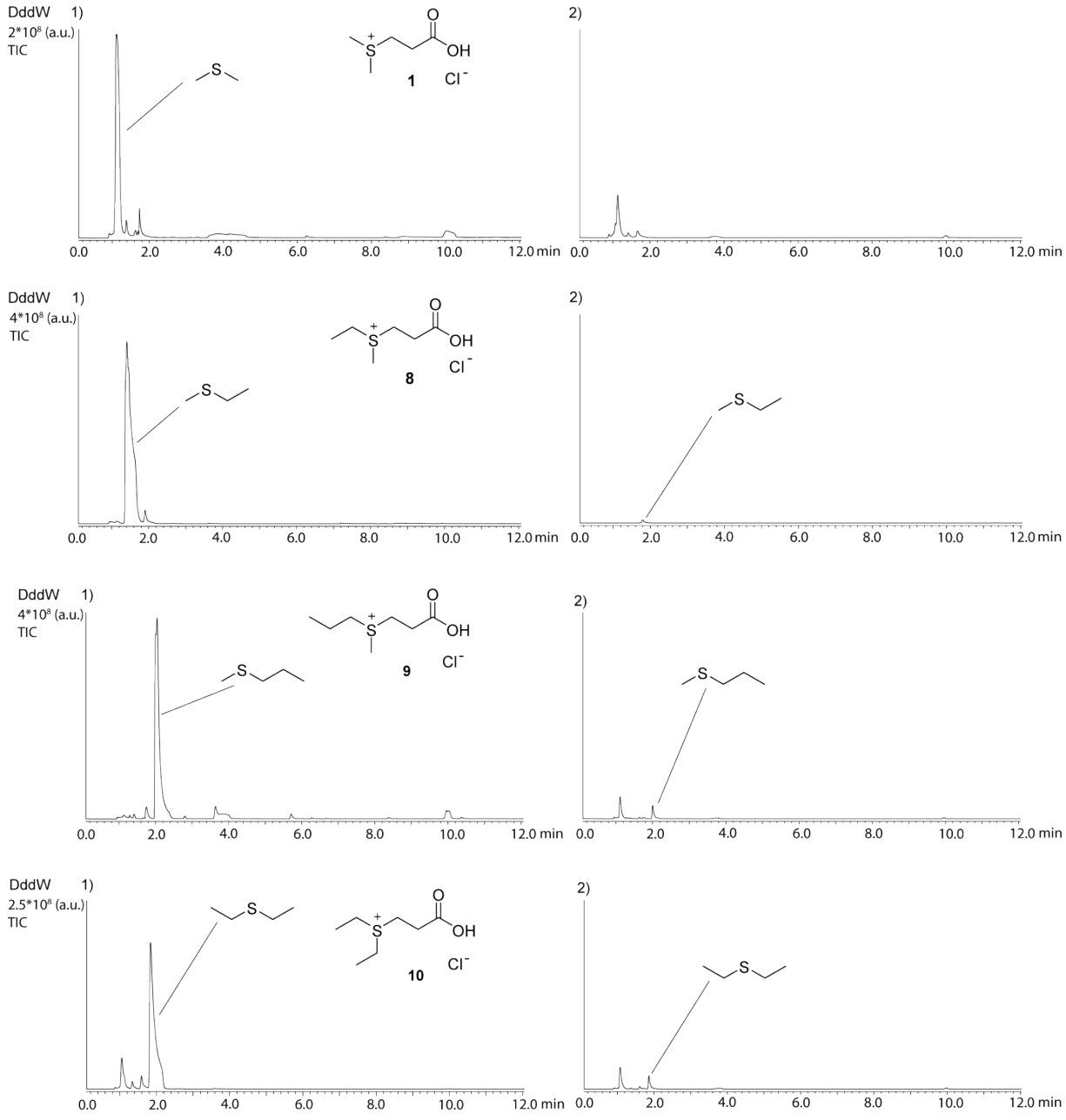

Figure S5 Chromatograms of SPME collected volatiles. 1) Incubations with shown substrate and DddW. 2) Incubations of substrates without enzyme. MS identified volatiles are labelled with corresponding structures.

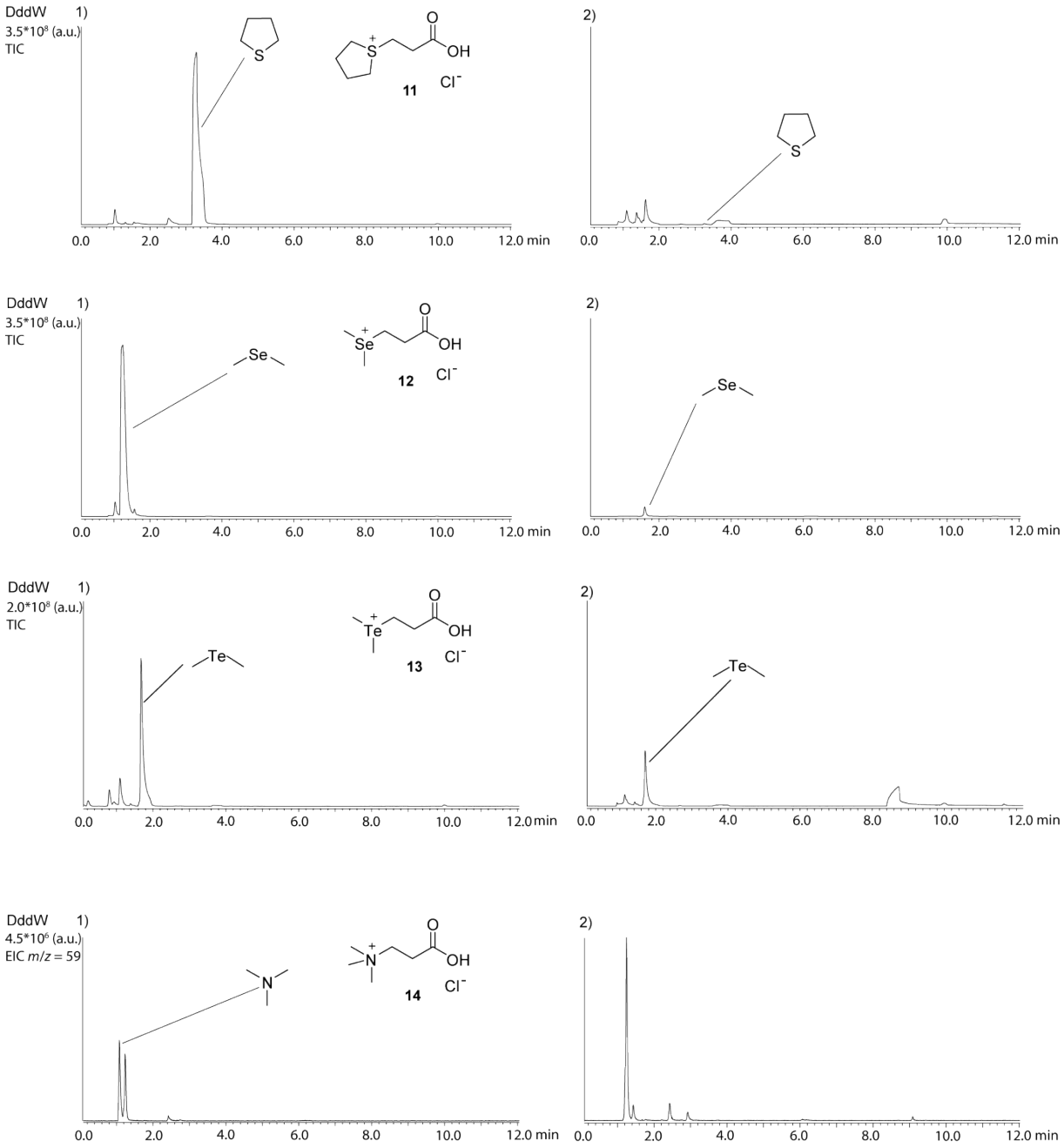

Figure S6 Chromatograms of SPME collected volatiles. 1) Incubations with shown substrate and DddW. 2) Incubations of substrates without enzyme. MS identified volatiles are labelled with corresponding structures.

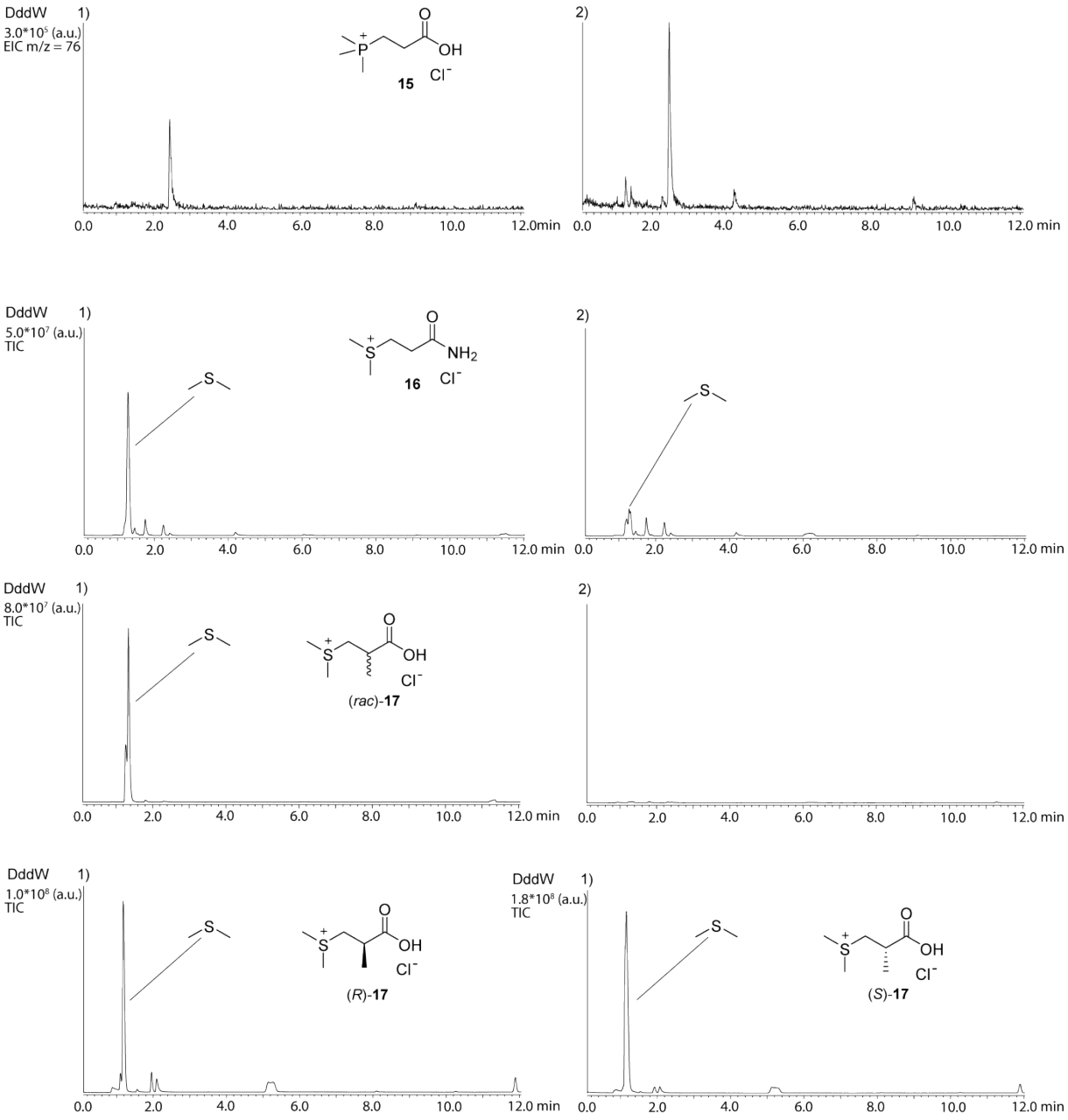

Figure S7 Chromatograms of SPME collected volatiles. 1) Incubations with shown substrate and DddW. 2) Incubations of substrates without enzyme. MS identified volatiles are labelled with corresponding structures.

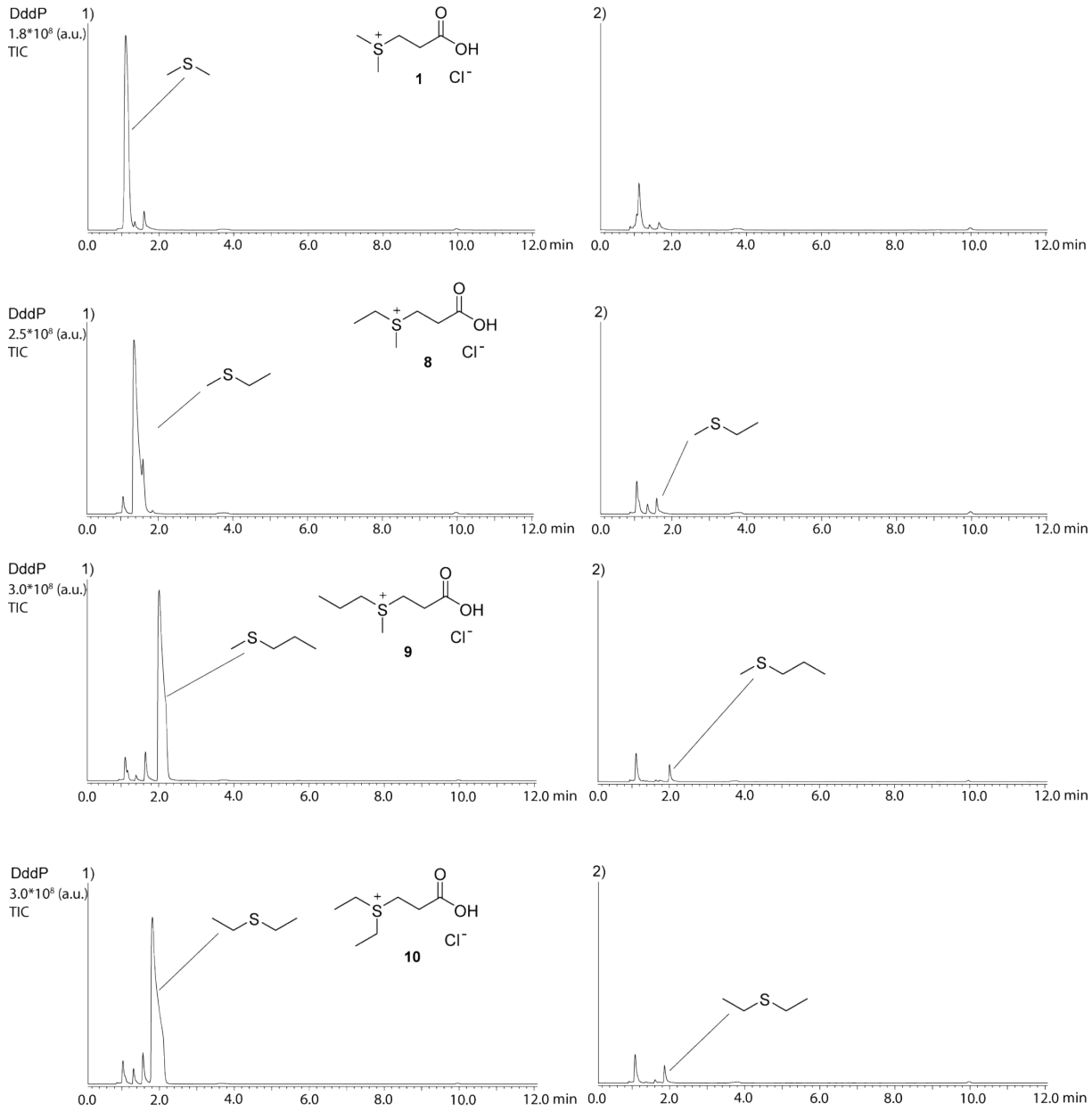

Figure S8 Chromatograms of SPME collected volatiles. 1) Incubations with shown substrate and DddP. 2) Incubations of substrates without enzyme. MS identified volatiles are labelled with corresponding structures.

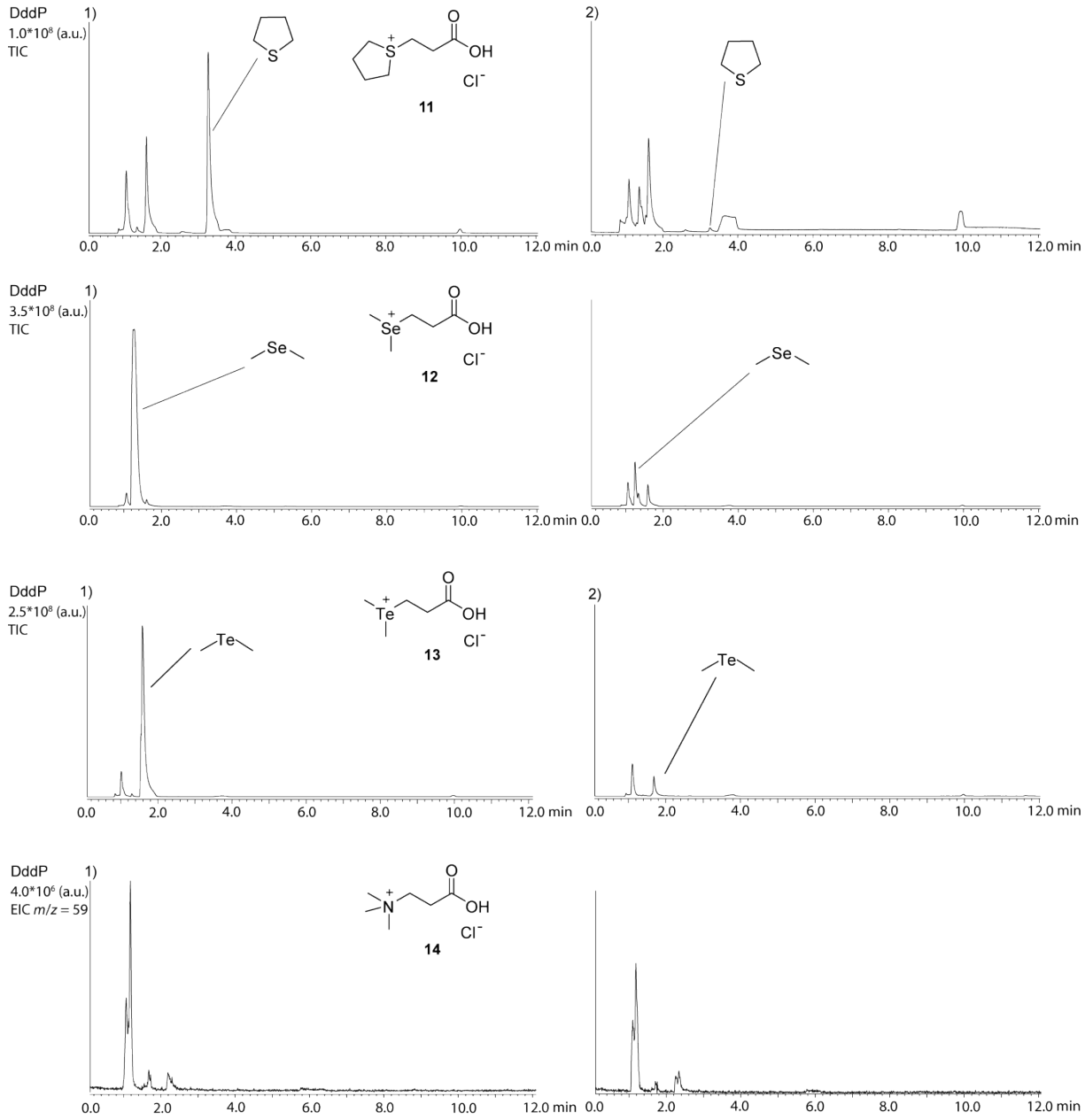

Figure S9 Chromatograms of SPME collected volatiles. 1) Incubations with shown substrate and DddP. 2) Incubations of substrates without enzyme. MS identified volatiles are labelled with corresponding structures.

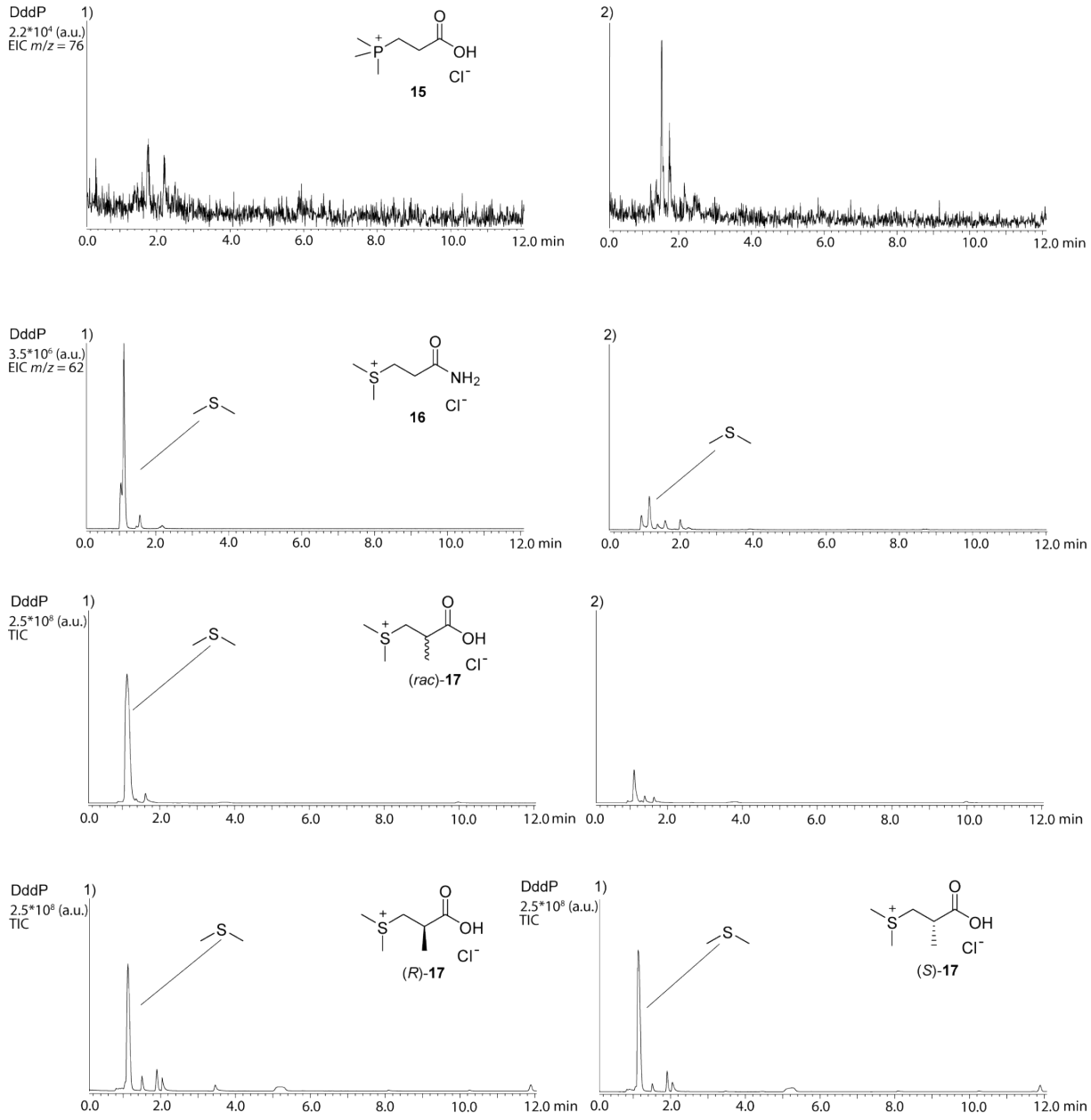

Figure S10 Chromatograms of SPME collected volatiles. 1) Incubations with shown substrate and DddP. 2) Incubations of substrates without enzyme. MS identified volatiles are labelled with corresponding structures.

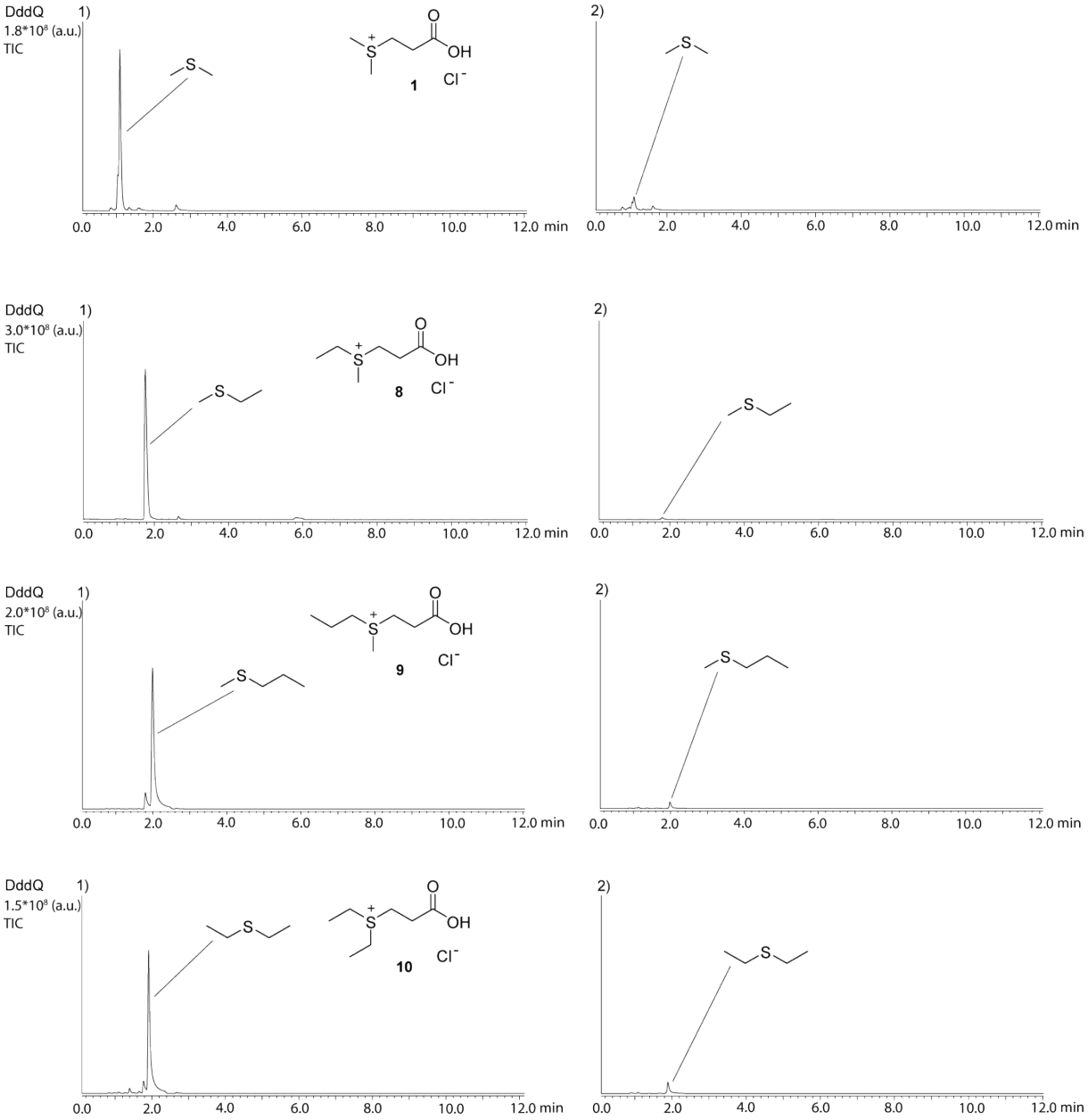

Figure S11 Chromatograms of SPME collected volatiles. 1) Incubations with shown substrate and DddQ. 2) Incubations of substrates without enzyme. MS identified volatiles are labelled with corresponding structures.

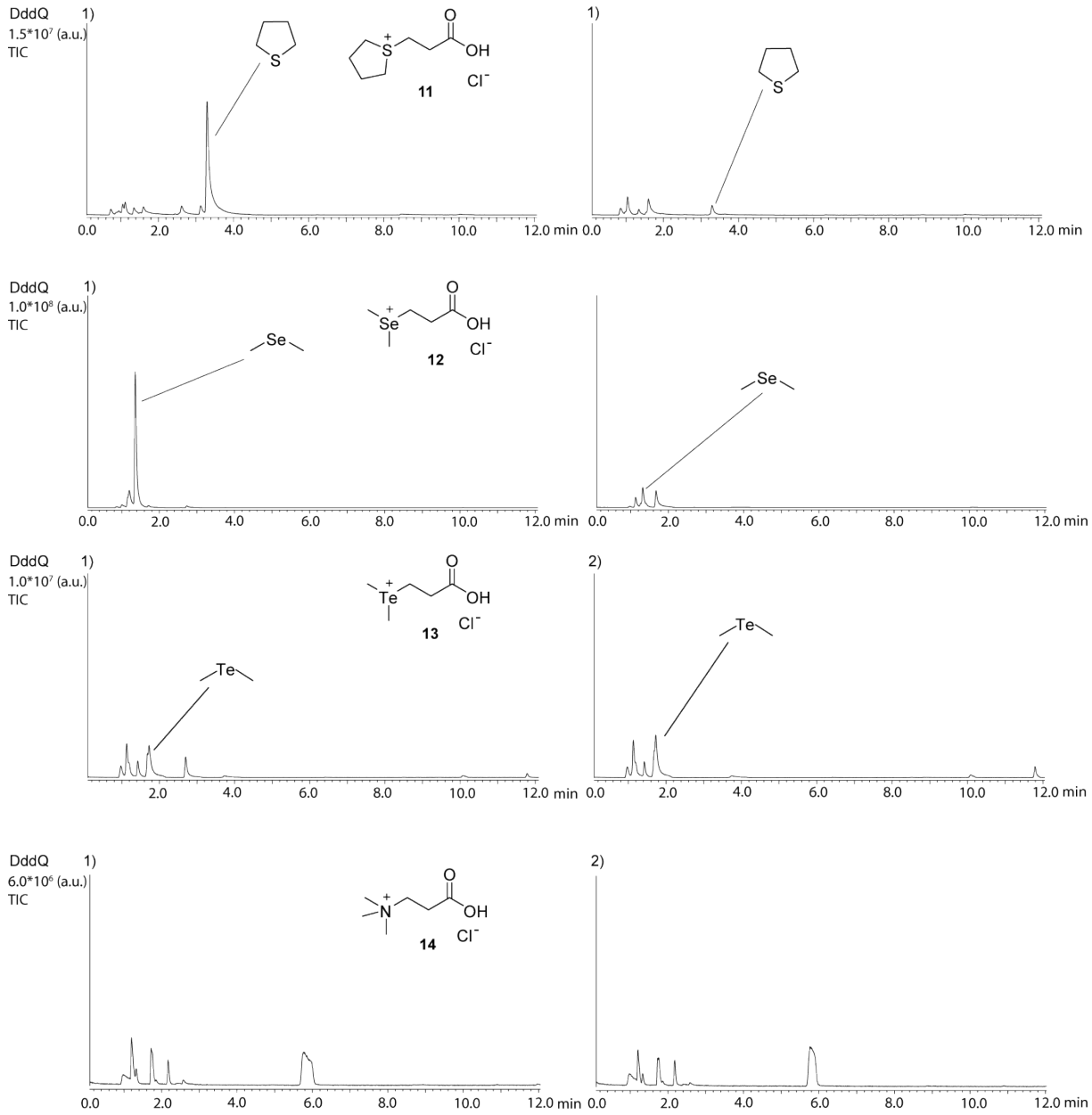

Figure S12 Chromatograms of SPME collected volatiles. 1) Incubations with shown substrate and DddQ. 2) Incubations of substrates without enzyme. MS identified volatiles are labelled with corresponding structures.

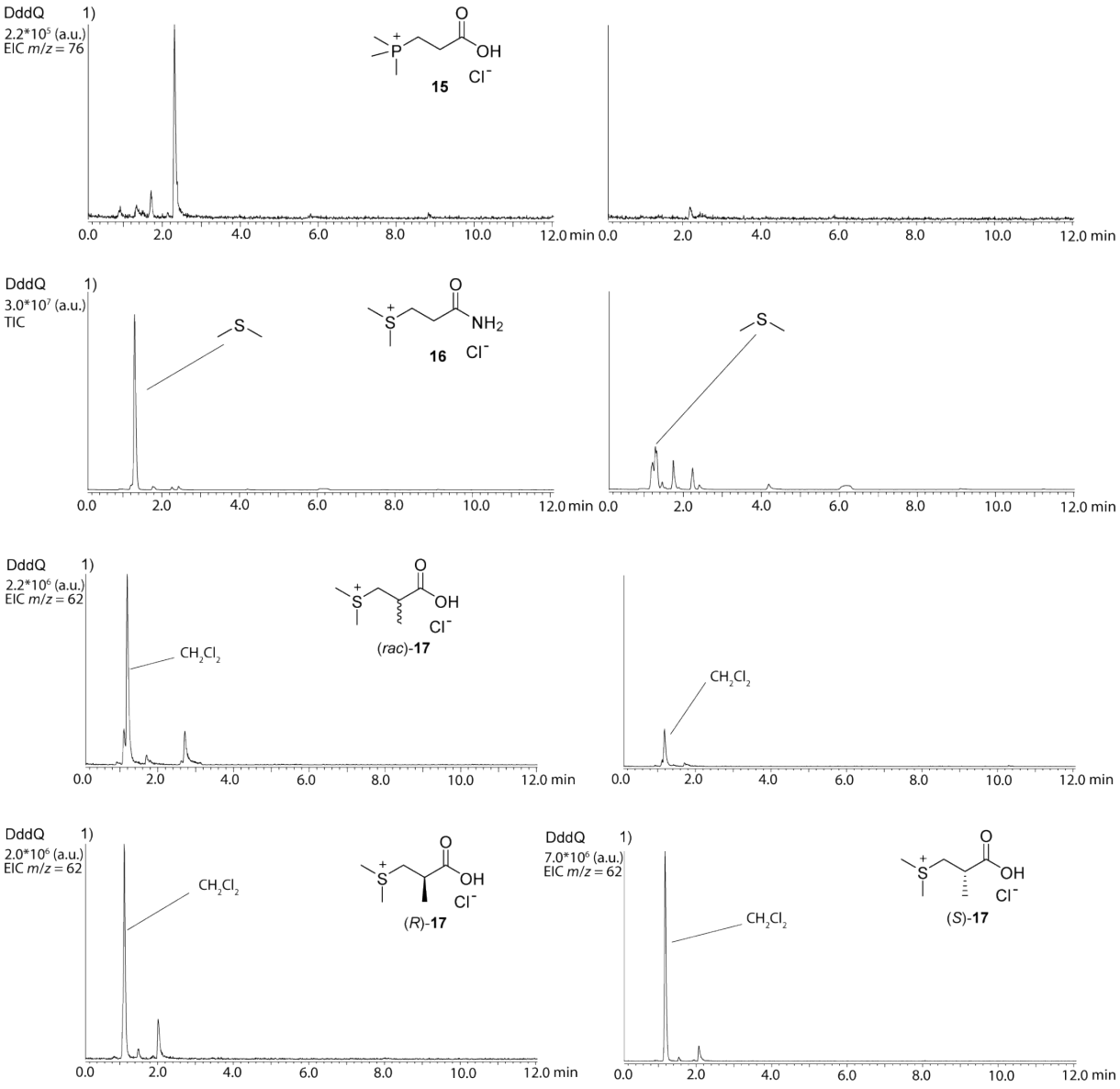

Figure S13 Chromatograms of SPME collected volatiles. 1) Incubations with shown substrate and DddQ. 2) Incubations of substrates without enzyme. MS identified volatiles are labelled with corresponding structures.

Assays for determination of kinetic parameters

A freshly prepared stock solution of the tested substrate was made immediately before the assay by solving it in suitable kinetic assay buffer (For DddW and DddQ: 50 mM HEPES, 50 mM NaCl, pH 8; For DddP: 20 mM MES, 50 mM NaCl, pH 6; final substrate concentration 0.8 M), adjusting the solution carefully to pH 6 using $NaHCO_3$ solution (0.8 M in the same buffer) and diluting it finally to 0.4 M. Assays were carried out by mixing the enzyme (0.9 µM) and the substrate (different concentrations, see Figs. S20-S45) in kinetic assay buffer at room temperature in a UV cuvette (2 mL or 200 µL reaction volume) and measuring the product absorption at a distinct wavelength (see Table S1) over 5-9 min. v_0 was determined from linear regression of the recorded plot in the Cary WinUV kinetics application (Agilent). The used wavelength for absorption measurements was chosen higher than λ_{max} (Figs. S14-19) to prevent exceeding the measurement range of the UV-spectrometer at high substrate concentrations. Correlation factors to connect measured absorption with product concentrations ($F_{abs->[c]}$, Table S1) were determined for every product by measuring absorptions of different concentrations at the chosen wavelength in a range of 0.01 – 2 mM in the respective buffer. Absorptions were plotted against measured concentrations and the slope was determined via linear regression, giving $F_{abs->[c]}$.

Table S1 Chosen wavelengths for measurement of corresponding buffer/product pairs and correlation factors for quantification of released product.

product	buffer	λ [nm]	$F_{abs->[c]}$
acrylic acid	MES	245	8.67±0.12
methacrylic acid	MES	245	5.27±0.05
acrylamide	MES	247	3.68±0.04
acrylic acid	HEPES	229	2.37±0.04
methacrylic acid	HEPES	255	13.59±0.19
acrylamide	HEPES	246	3.27±0.03

The measured v_0 values were plotted against the respective substrate concentrations and the Hill function (eq S1) was fitted to the data (Figs. S20-S45) using OriginPro 8G (OriginLab Corporation, Northampton, MA, USA), defining n = 1 to give the Michaelis-Menten equation.

$$v_0 = v_{max}\frac{([S]^n)}{K^n + [S]^n}$$

(S1)

v_0 = initial velocity, v_{max} = maximal velocity at enzyme saturation, [*S*] = substrate concentration, $K = K_m$ = Michaelis constant, n = Hill coefficient.

DddP showed substrate inhibition at higher substrate concentrations that cannot be described by the standard Hill equation. Since DddP is an active homodimer displaying two active sites, in the case of observed substrate inhibition a semiempirical modified Hill equation designed to describe allosteric inhibition was implemented in the Origin software and used to fit the obtained data:[4, 5]

$$v_0 = \frac{v_{max} + v_i\left(\frac{[S]^x}{K_i{}^x}\right)}{1 + \left(\frac{K^n}{[S]^n}\right) + \left(\frac{[S]^x}{K_i{}^x}\right)}$$

(S2)

v_0 = initial velocity, v_{max} = maximal velocity at enzyme saturation, v_i = velocity at maximal inhibition, [*S*] = substrate concentration, $K = K_m$, K_i = half maximal inhibitory substrate concentration, n = Hill coefficient, x = second Hill coefficient for binding of substrate in inhibitory mode. For a converging fit n and x need to be fixed. n was defined as 1 and the value for x was determined empirically. For discussion in the main text, eq (S1) was fitted to values in the Michaelis-Menten region of the data. Values derived from fits of equation (S2) to the whole range are shown in Table S2.

Table S2 Kinetic parameters for DddP derived from fitting eq (S2) to the obtained data. Values for x as well as n were fixed and determined empirically. Shown deviations are derived from standard error of the individual fits.

substrate	k_{cat} [s^{-1}]	k_i [s^{-1}]	K_m [mM]	K_i [mM]	x	n
DMSP	4.00±0.23	0.00±2.21	37.3±5.0	153±17	10	1
EMSP	2.12±0.12	1.05±0.04	34.7±4.1	94.5±6.7	6	1
MPSP	2.01±0.10	0.79±0.02	38.0±3.3	74.3±2.4	6	1
DESP	1.83±0.09	0.67±0.08	18.7±2.1	92.0±5.6	6	1
TMSP	–	–	–	–	–	–
DMSeP	4.20±0.37	0.49±0.07	20.9±3.7	48.0±1.5	8	1
Me-DMSP	1.10±0.04	0.39±0.06	7.0±0.9	108±7	6	1
(*R*)-Me-DMSP	1.61±0.07	0.92±1.06	22.4±2.4	164±197	3	1
(*S*)-Me-DMSP	1.50±0.06	0.56±0.10	8.1±1.0	101±11	4	1

UV-spectra of detected products in respective buffers

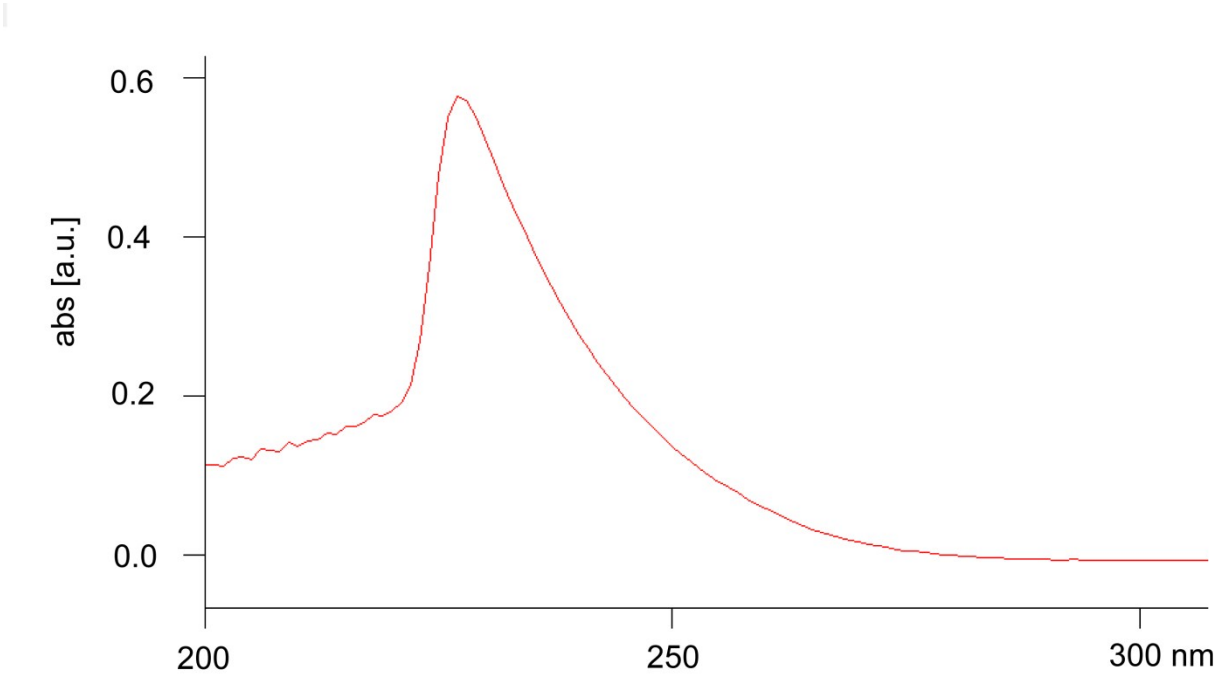

Figure 14 UV spectrum of acrylic acid in 50 mM HEPES buffer at pH 8.

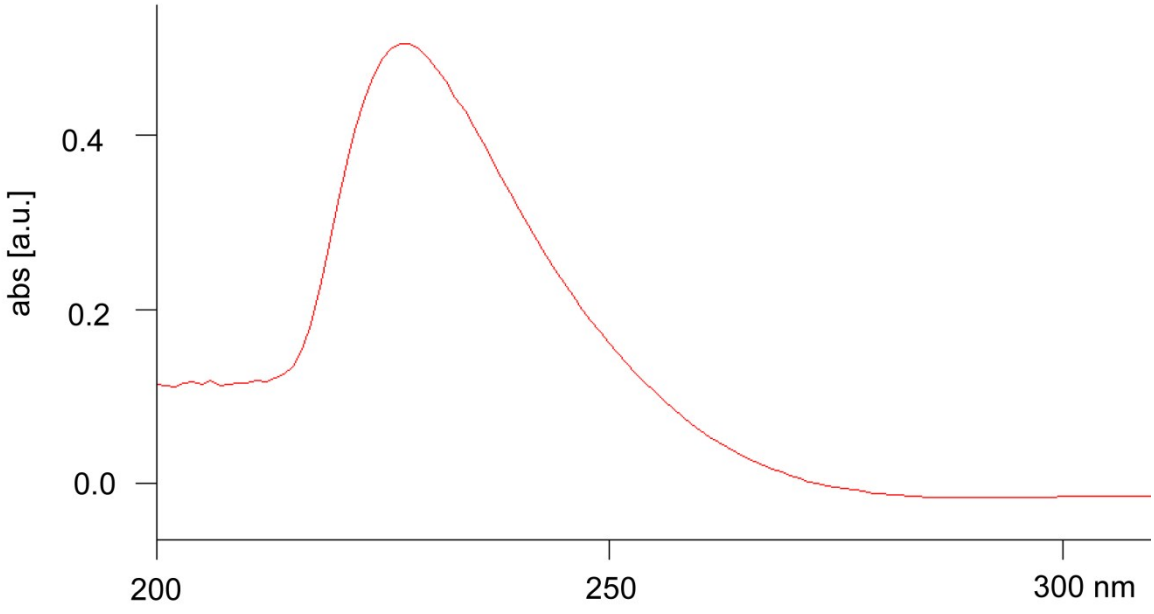

Figure S15 UV spectrum of acrylic acid in 20 mM MES buffer at pH 6.

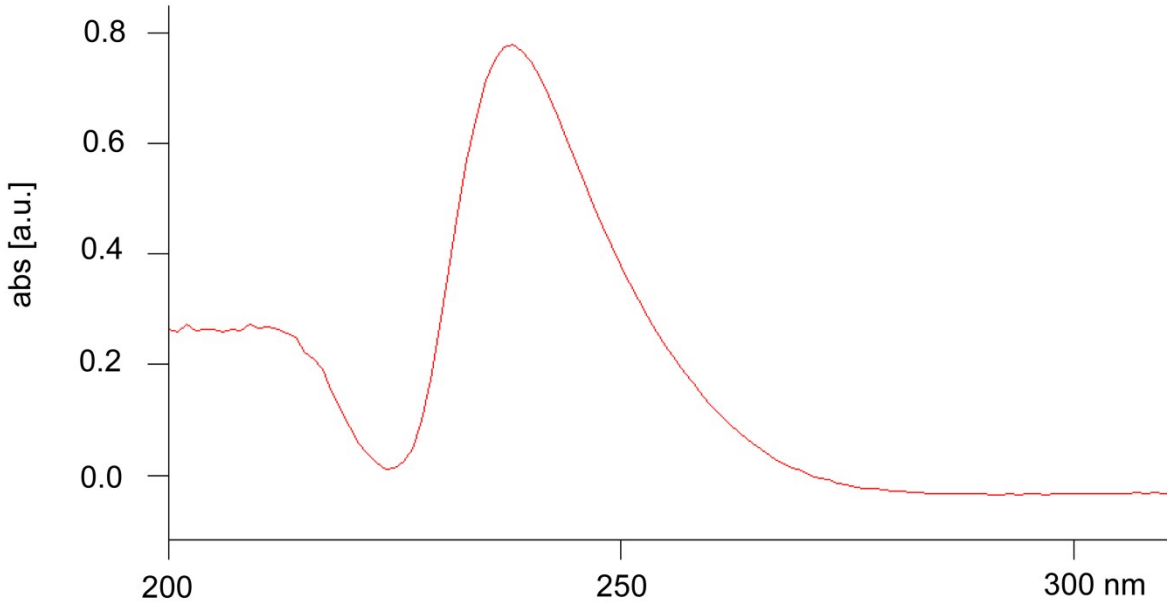

Figure S16 UV spectrum of methacrylic acid in 50 mM HEPES buffer at pH 8.

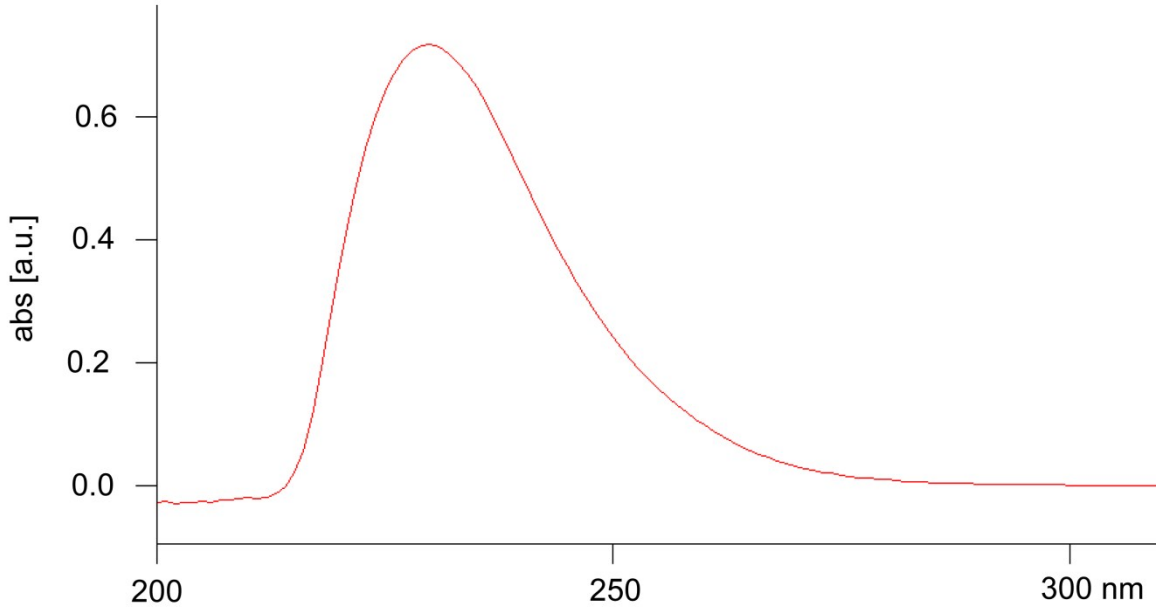

Figure S17 UV spectrum of methacrylic acid in 20 mM MES buffer at pH 6.

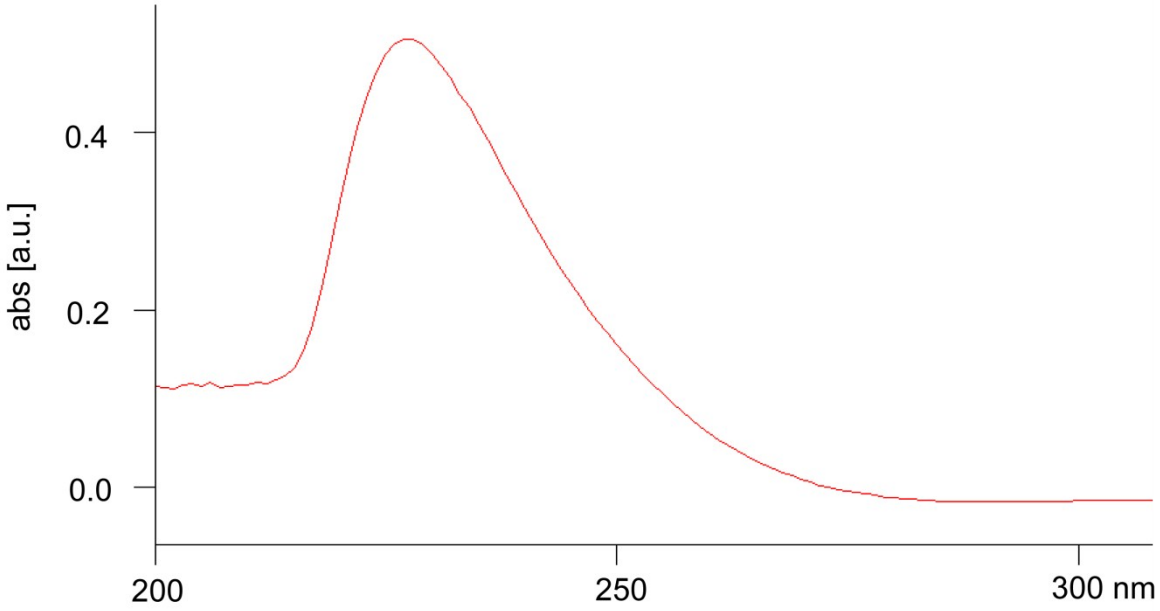

Figure S18 UV-spectrum of acrylamide in 50 mM HEPES buffer at pH 8.

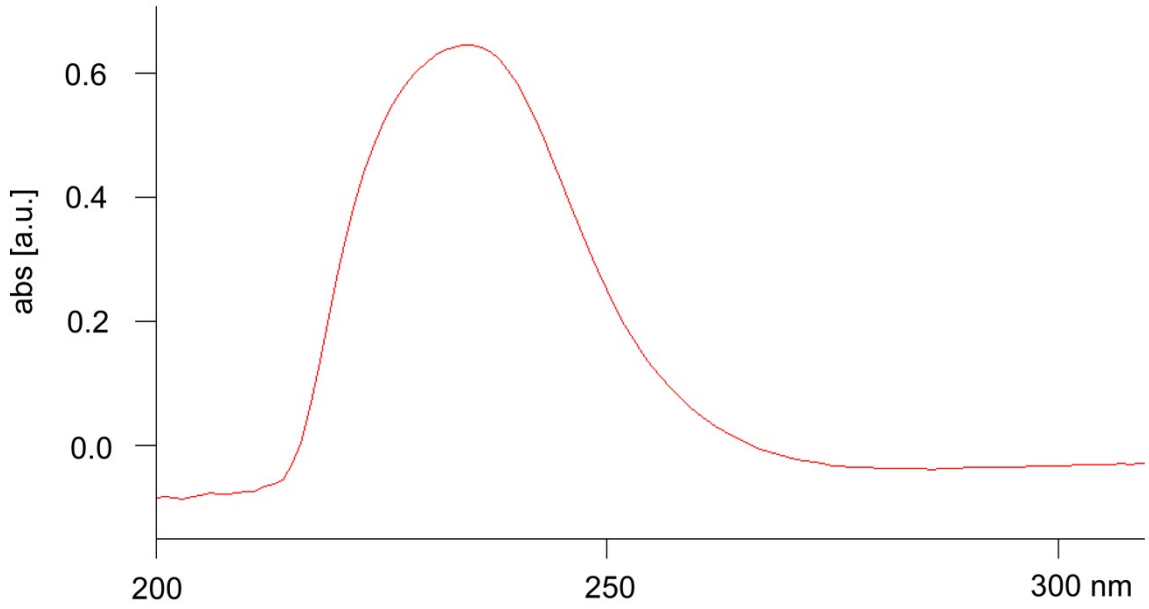

Figure S19 UV-spectrum of acrylamide in 20 mM MES buffer at pH 6.

Kinetic plots

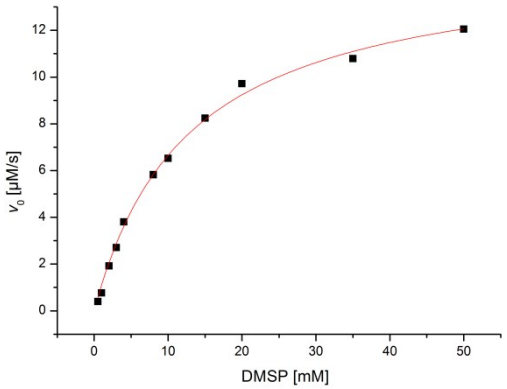

Figure S20 Kinetic data of DMSP conversion by DddW with fit of eq (S1).

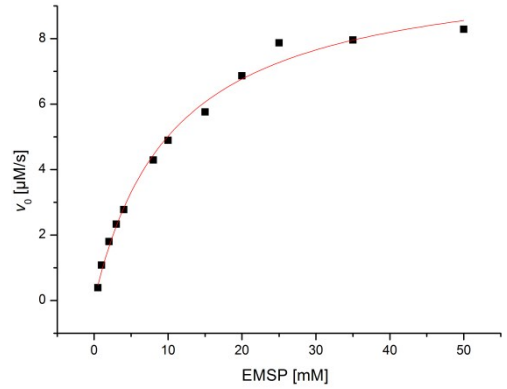

Figure S21 Kinetic data EMSP conversion by DddW with fit of eq (S1).

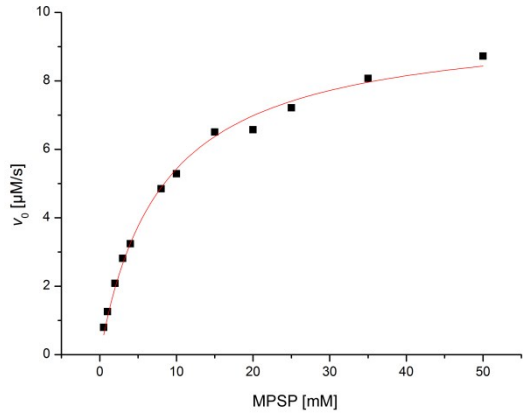

Figure S22 Kinetic data of MPSP conversion by DddW with fit of eq (S1).

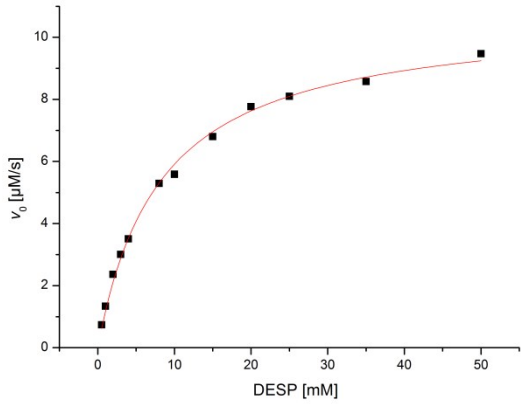

Figure S23 Kinetic data of DESP conversion by DddW with fit of eq (S1).

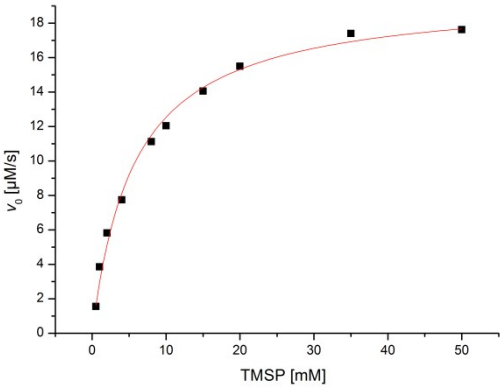

Figure S24 Kinetic data of TMSP conversion by DddW with fit of eq (S1).

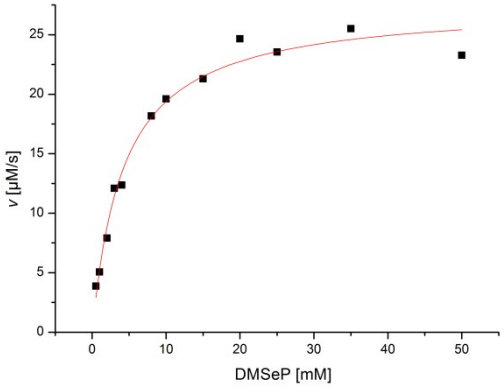

Figure S25 Kinetic data of DMSeP conversion by DddW with fit of eq (S1).

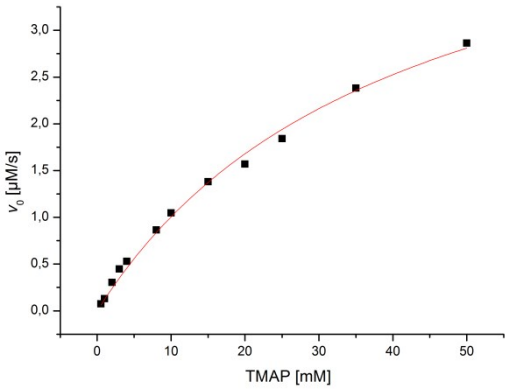

Figure S26 Kinetic data of TMAP conversion by DddW with fit of eq (S1).

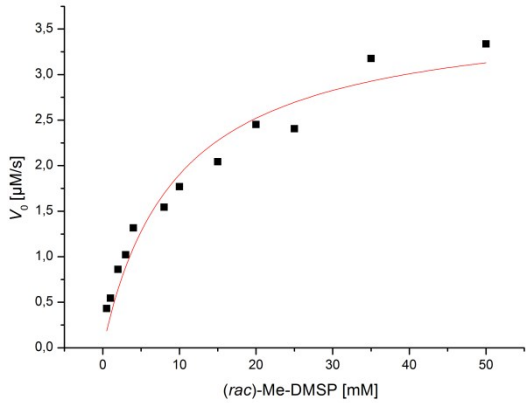

Figure S27 Kinetic data of (*rac*)-Me-DMSP conversion by DddW with fit of eq (S1).

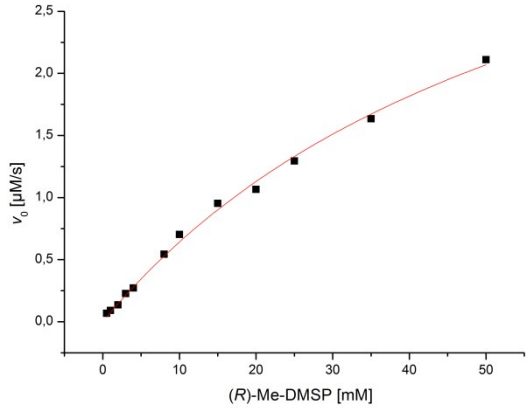

Figure S28 Kinetic data of (*R*)-Me-DMSP conversion by DddW with fit of eq (S1).

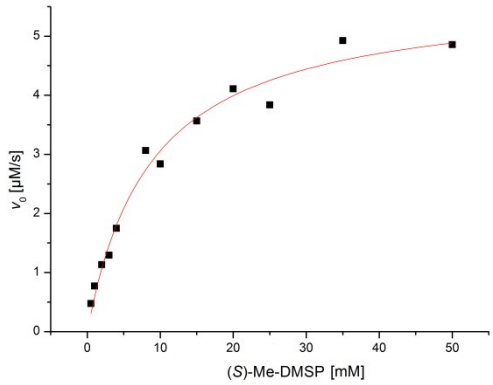

Figure S29 Kinetic data of (*S*)-Me-DMSP conversion by DddW with fit of eq (S1).

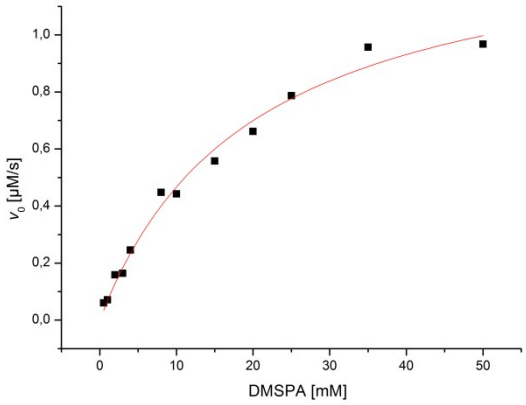

Figure S30 Kinetic data of DMSPA conversion by DddW with fit of eq (S1).

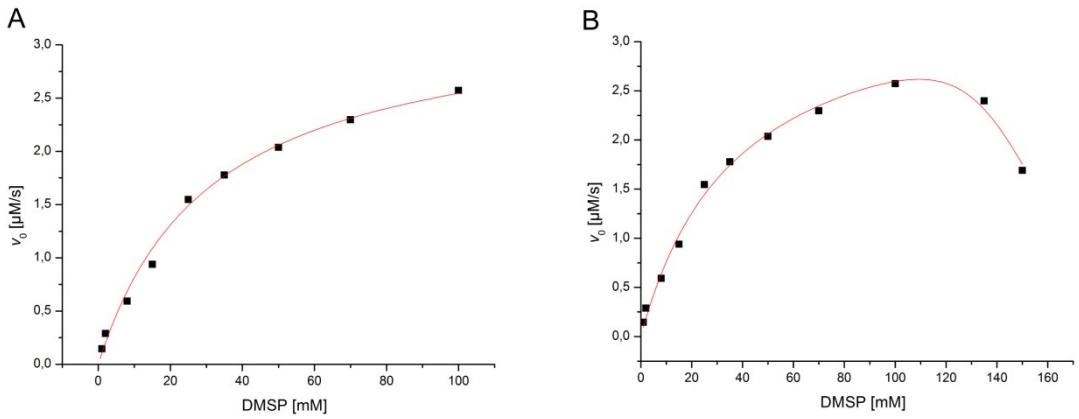

Figure S31 Kinetic data of DMSP conversion by DddP (A) with fit of eq (S1) and (B) with fit of eq (S2).

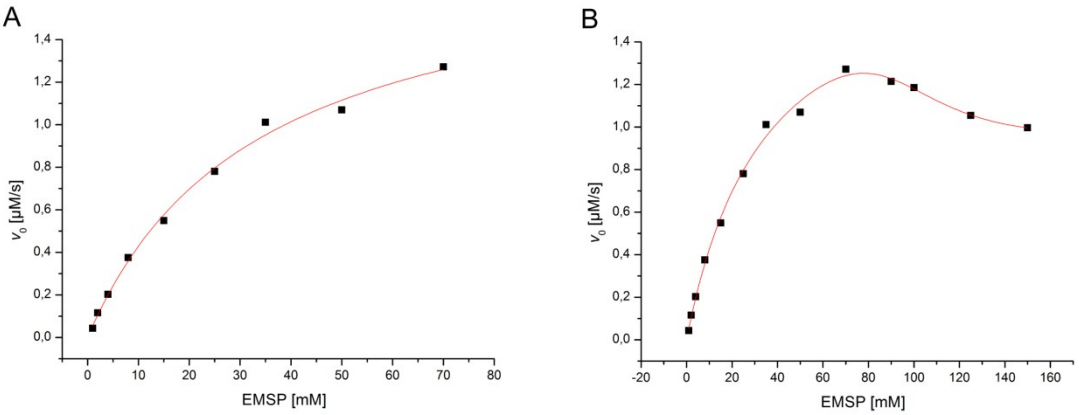

Figure S32 Kinetic data of EMSP conversion by DddP (A) with fit of eq (S1) and (B) with fit of eq (S2).

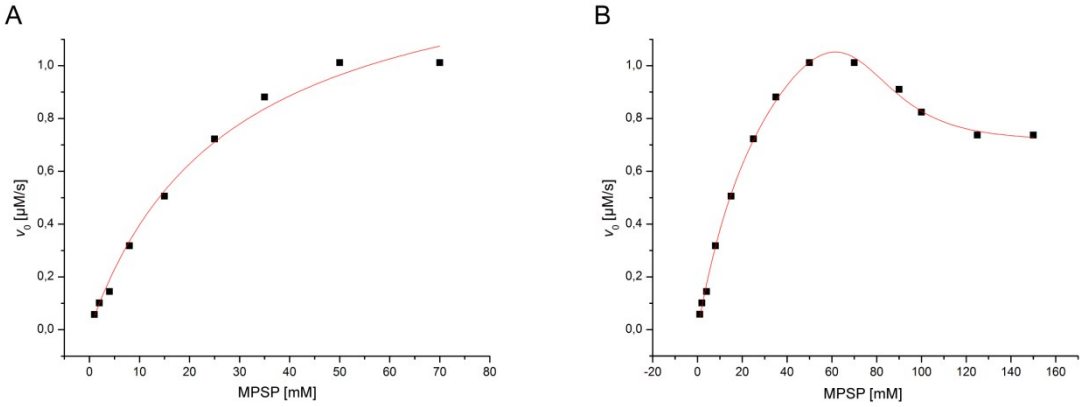

Figure S33 Kinetic data of MPSP conversion by DddP (A) with fit of eq (S1) and (B) with fit of eq (S2).

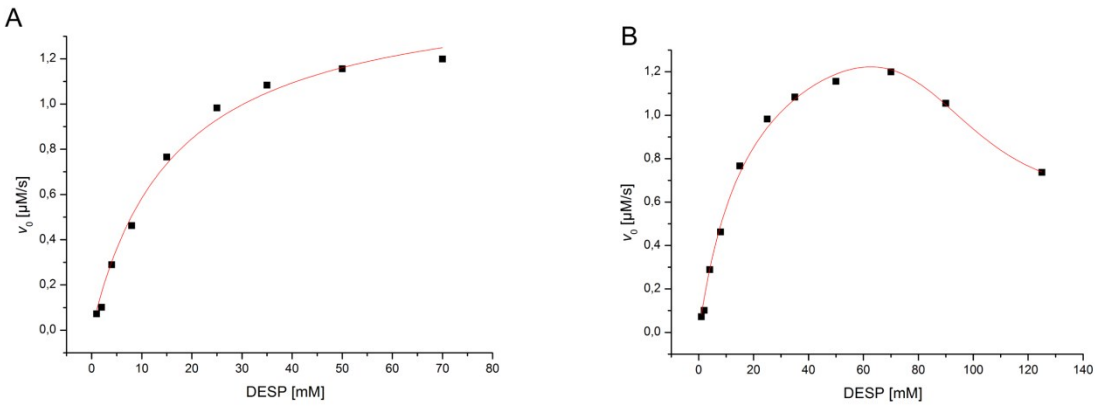

Figure S34 Kinetic data of DESP conversion by DddP (A) with fit of eq (S1) and (B) with fit of eq (S2).

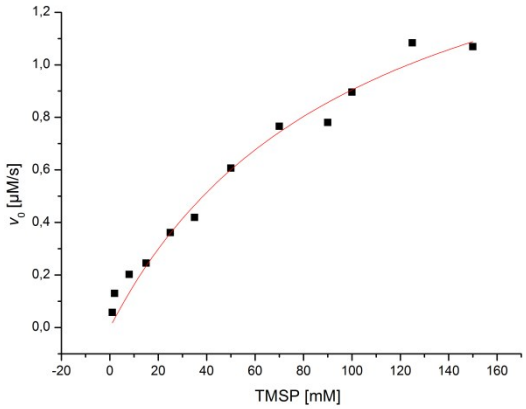

Figure S35 Kinetic data of TMSP conversion by DddP with fit of eq (S1).

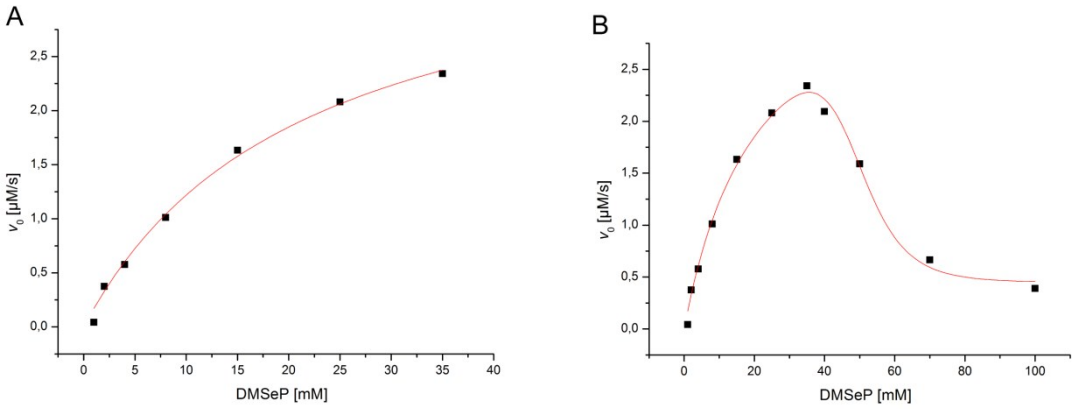

Figure S36 Kinetic data of DMSeP conversion by DddP (A) with fit of eq (S1) and (B) with fit of eq (S2).

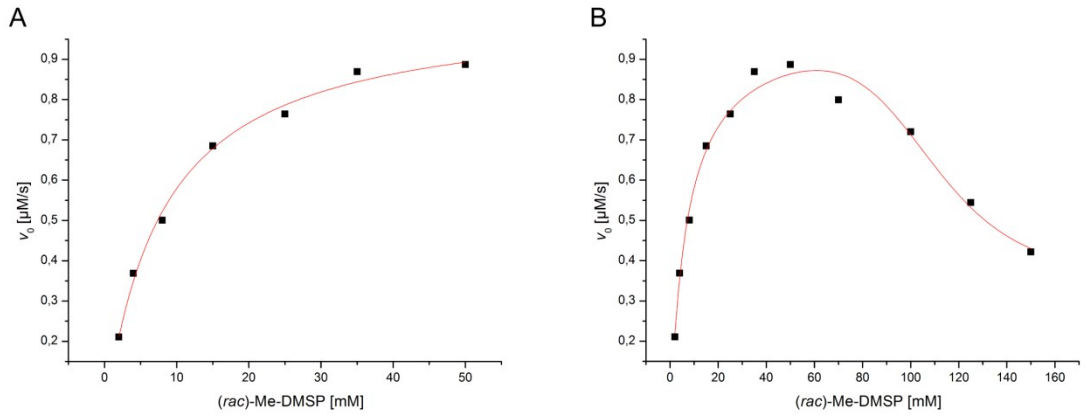

Figure S37 Kinetic data of (*rac*)-Me-DMSP conversion by DddP (A) with fit of eq (S1) and (B) with fit of eq (S2).

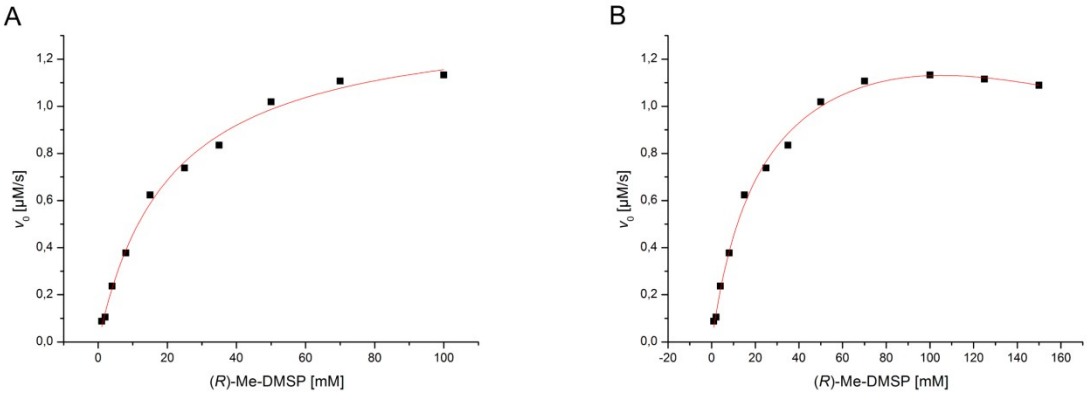

Figure S38 Kinetic data of (*R*)-Me-DMSP conversion by DddP (A) with fit of eq (S1) and (B) with fit of eq (S2).

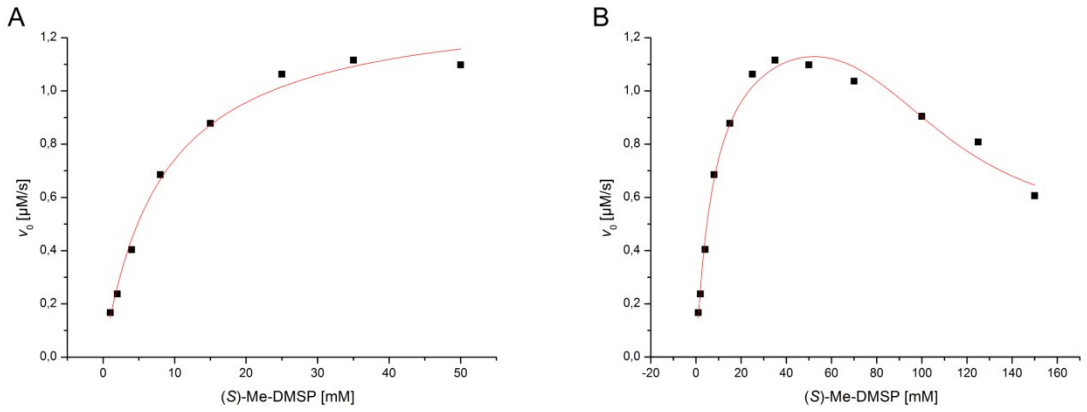

Figure S39 Kinetic data of (*S*)-Me-DMSP conversion by DddP (A) with fit of eq (S1) and (B) with fit of eq (S2).

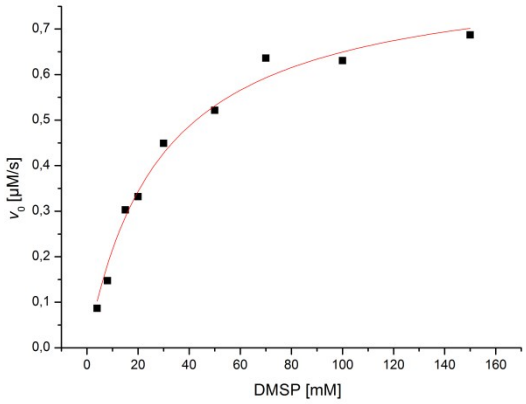

Figure S40 Kinetic data of DMSP conversion by DddQ with fit of eq (S1).

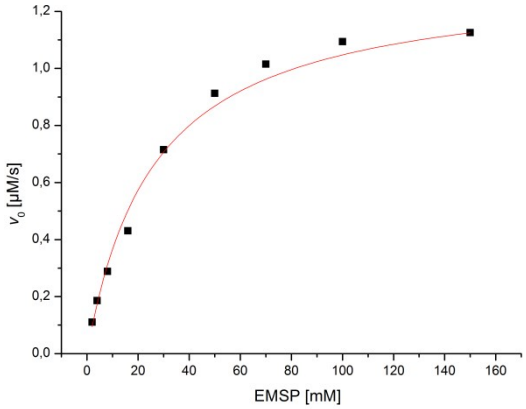

Figure S41 Kinetic data of EMSP conversion by DddQ with fit of eq (S1).

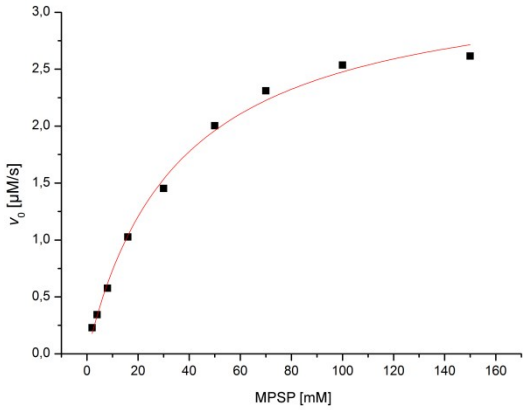

Figure S42 Kinetic data of MPSP conversion by DddQ with fit of eq (S1).

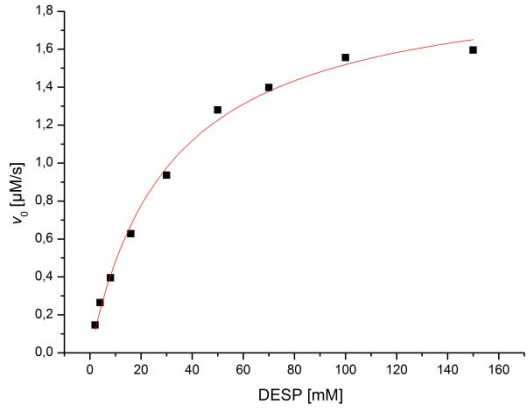

Figure S43 Kinetic data of DESP conversion by DddQ with fit of eq (S1).

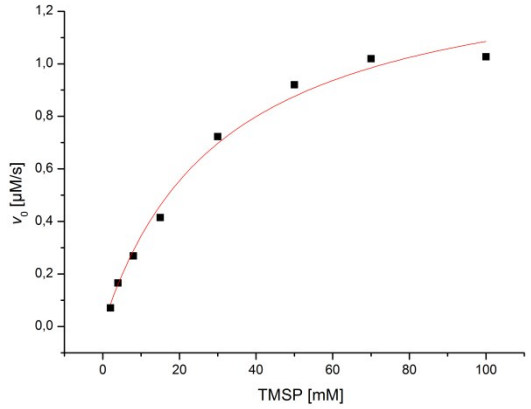

Figure S44 Kinetic data of TMSP conversion by DddQ with fit of eq (S1).

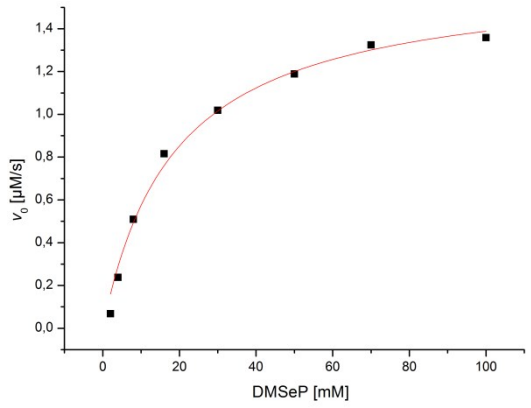

Figure S45 Kinetic data of DMSeP conversion by DddQ with fit of (S1).

Protein structures and CAVER analyses[6]

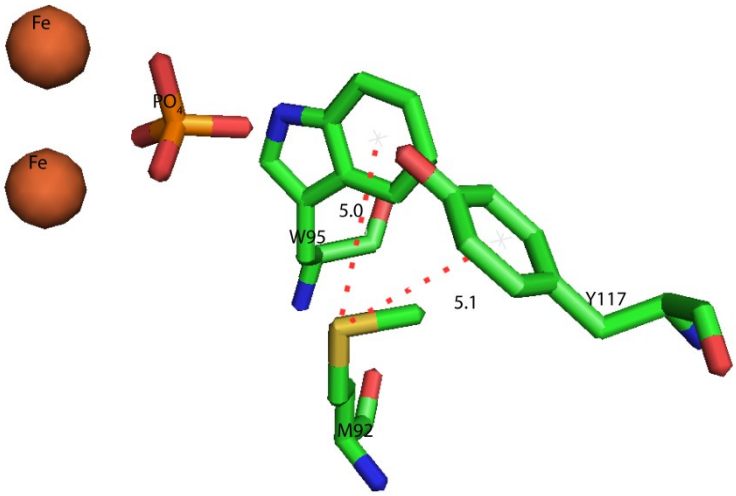

Figure S46 Residues W95, Y117 and M92 from the active site of DddP. Methionine-π interactions hold the two aromatic amino acids in the right position for a substrate molecule to coordinate. Distances are shown as dashed red lines in Å. Methionine-π interactions are a common structural motif in proteins.[7] The two irons and the bound phosphate from the active center are also displayed. Image was generated with Pymol. PDB code: 4RZZ.[8]

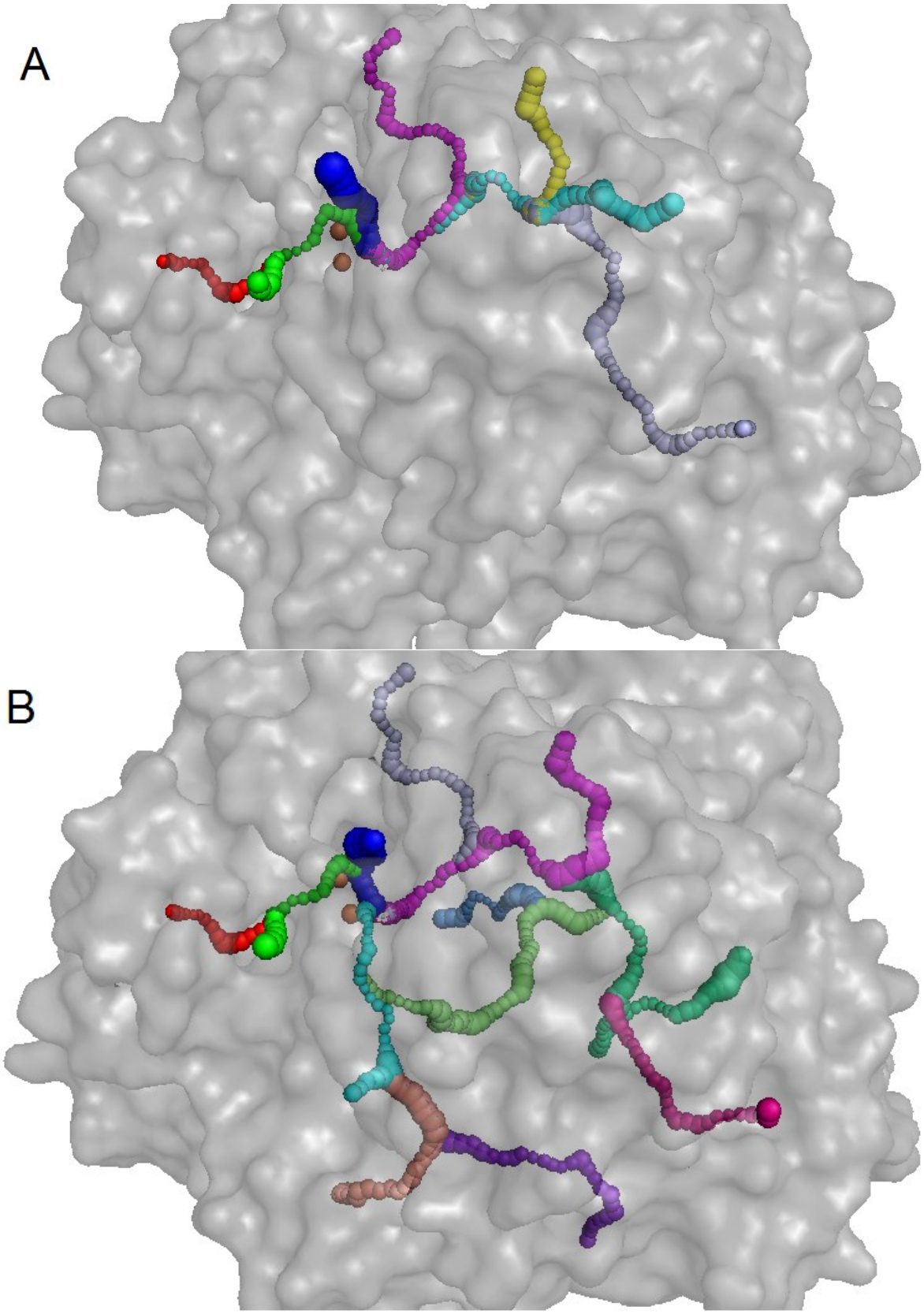

Figure S47 CAVER analysis of (A) MES bound DddP dimer, and (B) PO_4^{3-} bound DddP dimer. Different channels from the active site to the protein surface are shown as coloured spheres. The shortest and widest channel (blue) is found in both structures and harbours several water molecules (not shown for clear view), possibly serving as entrance point for the permanently charged substrates. The simulations show different courses of longer tunnels that could serve as channels for release of hydrophobic products. The two irons in one active center used as start for the simulation are shown as spheres (rust). Pictures were generated with PyMOL. PDB codes: 4RZY; 4RZZ.[8]

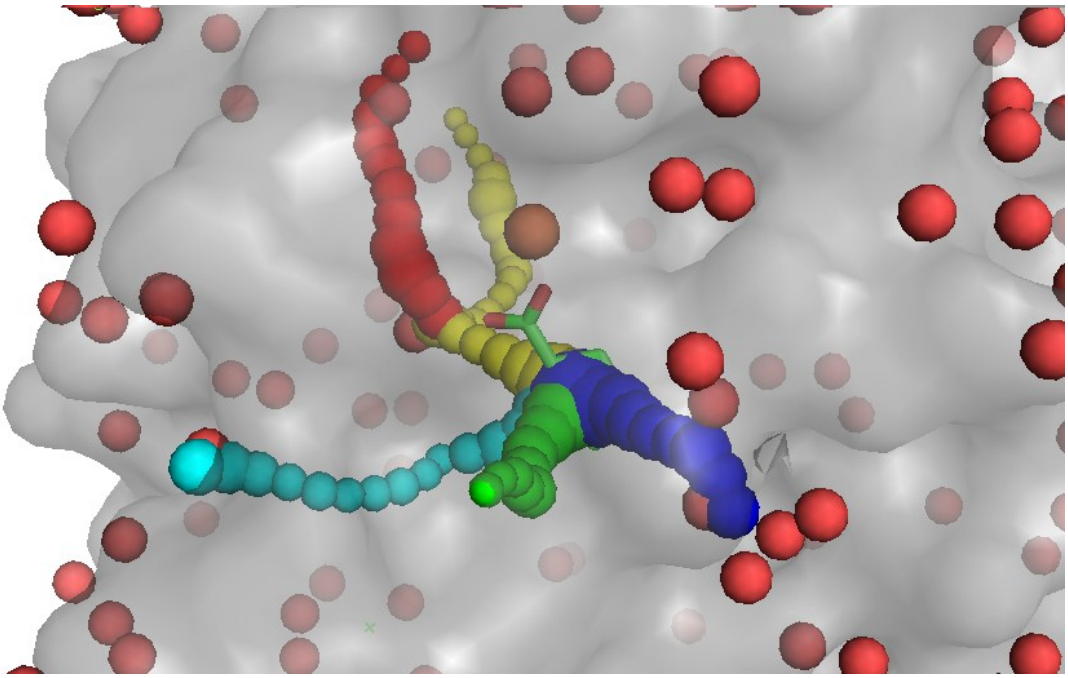

Figure S48 Caver analysis of DMSP bound DddQ crystal structure from *R. lacuscaerulensis*. The start of the simulation is the sulfur atom of DMSP. Water molecules are shown as red spheres. The two most probable channels (with respect to shortness and diameter) are shown in ultramarin and cyan. Both channels contain no water over most space, although five water molecules are located at the entrance of the blue channel, indicating hydrophilic character towards the surface. This is most likely the entrance point for the charged substrate molecule. The cyan and green channel show no water (only one water molecule is localised next to the opening of the cyan channel at the surface), being possible exits for the small, unpolar DMS or derivatives thereof. The red and yellow channels are likely not of importance for being much longer than the others and narrow at the endings. PDB code: 5JSP.[9] Image was generated with Pymol.

NMR Spectra

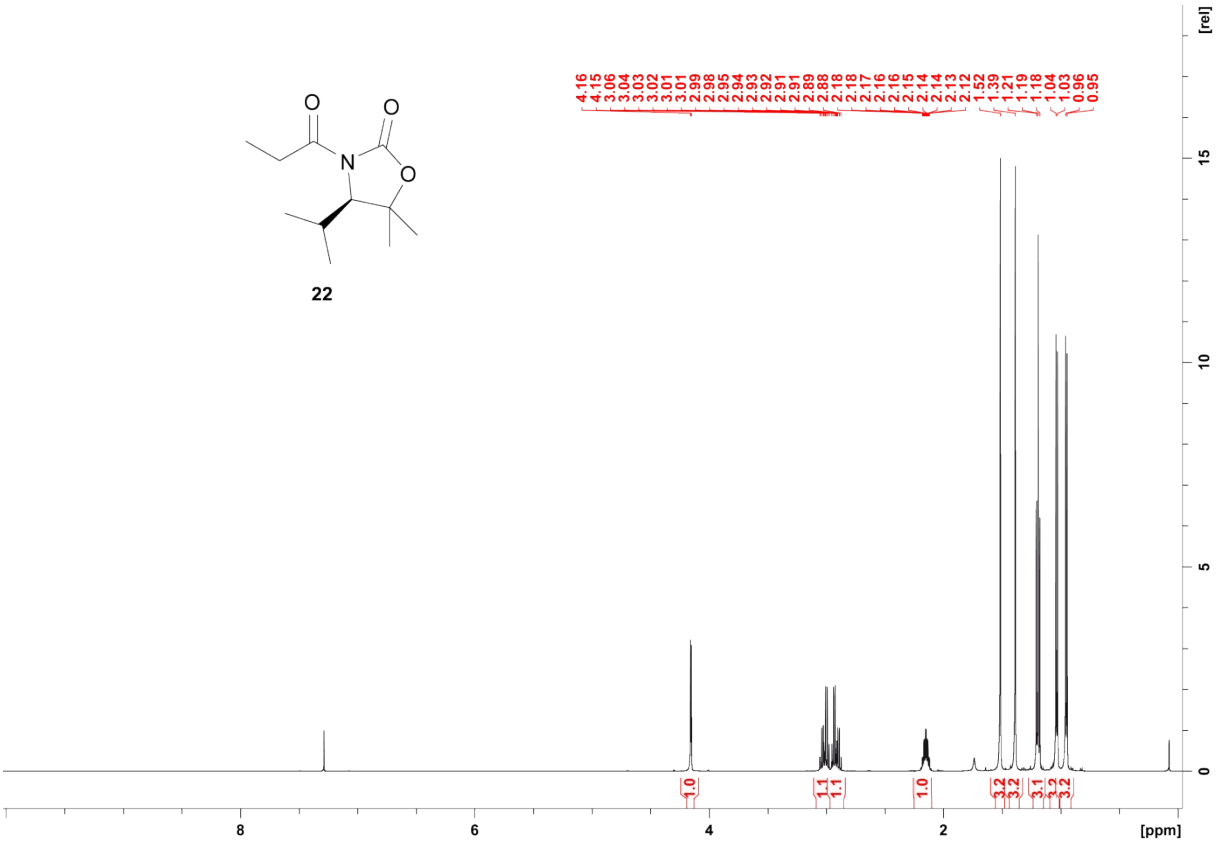

Figure S49 ^{1}H-NMR spectrum of **22** (500 MHz, $CDCl_3$).

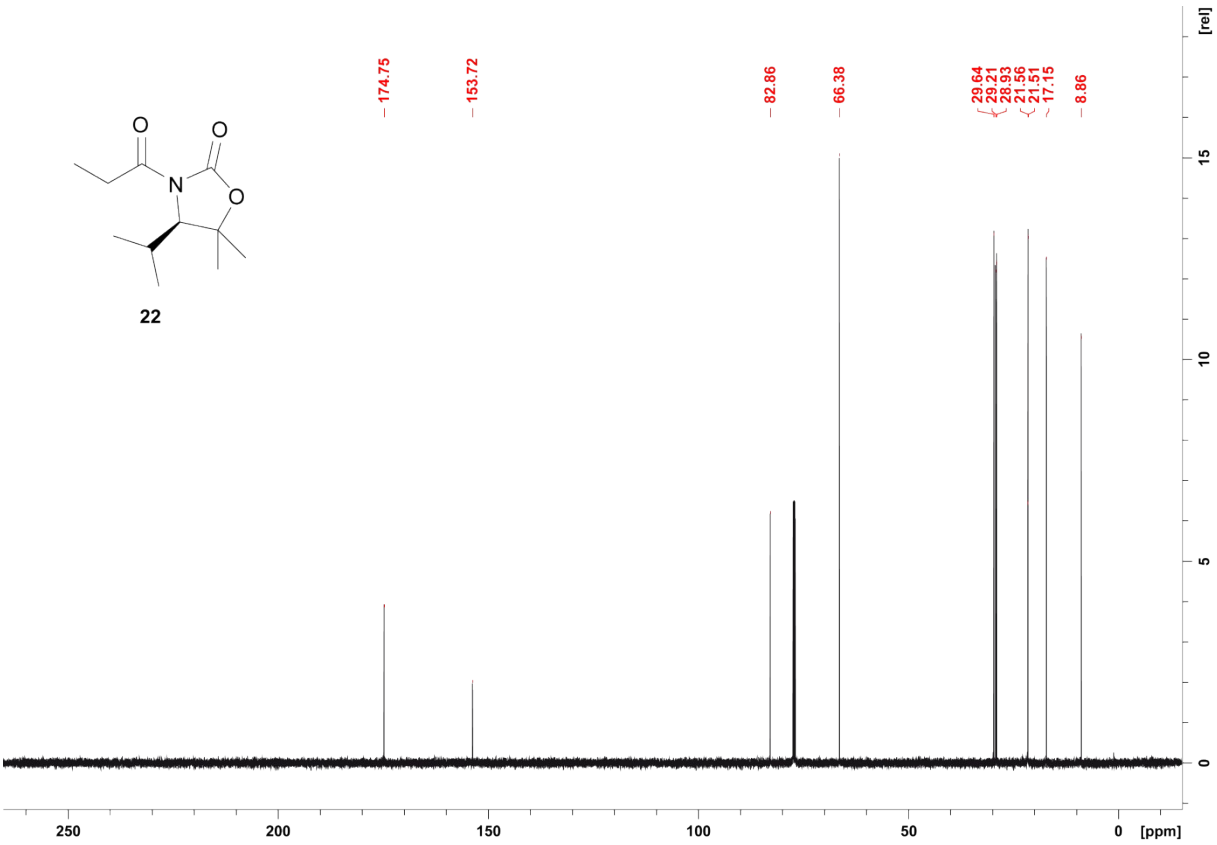

Figure S50 ^{13}C-NMR spectrum of **22** (125 MHz, $CDCl_3$).

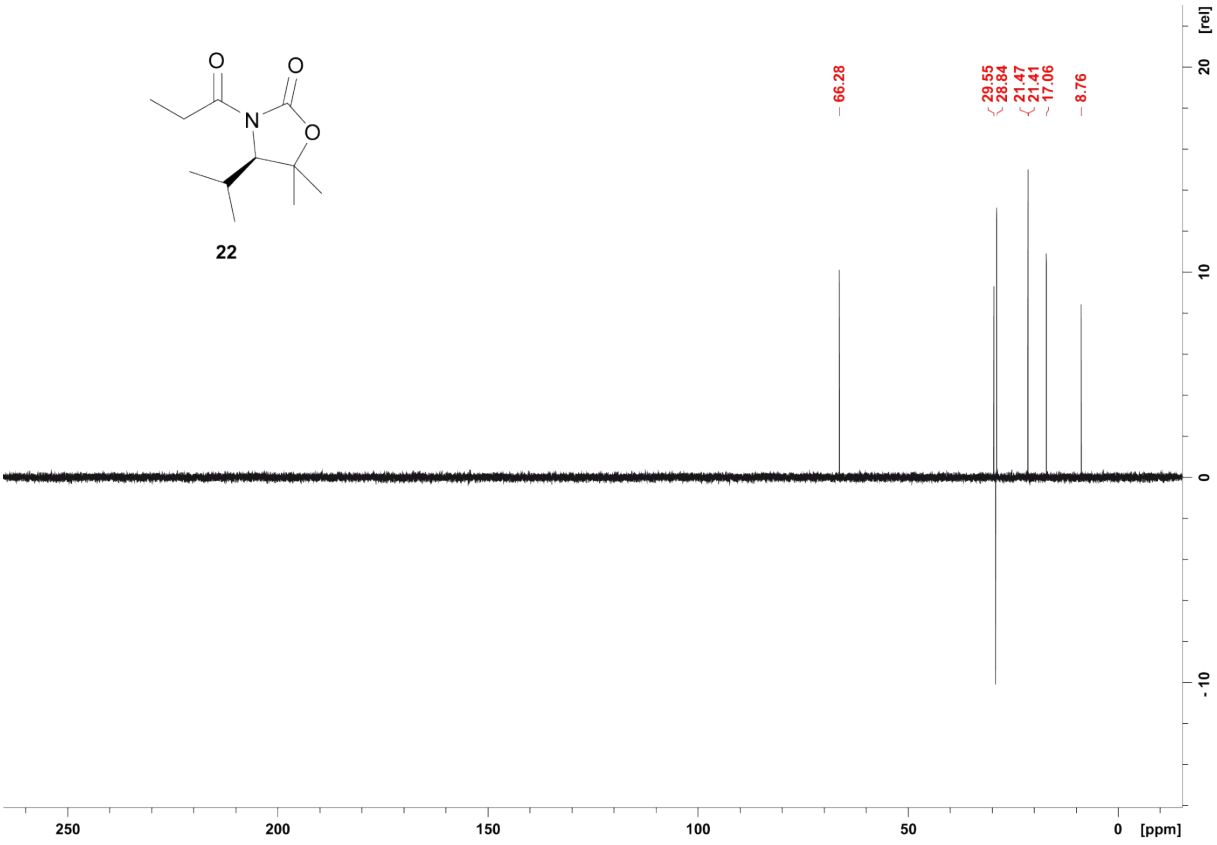

Figure S51 ^{13}C-DEPT-NMR spectrum of **22** (125 MHz, $CDCl_3$).

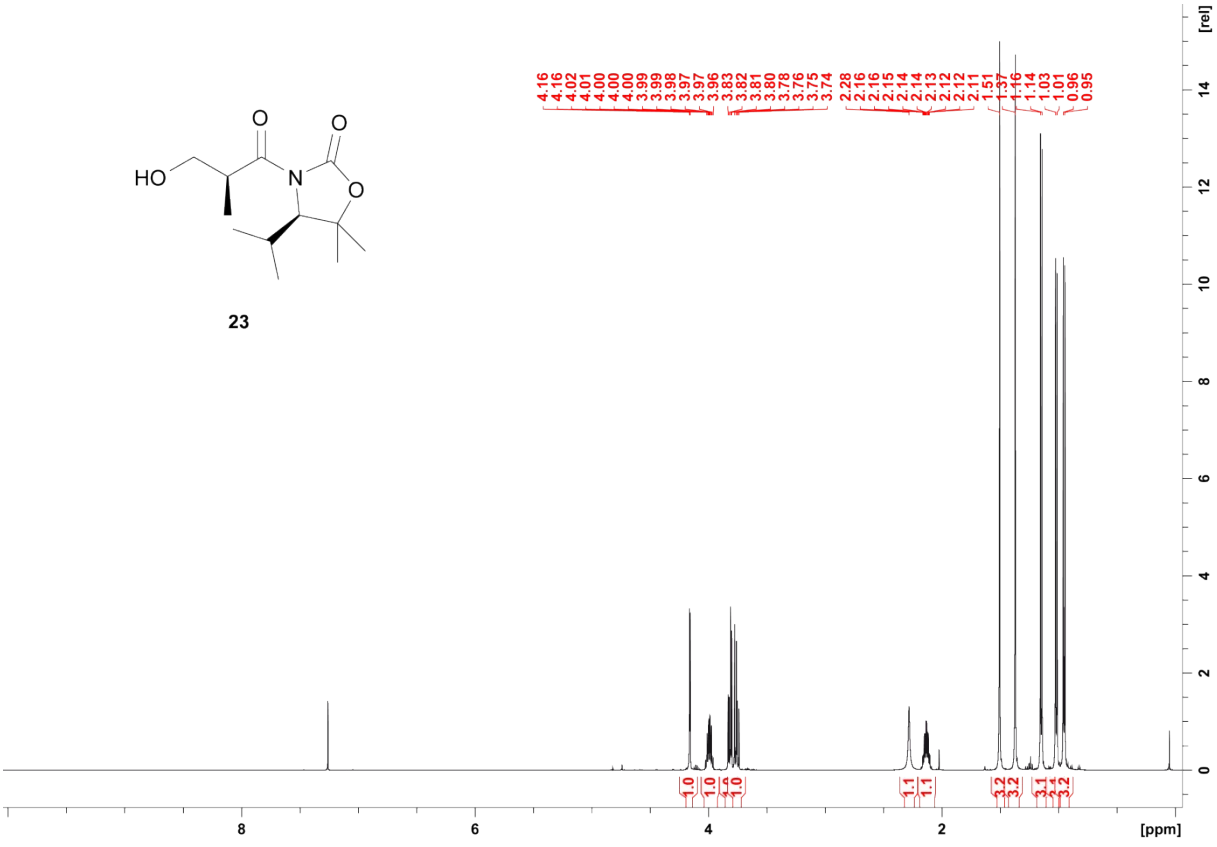

Figure S52 ^{1}H-NMR spectrum of **23** (500 MHz, $CDCl_3$).

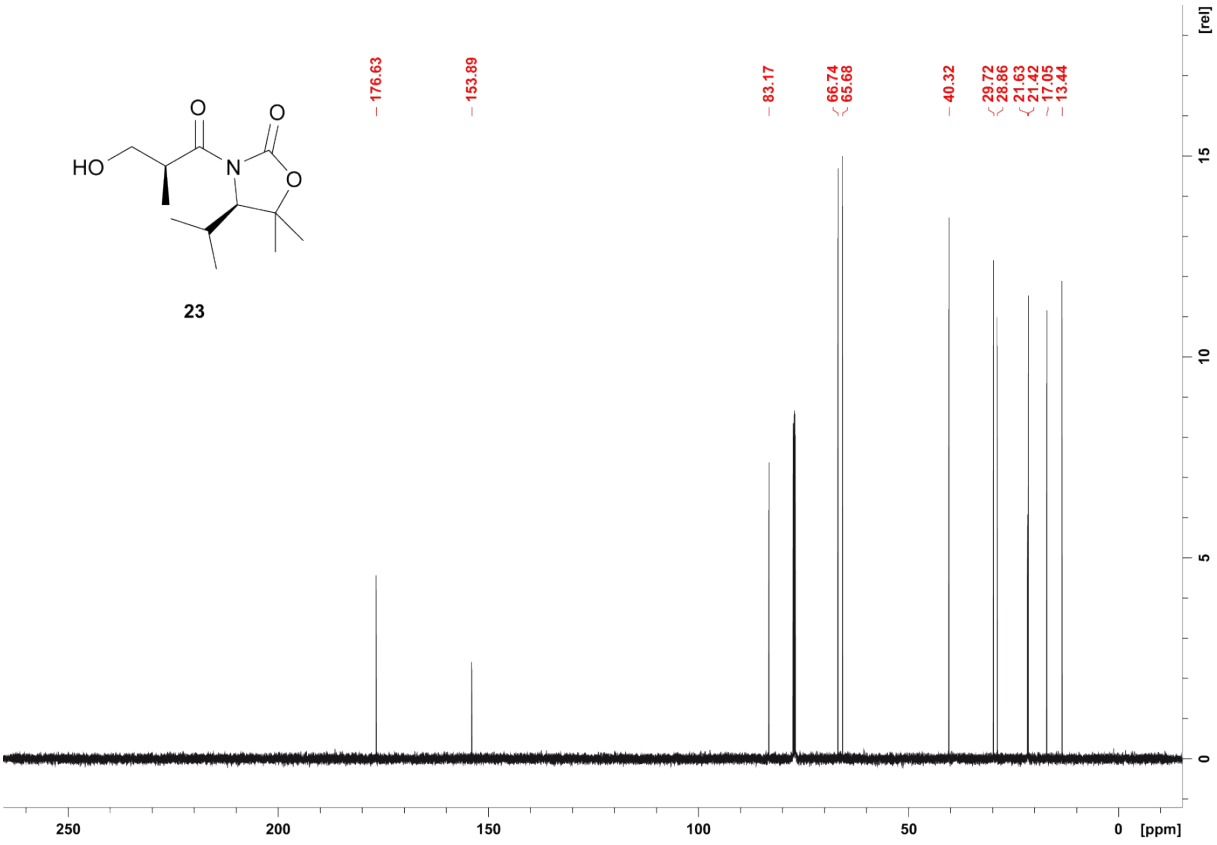

Figure S53 ^{13}C-NMR spectrum of **23** (125 MHz, $CDCl_3$).

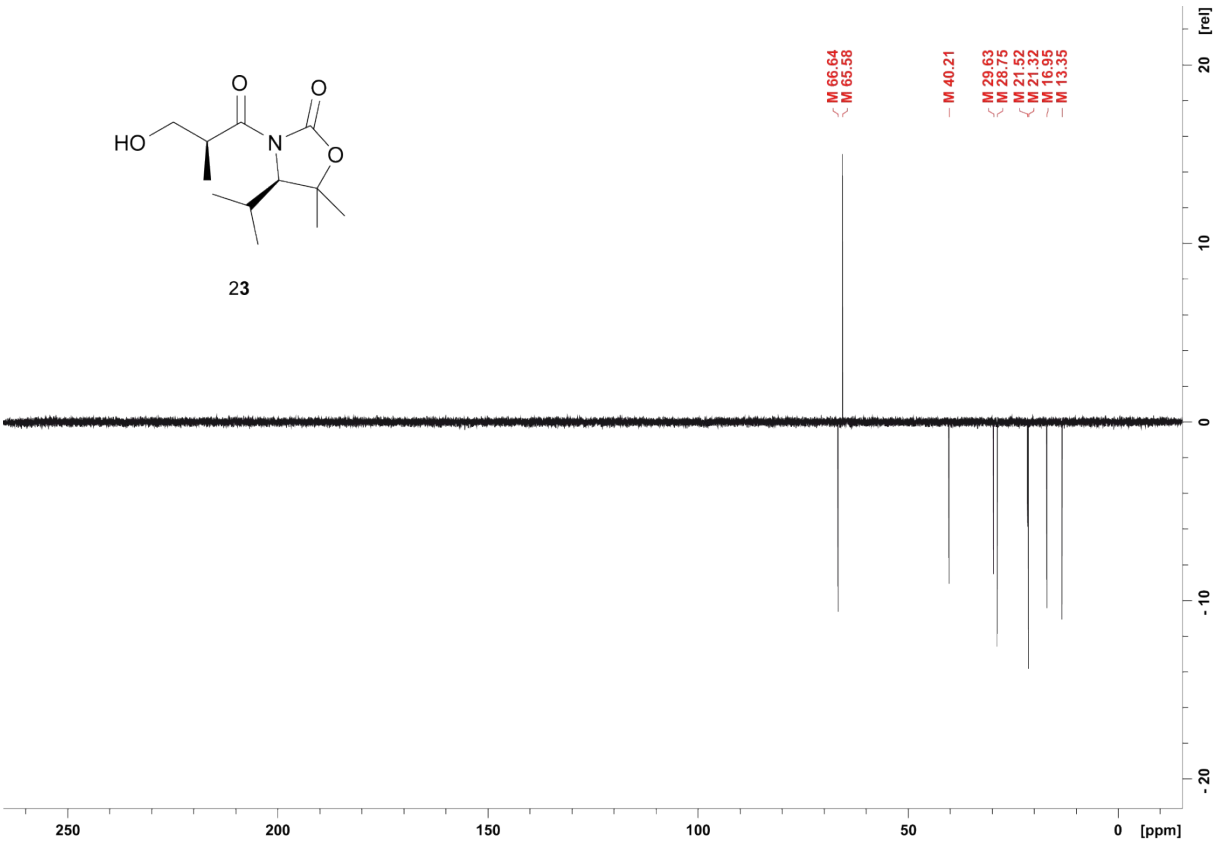

Figure S54 ^{13}C-DEPT-NMR spectrum of **23** (125 MHz, $CDCl_3$).

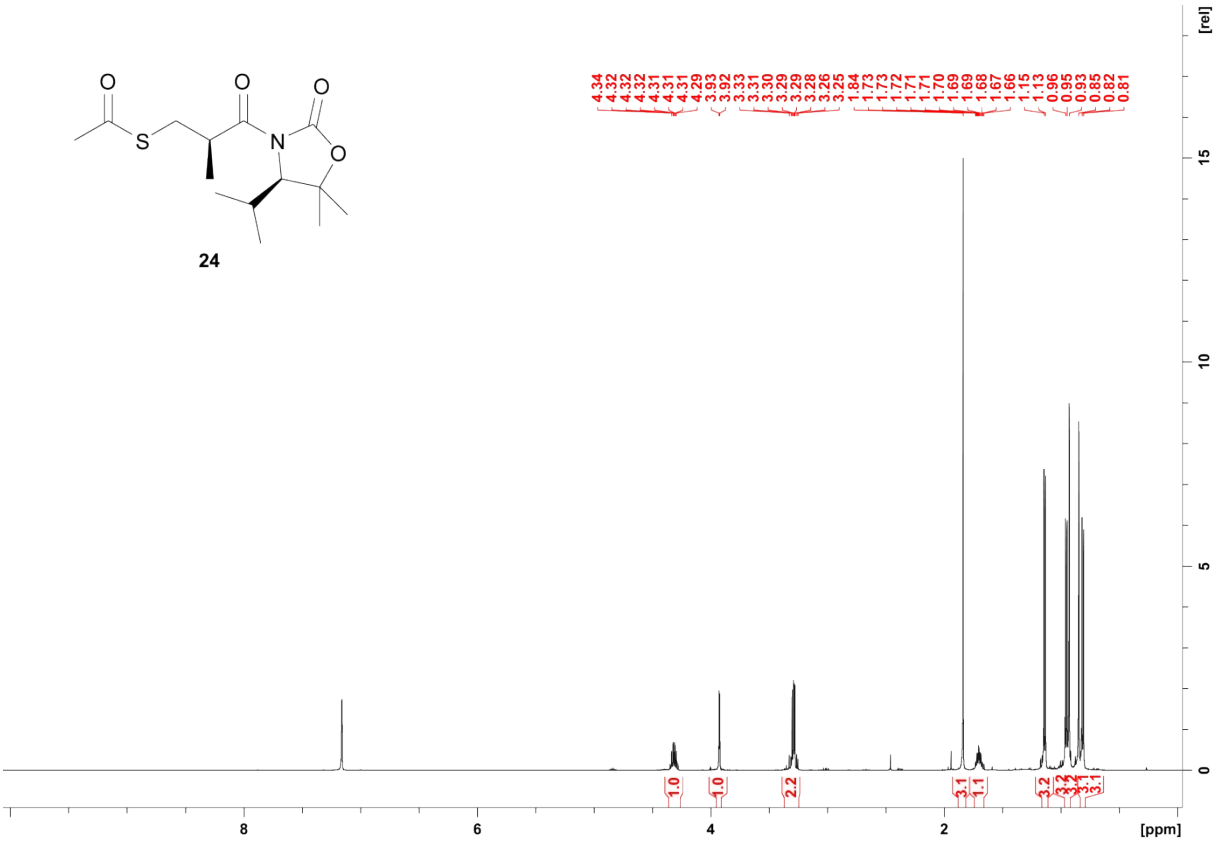

Figure S55 ^{1}H-NMR spectrum of **24** (500 MHz, C_6D_6).

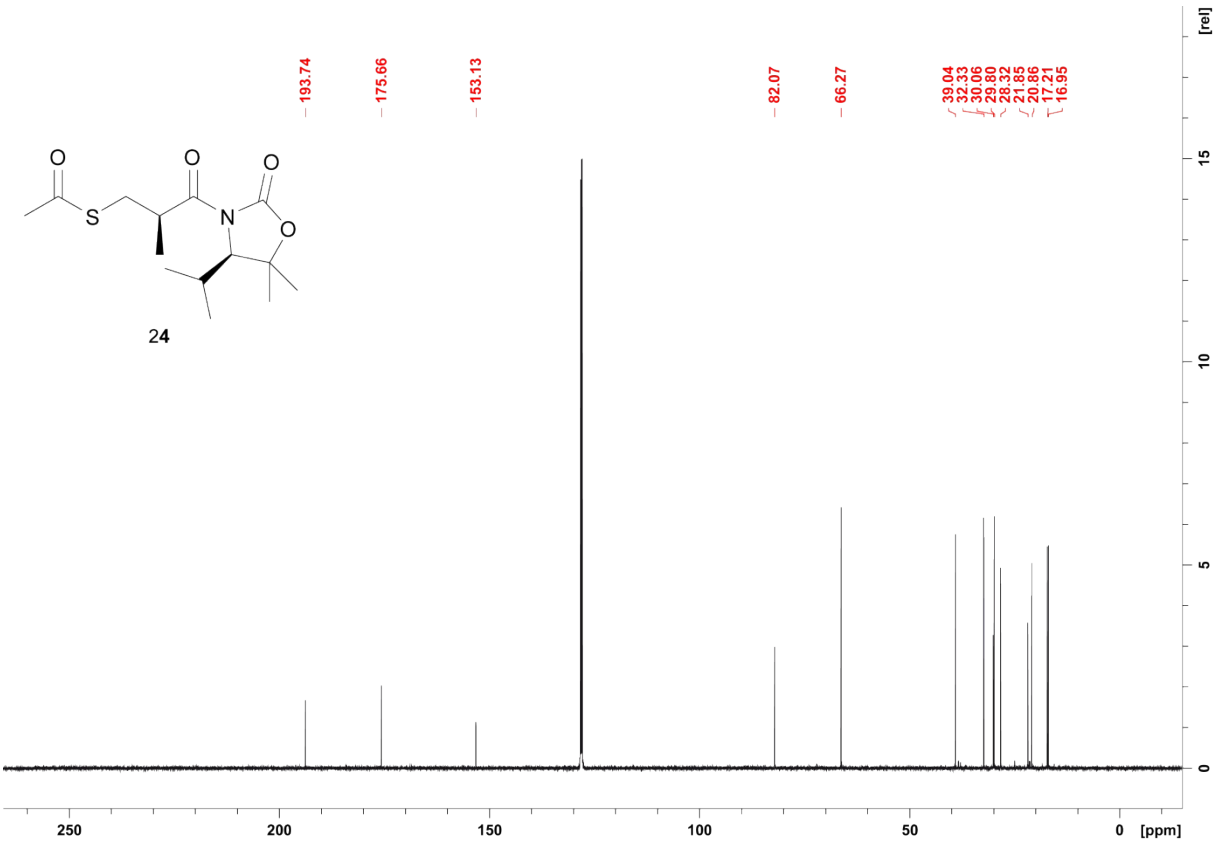

Figure S56 ^{13}C-NMR spectrum of **24** (125 MHz, C_6D_6).

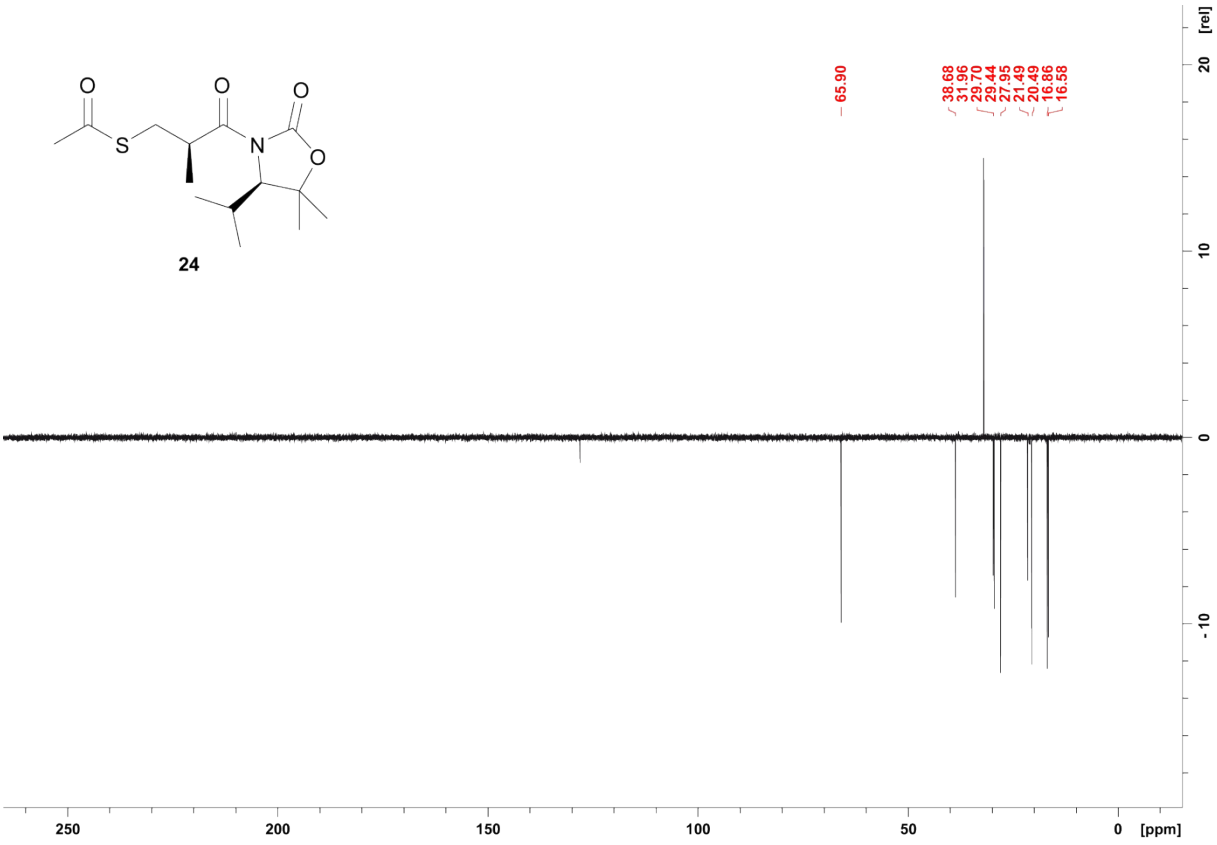

Figure S57 ^{13}C-DEPT-NMR spectrum of **24** (125 MHz, C_6D_6).

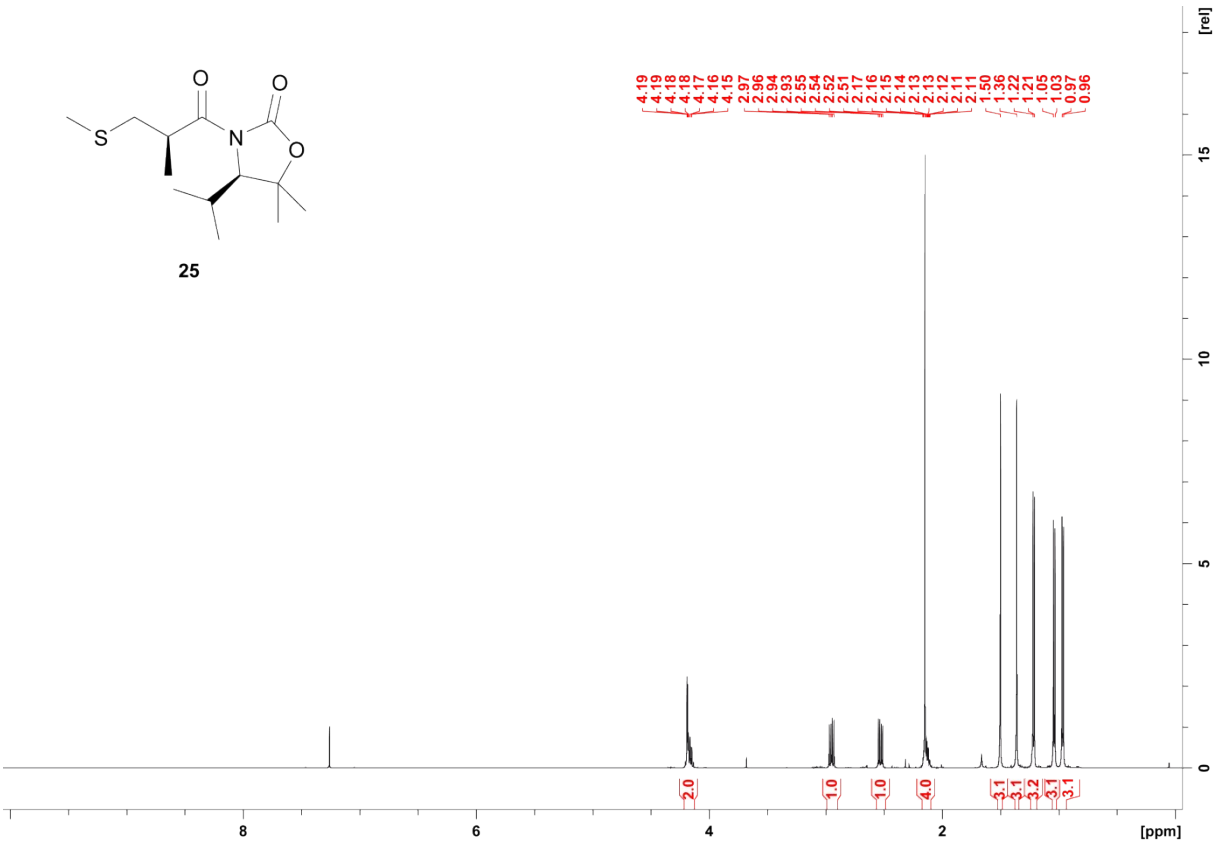

Figure S58 ^{1}H-NMR spectrum of **25** (500 MHz, $CDCl_3$).

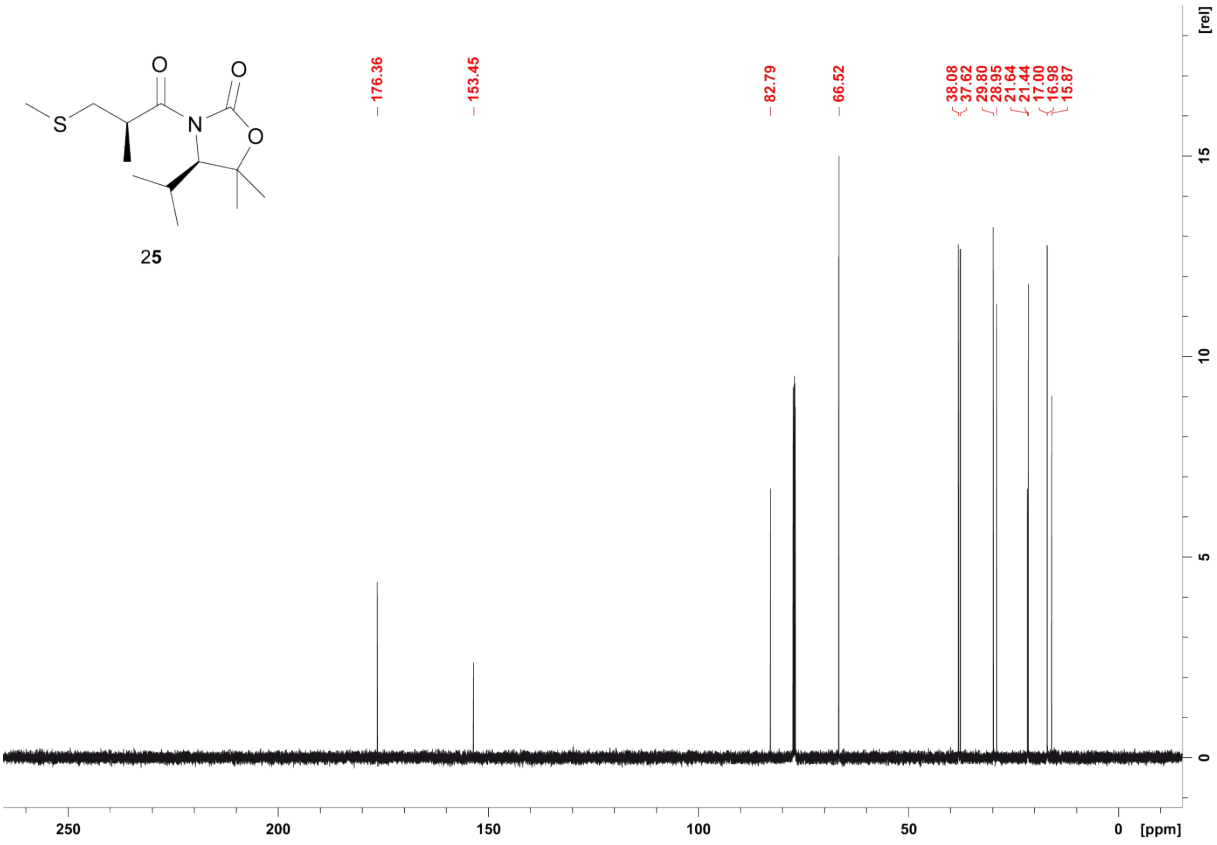

Figure S59 ^{13}C-NMR spectrum of **25** (125 MHz, $CDCl_3$).

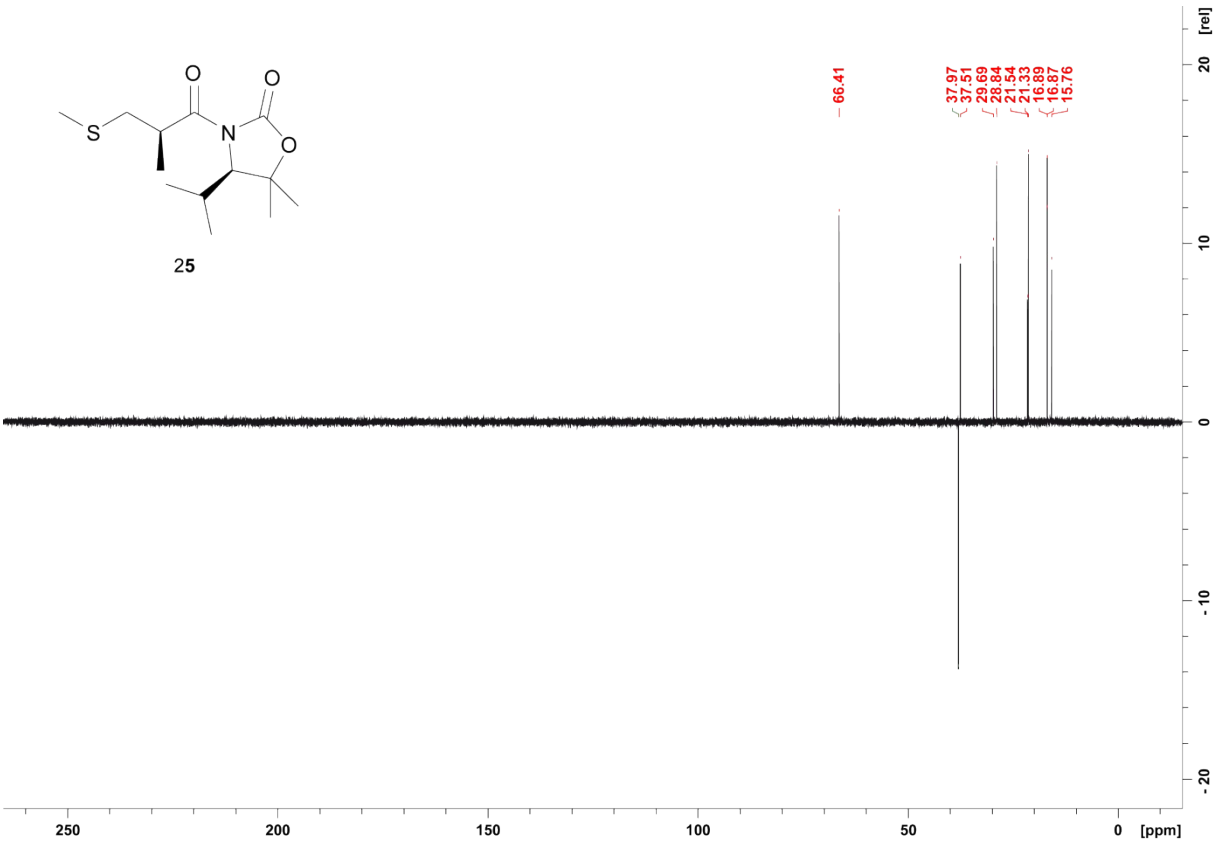

Figure S60 ^{13}C-DEPT-NMR spectrum of **25** (125 MHz, $CDCl_3$).

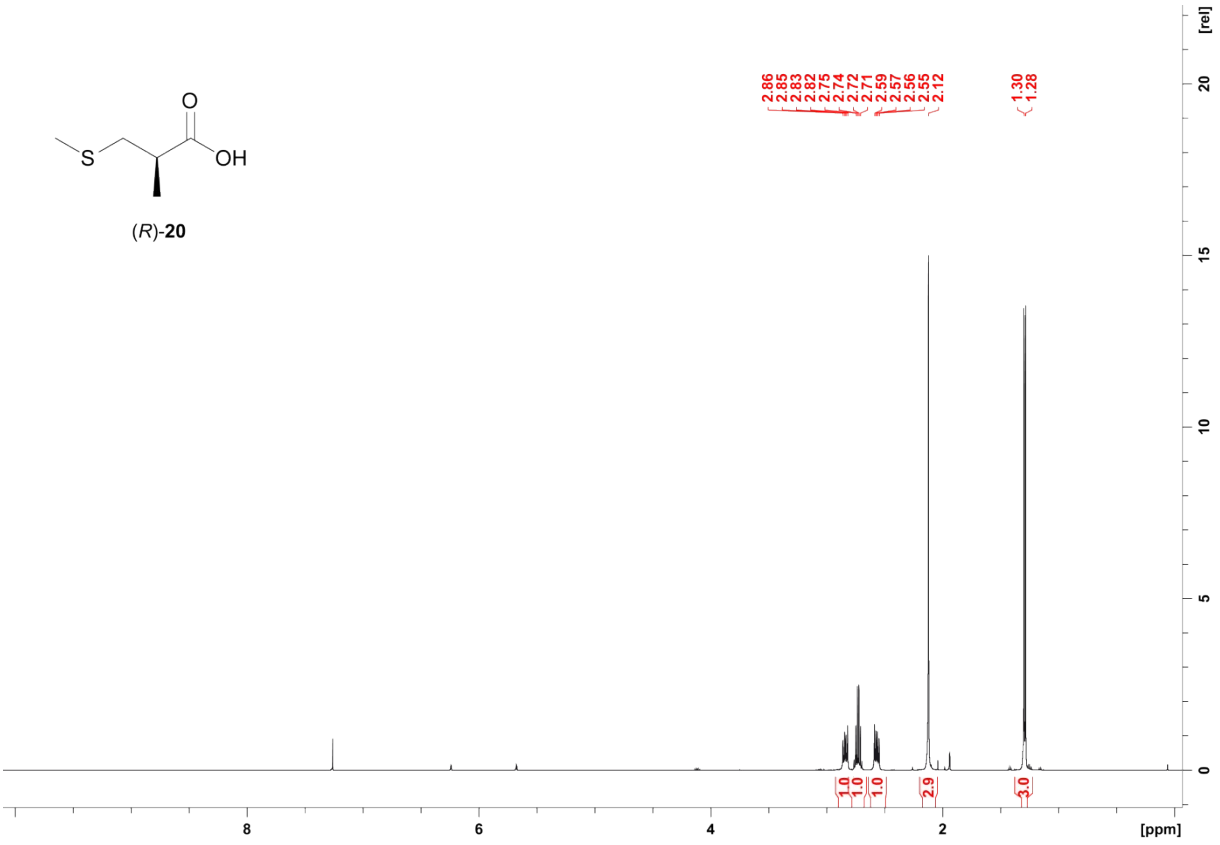

Figure S61 ^{1}H-NMR spectrum of (*R*)-**20** (500 MHz, $CDCl_3$).

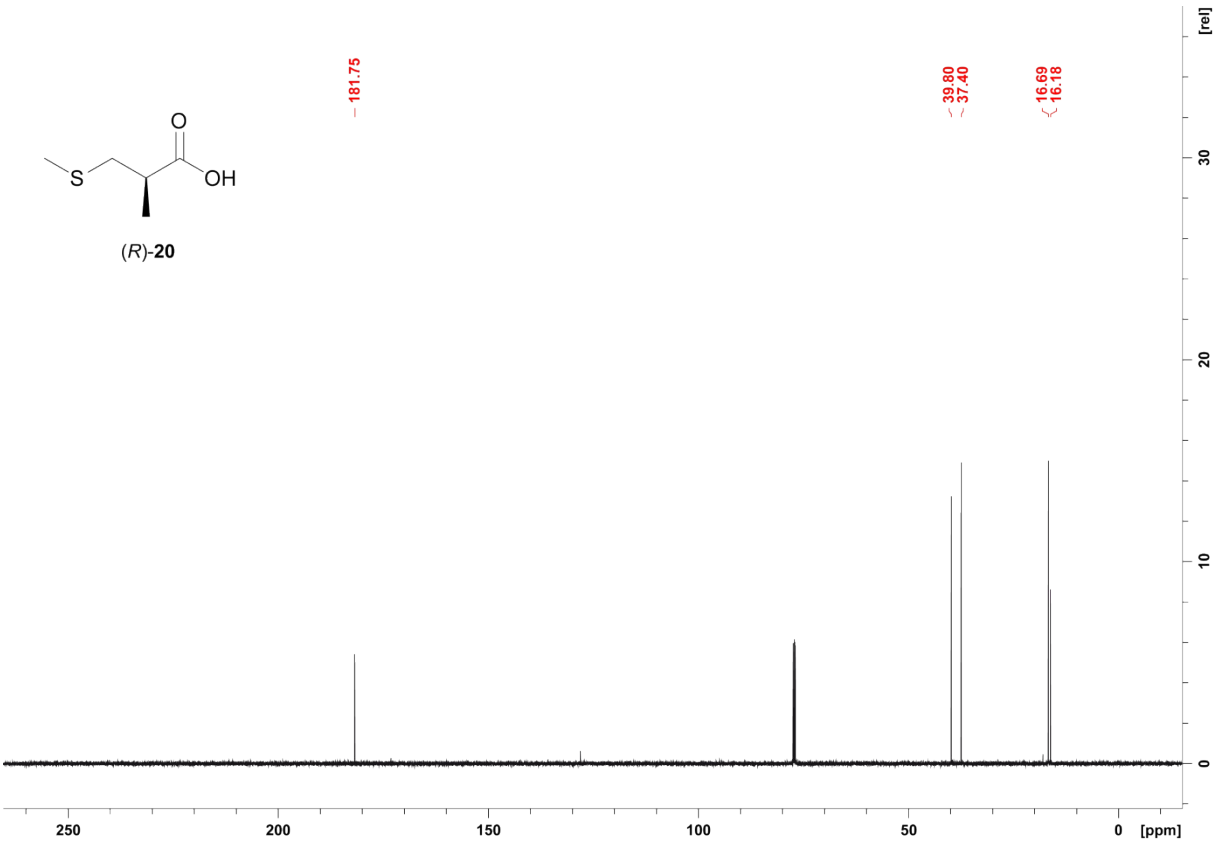

Figure S62 ^{13}C-NMR spectrum of (*R*)-**20** (125 MHz, $CDCl_3$).

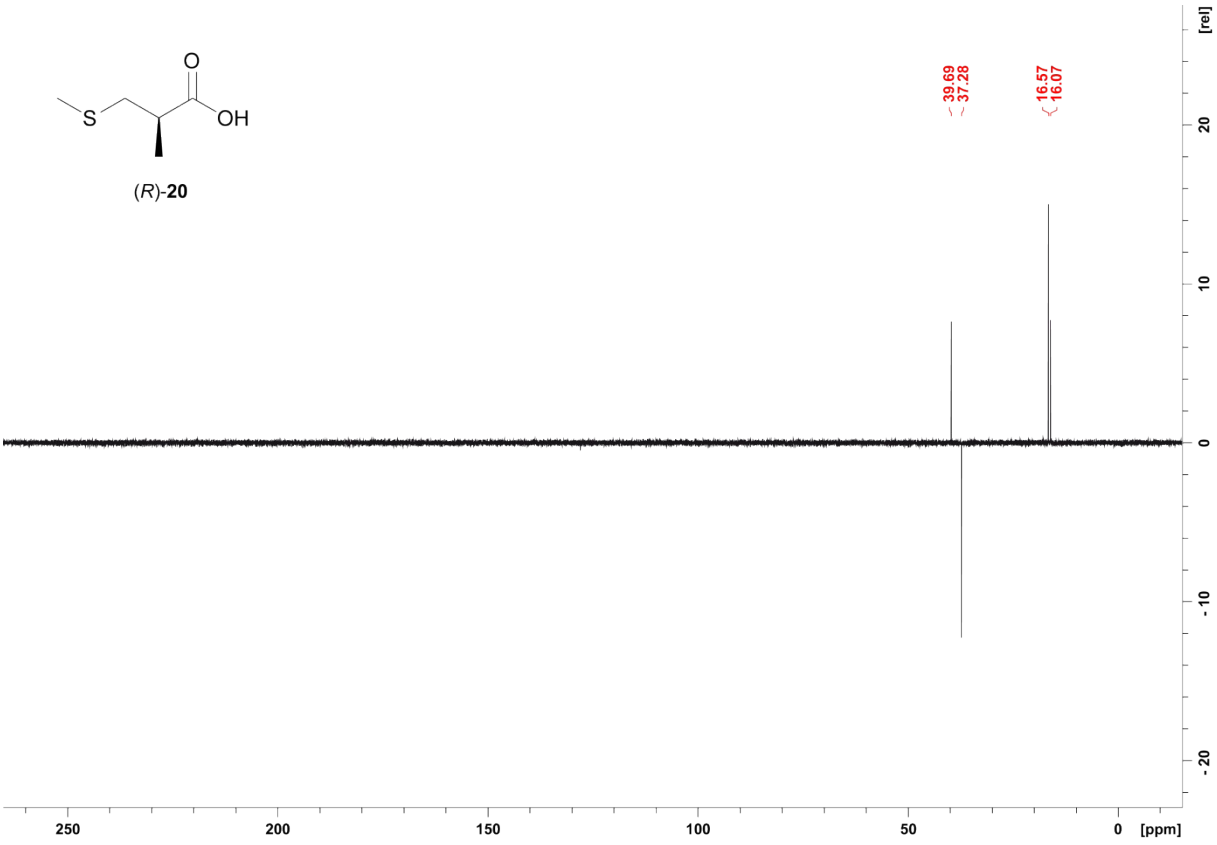

Figure S63 ^{13}C-DEPT-NMR spectrum of (*R*)-**20** (125 MHz, $CDCl_3$).

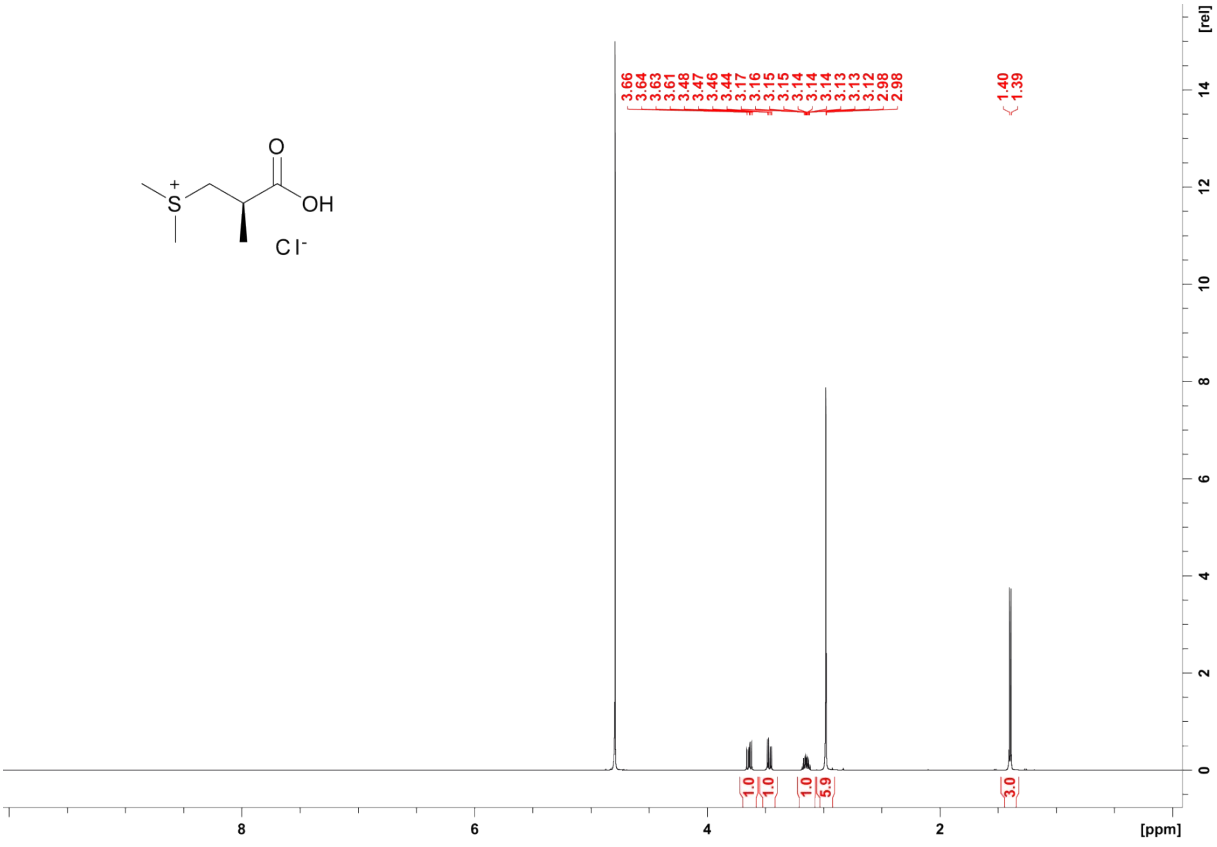

Figure S64 ^{1}H-NMR spectrum of (*R*)-**17** (500 MHz, D_2O).

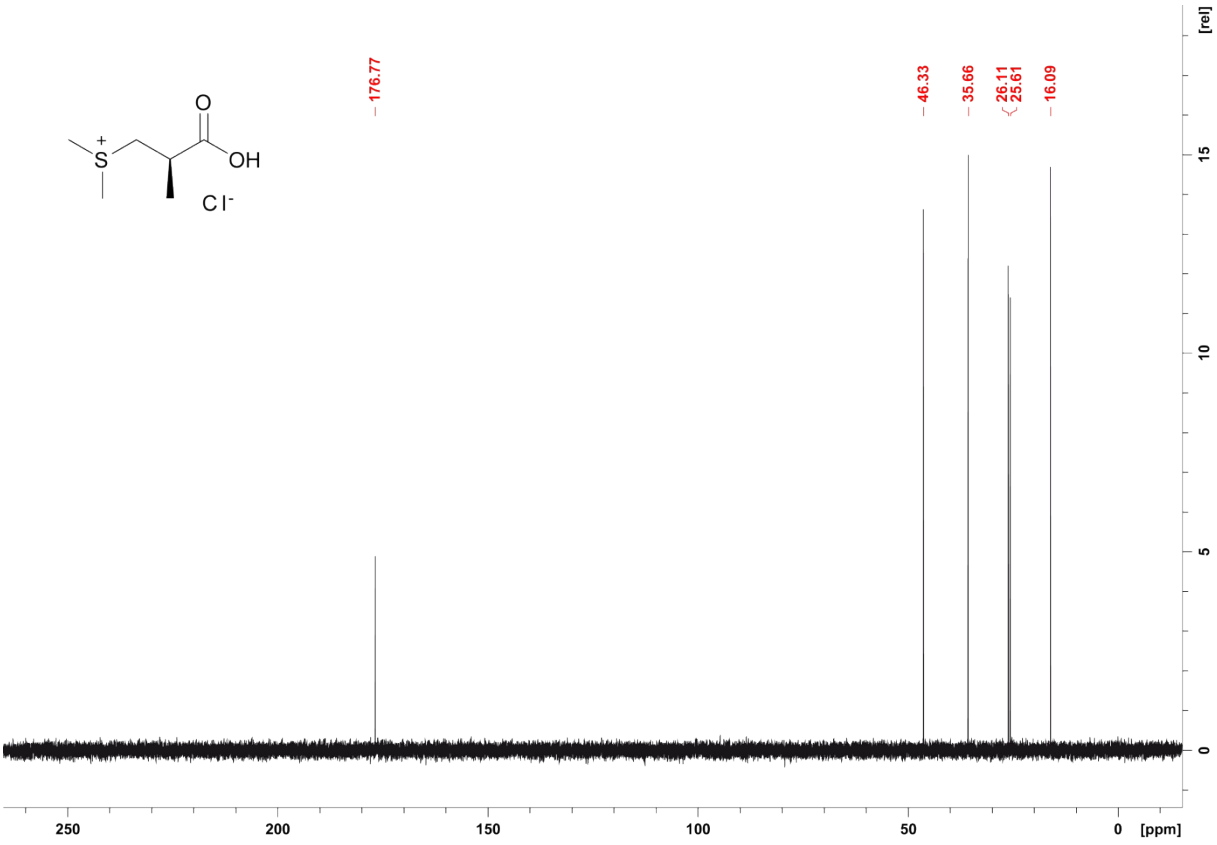

Figure S65 ^{13}C-NMR spectrum of (*R*)-**17** (125 MHz, D_2O).

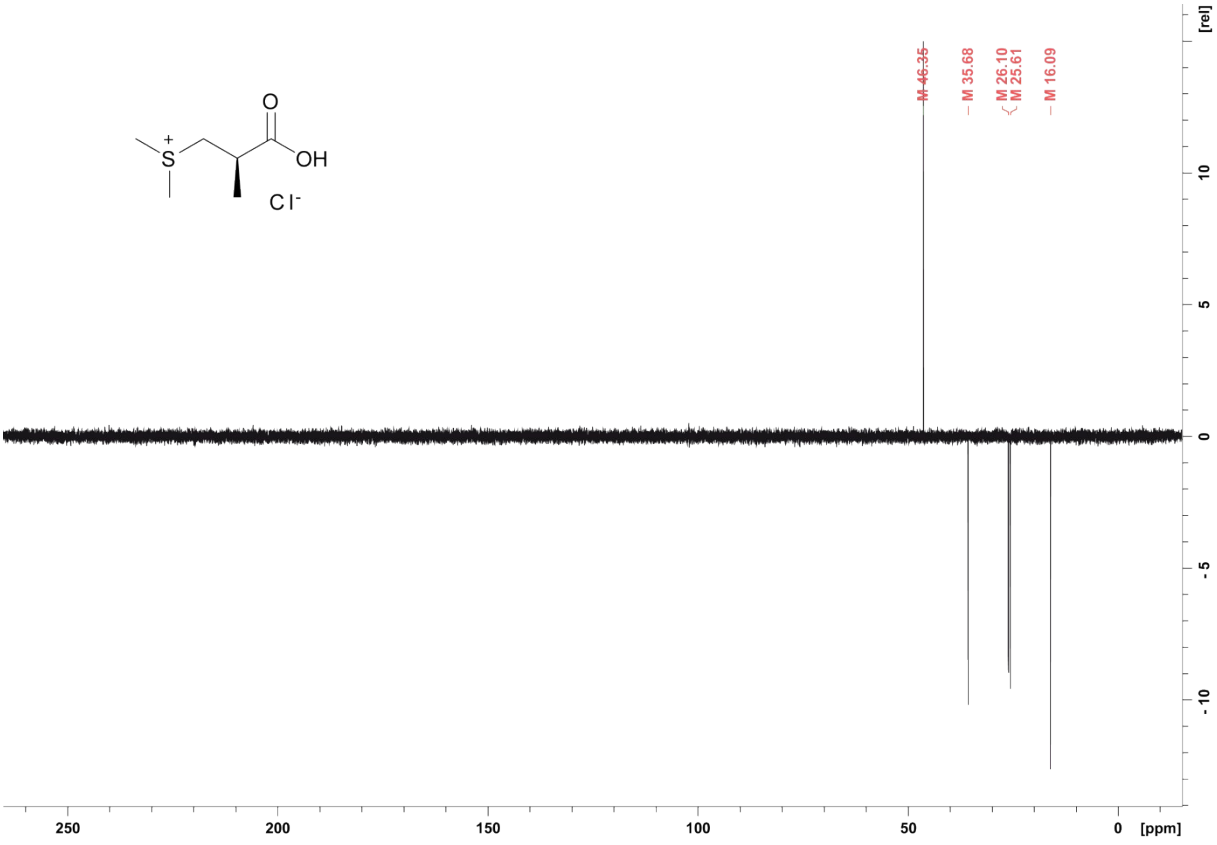

Figure S66 ^{13}C-DEPT-NMR spectrum of (*R*)-**17** (125 MHz, D_2O).

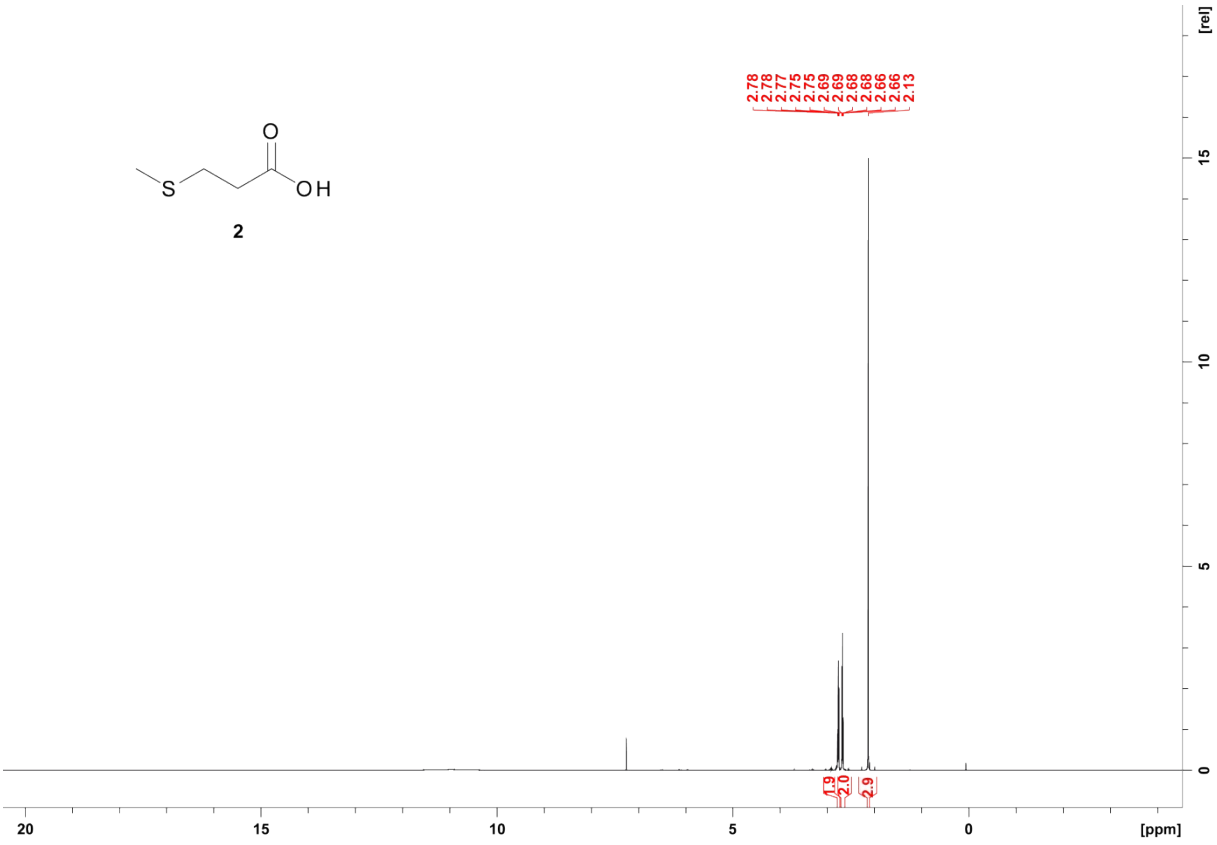

Figure S67 ^{1}H-NMR spectrum of **2** (500 MHz, $CDCl_3$).

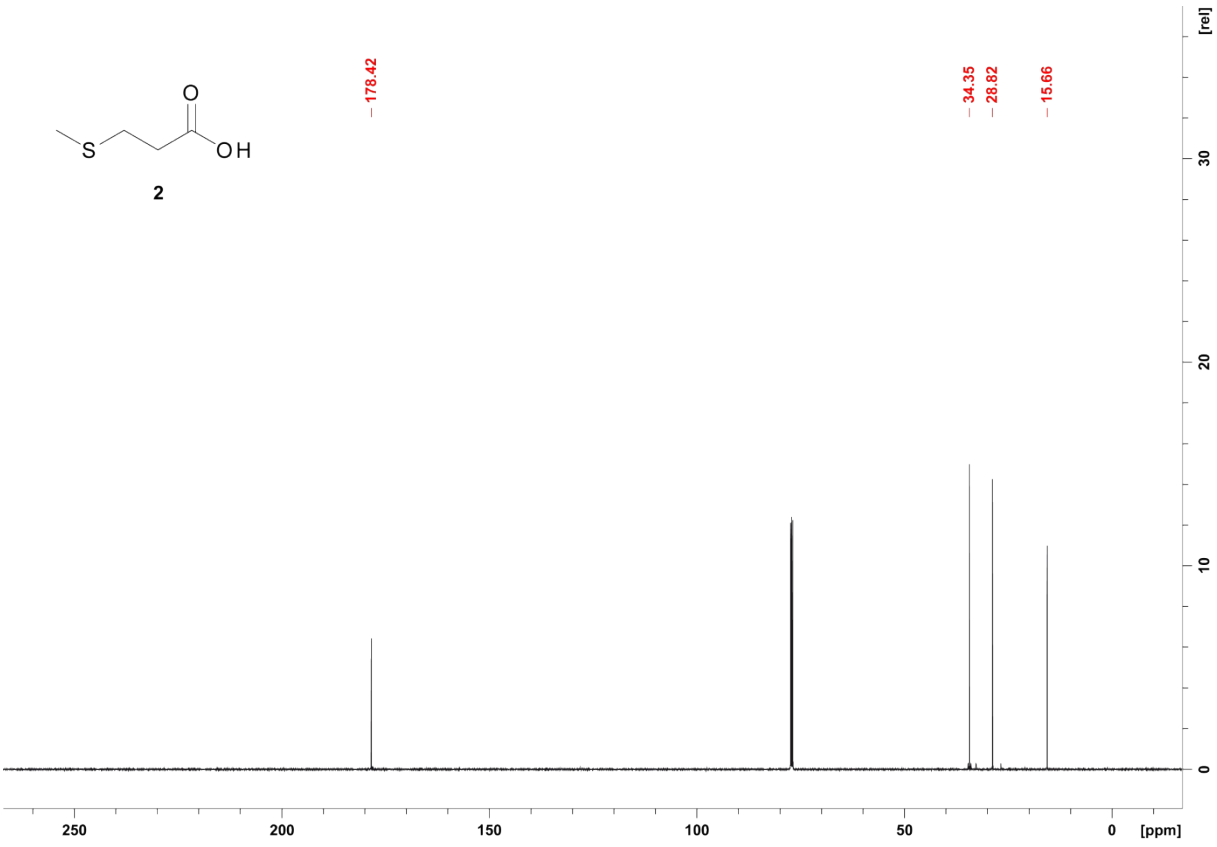

Figure S68 ^{13}C-NMR spectrum of **2** (125 MHz, $CDCl_3$).

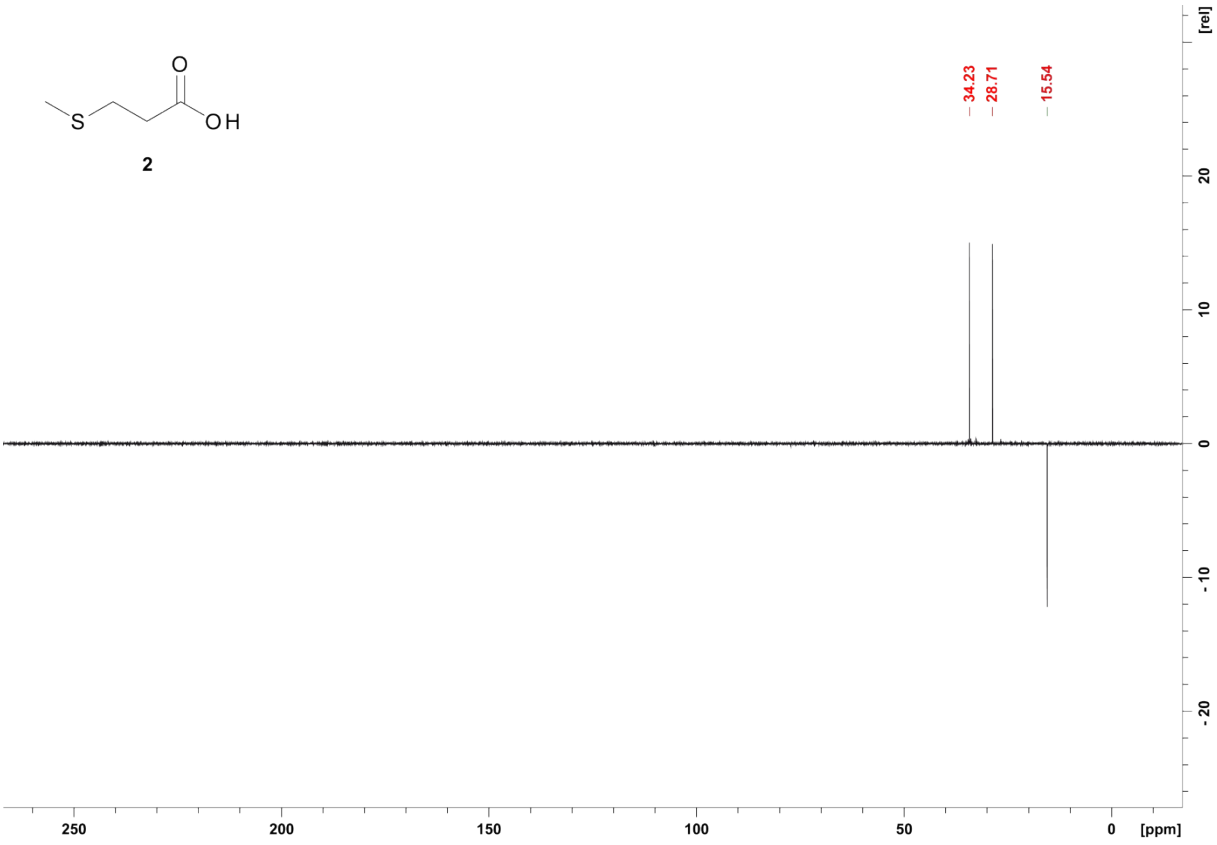

Figure S69 ^{13}C-DEPT-NMR spectrum of **2** (125 MHz, $CDCl_3$).

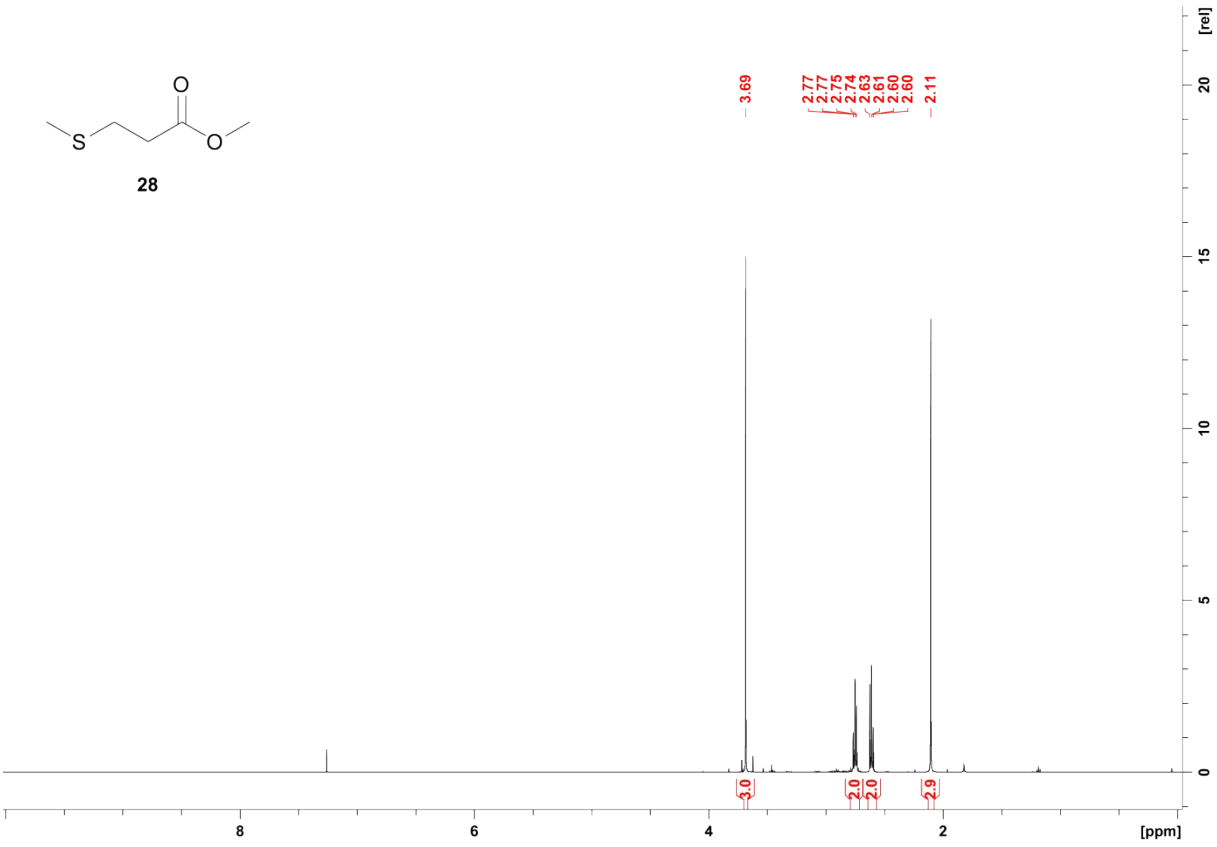

Figure S70 ^{1}H-NMR spectrum of **28** (500 MHz, $CDCl_3$).

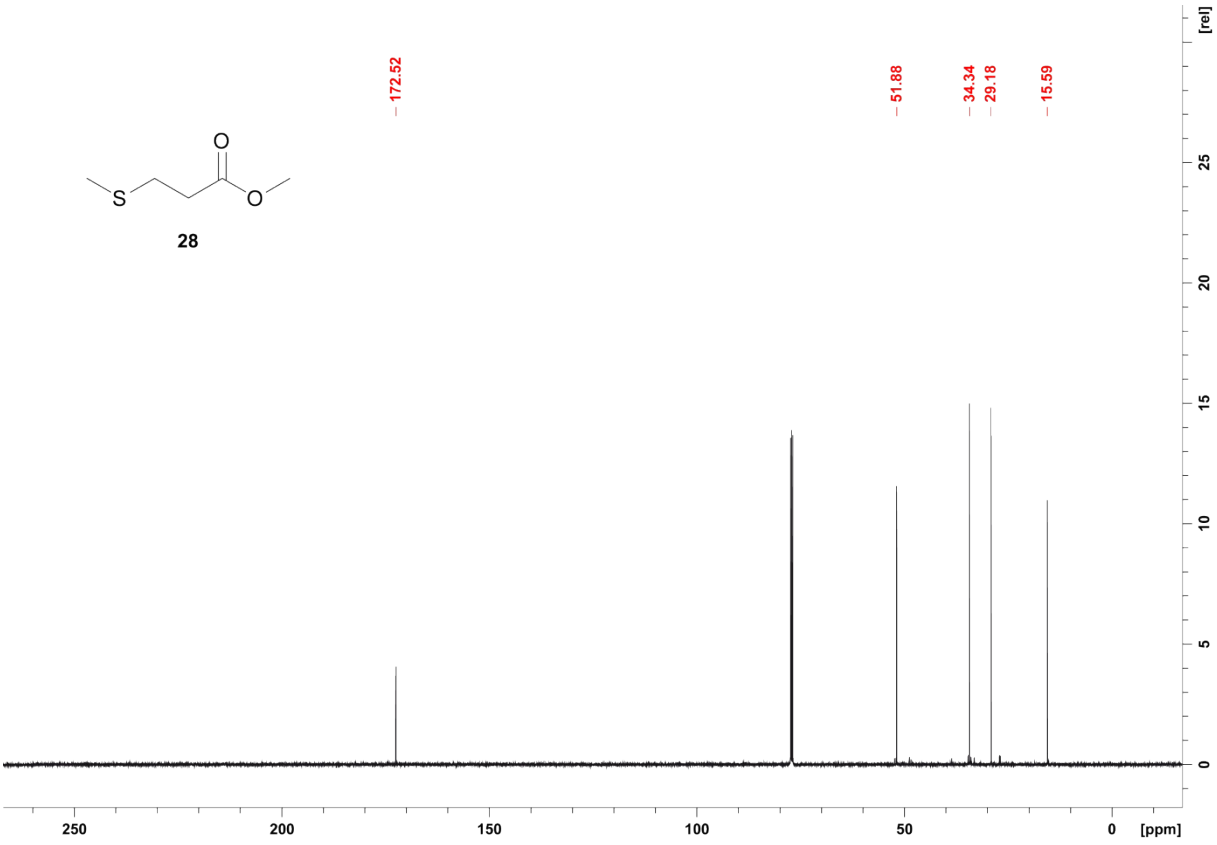

Figure S71 ^{13}C-NMR spectrum of **28** (125 MHz, $CDCl_3$).

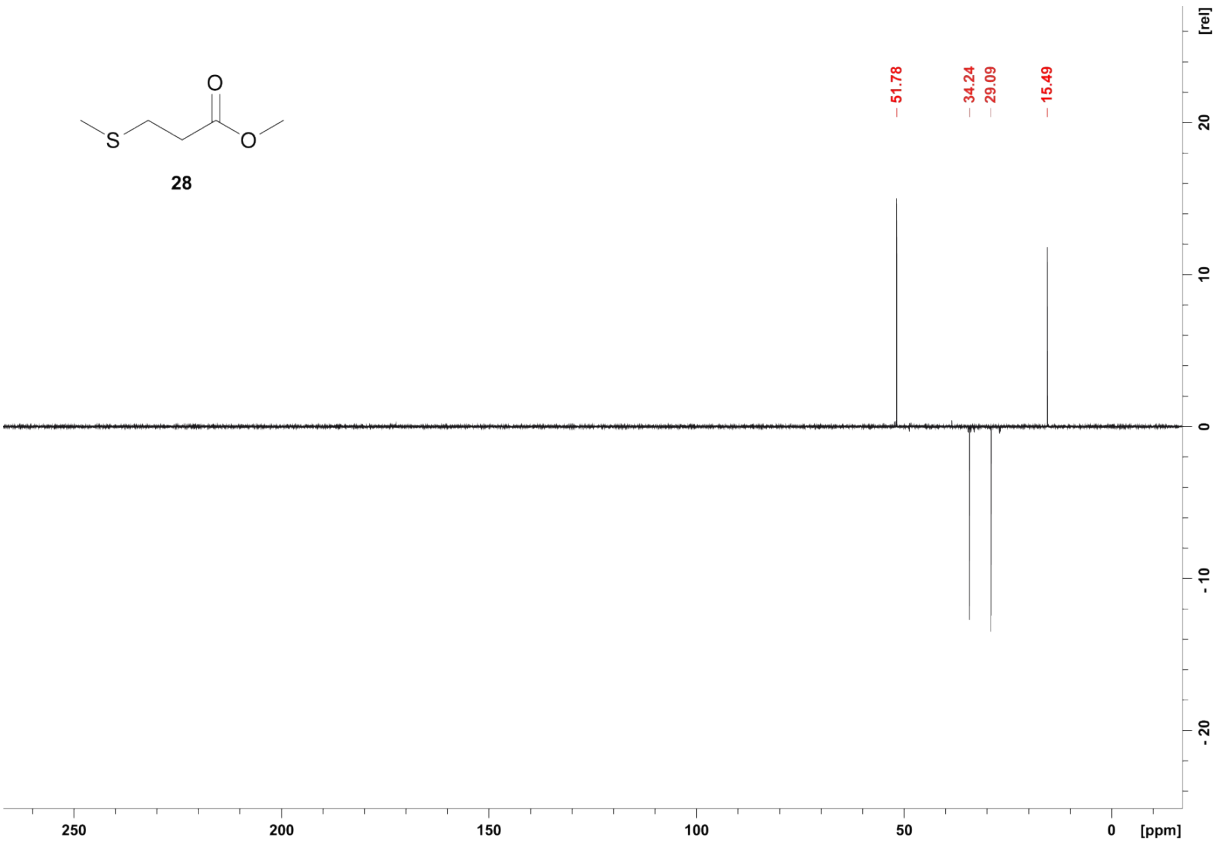

Figure S72 ^{13}C-DEPT-NMR spectrum of **28** (125 MHz, $CDCl_3$).

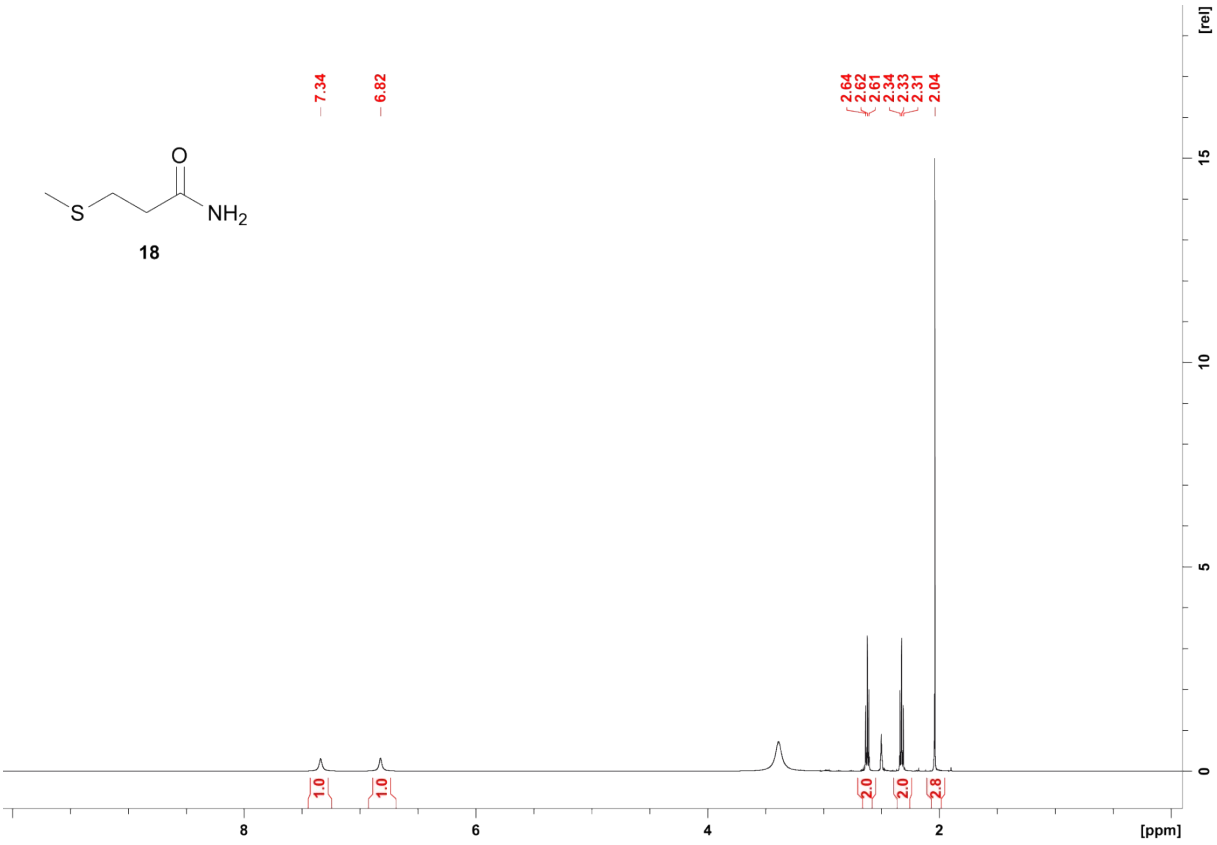

Figure S73 ^{1}H-NMR spectrum of **18** (500 MHz, DMSO-d_6).

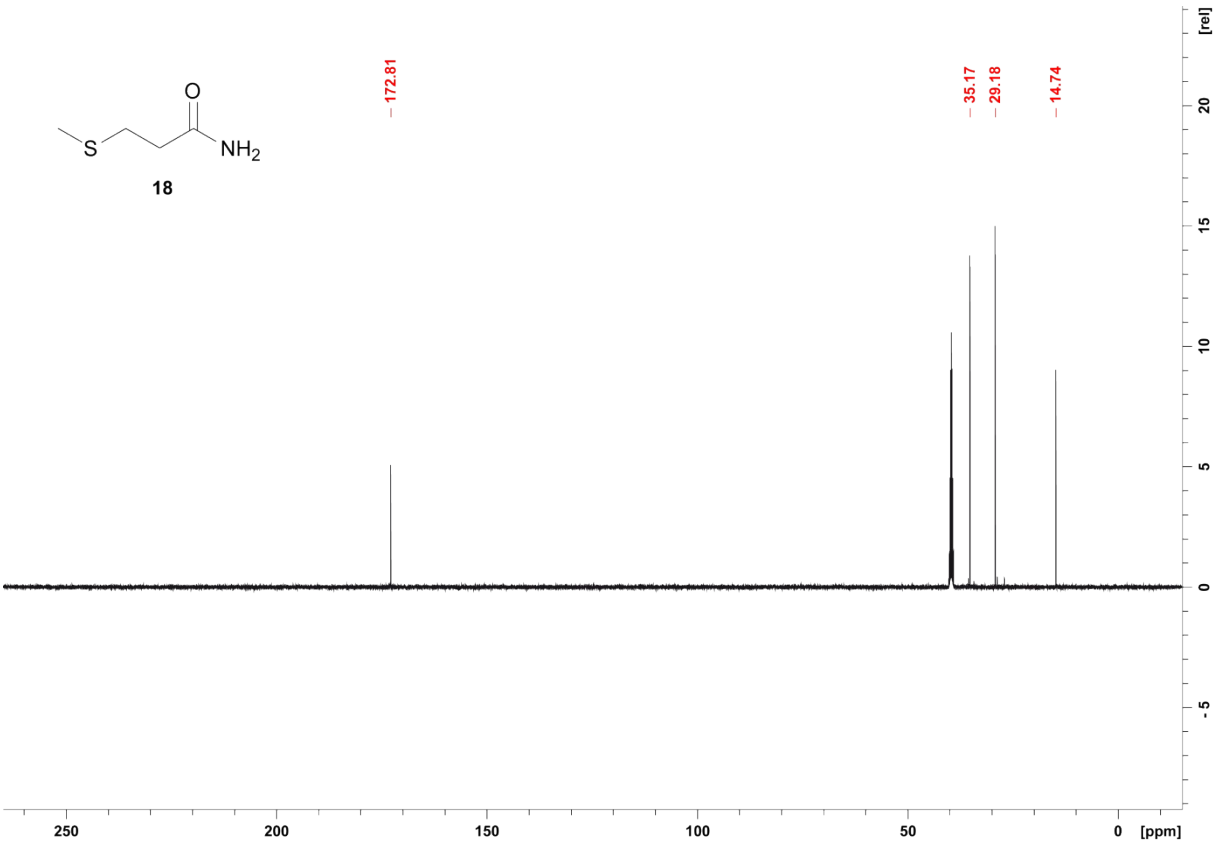

Figure S74 ^{13}C-NMR spectrum of **18** (125 MHz, DMSO-d_6).

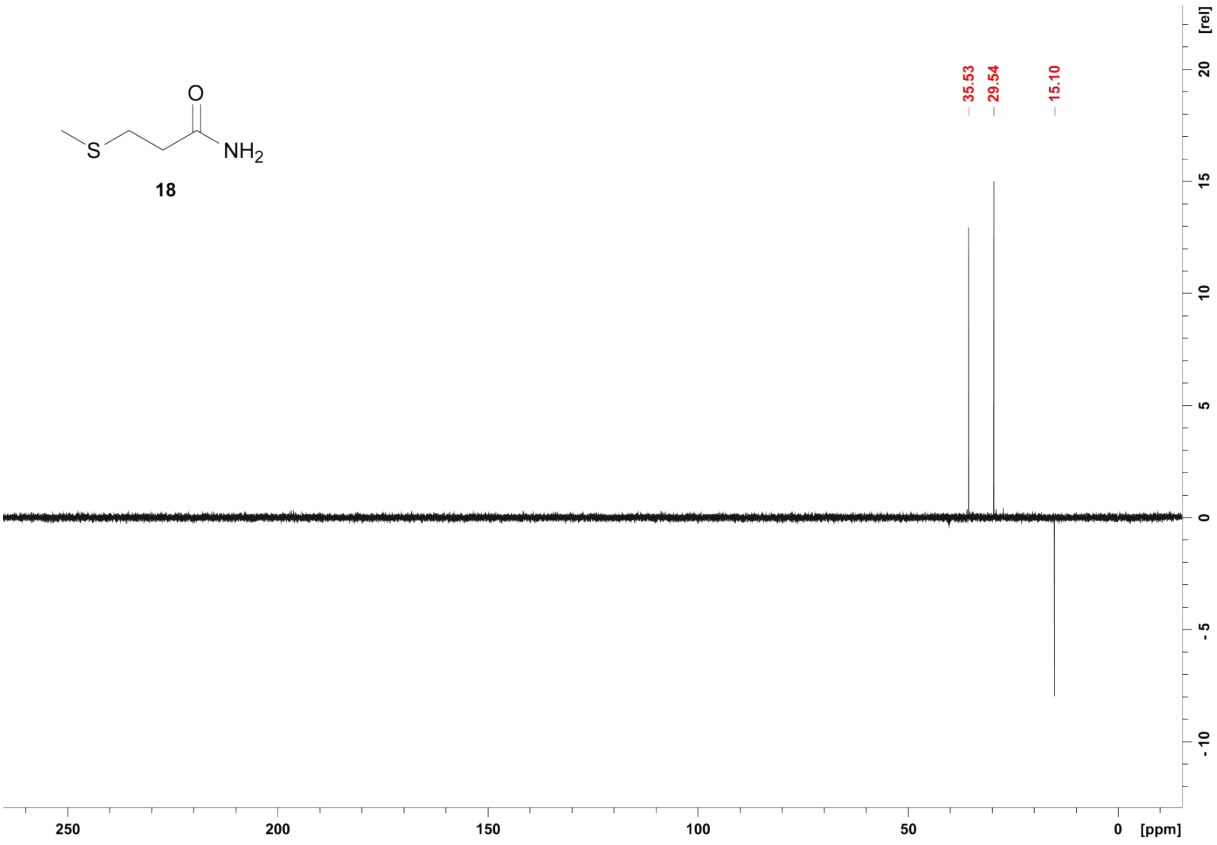

Figure S75 ^{13}C-DEPT-NMR spectrum of **18** (125 MHz, DMSO-d_6).

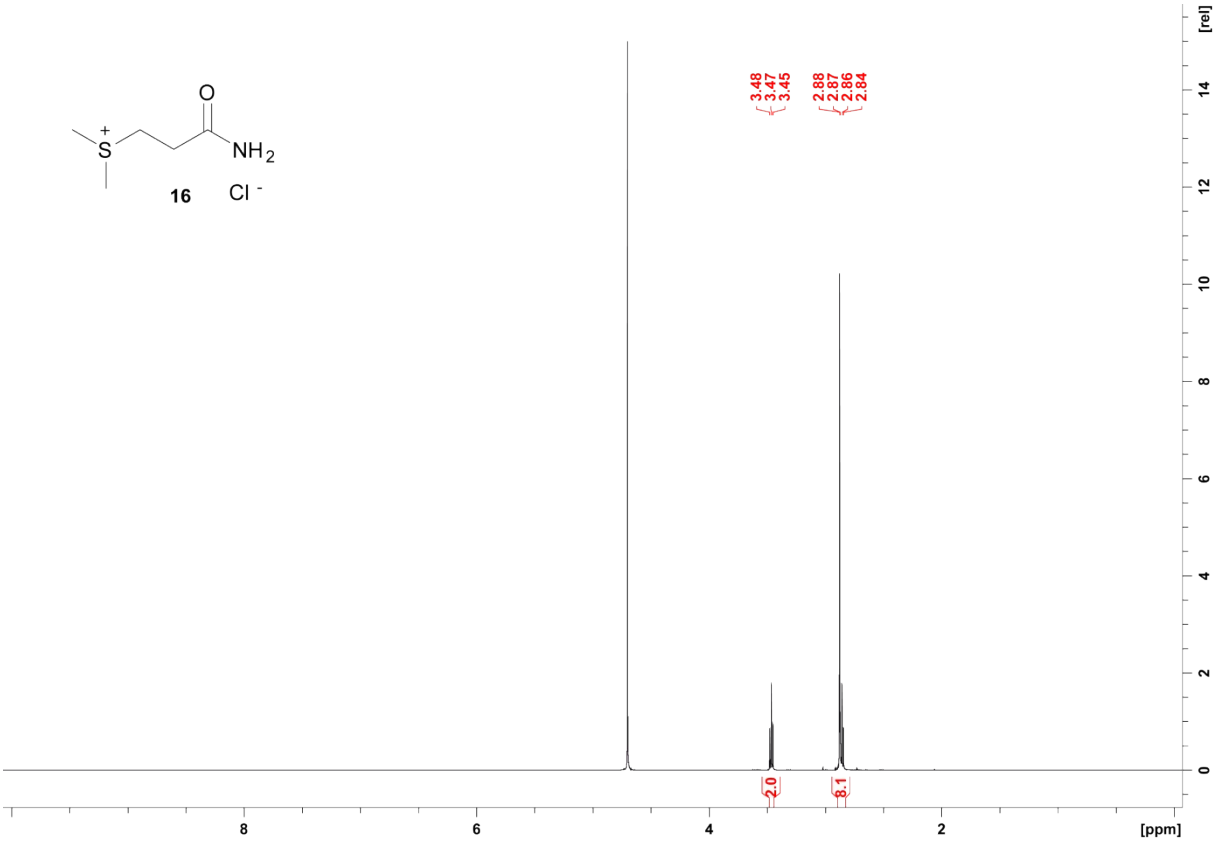

Figure S76 ^{1}H-NMR spectrum of **16** (500 MHz, D_2O).

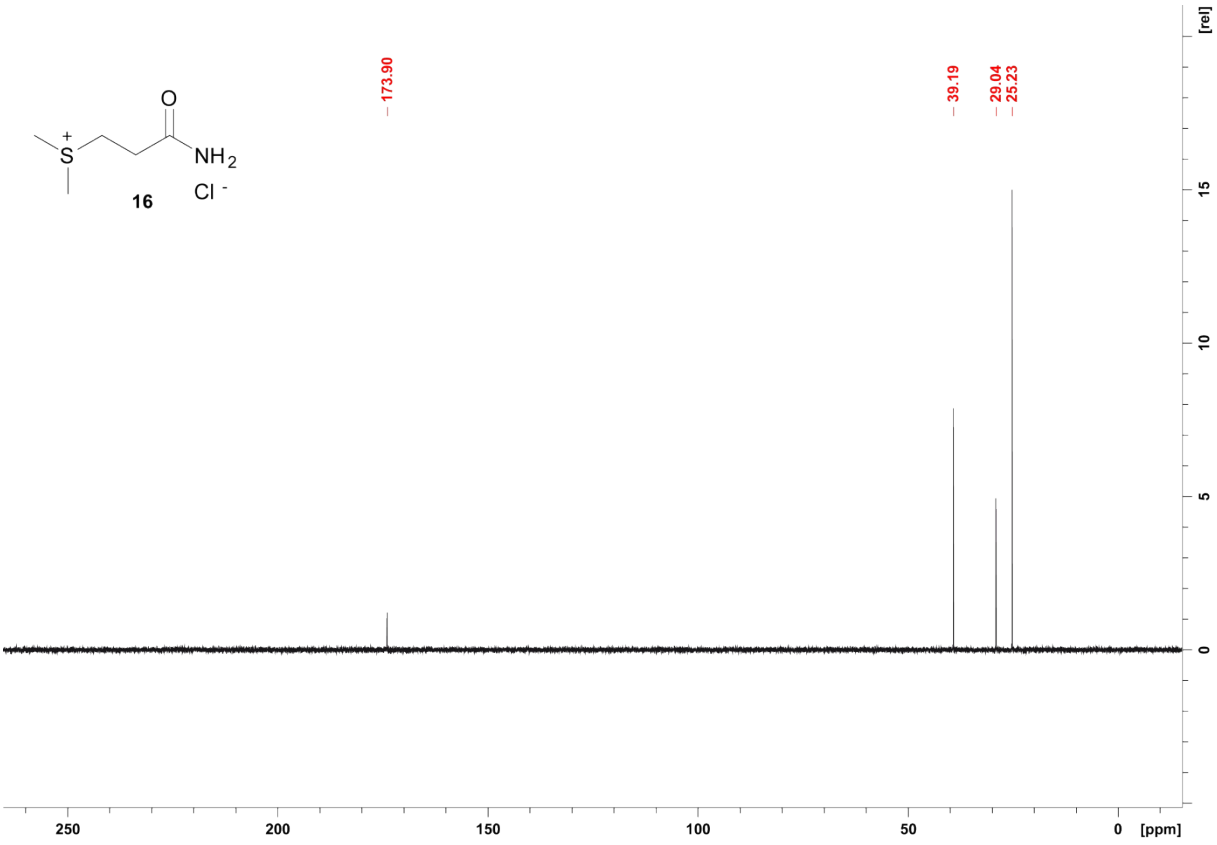

Figure S77 ^{13}C-NMR spectrum of **16** (125 MHz, D_2O).

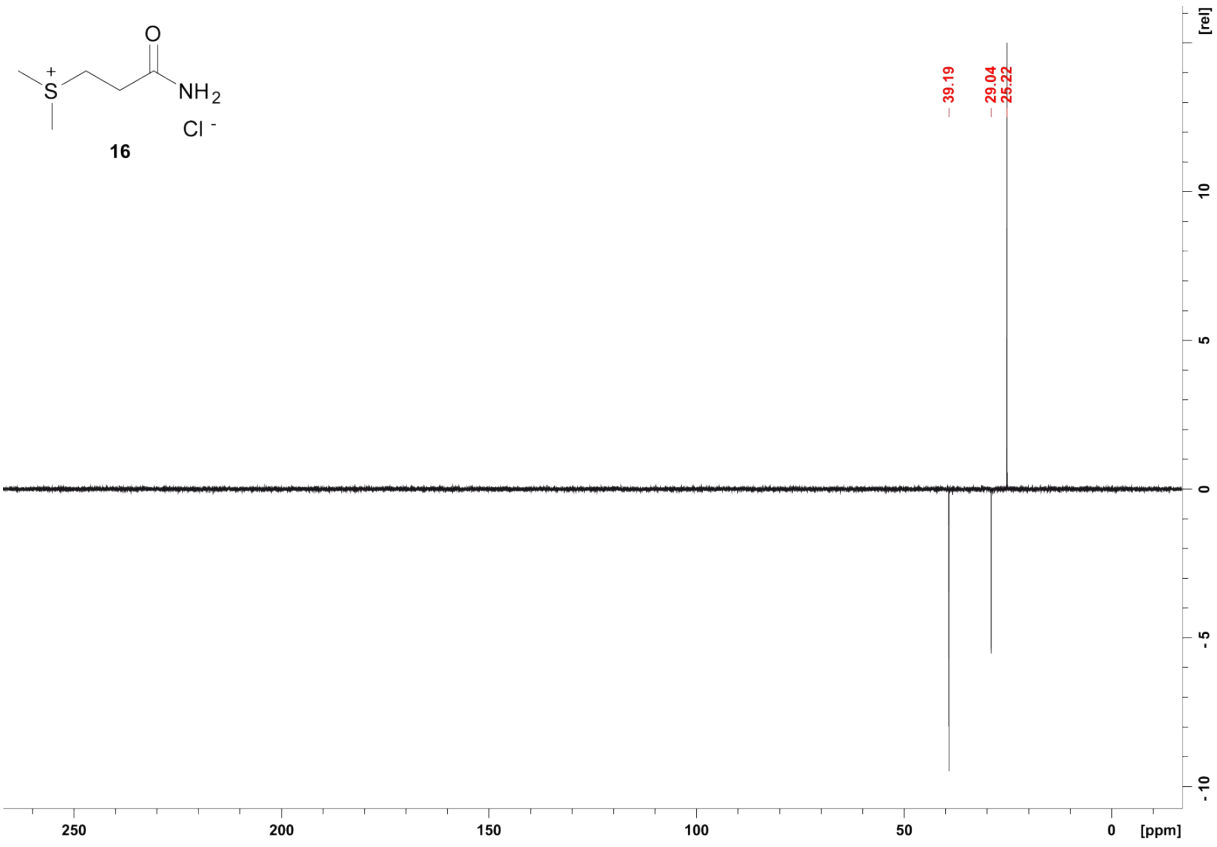

Figure S78 ^{13}C-DEPT-NMR spectrum of **16** (125 MHz, D_2O).

References

[1] J. S. Dickschat, K. A. K. Pahirulzaman, P. Rabe and T. A. Klapschinski, *ChemBioChem*, 2014, **15**, 810.

[2] R. D. Gietz and R. H. Schiestl, *Nat. Protoc.*, 2007, **2**, 31.

[3] S. C. Gill and P. H. von Hippel, *Anal. Biochem.*, 1989, **182**, 319.

[4] R. L. Burton, S. Chen, X. L. Xu and G. A. Grant, *J. Biol. Chem.*, 2007, **282**, 31517.

[5] V. J. LiCata and N. M. Allewell, *Biophys. Chem.*, 1997, **64**, 225.

[6] (a) E. Chovancová, A. Pavelka , P. Beneš, O. Strnad, J. Brezovský, B. Kozlíková, A. Gora, V. Šustr, M. Klvaňa, P. Medek, L. Biedermannová, J. Sochor, J. Damborský, *PLOS Comput. Biol.*, 2012, **8**, e1002708; (b) A. Pavelka, E. Šebestová, B. Kozlíková, J. Brezovský, J. Sochor and J. Damborský, *IEEE/ACM Trans. Comput. Biol. Bioinf., 2016*, **13**, 505.

[7] C. C. Valley, A. Cembran, J. D. Perlmutter, A. K. Lewis, N. P. Labello, J. Gao and J. N. Sachs, *J. Biol. Chem.*, 2012, **287**, 34979.

[8] P. Wang, X.-L. Chen, C.-Y. Li, X. Gao, D.-Y. Zhu, B.-B. Xie, Q.-L. Qin, X.-Y. Zhang, H.-N. Su, B.-C. Zhou, L.-Y. Xun and Y.-Z. Zhang, *Mol. Microbiol.*, 2015, **98**, 289.

[9] A. E. Brummett and M. Dey, *Biochemistry*, 2016, **55**, 6162.